Investigations on PD Source Localization in Power Transformer using Non-Invasive Monitoring Techniques

A Thesis Submitted in partial fulfillment of the
Requirements for the award of the degree of

Doctor of Philosophy

in

Electrical Engineering

by

M. Kalyan Chakravarthi
(Roll No. 701410)

Supervisors

Dr. A.V. Giridhar Associate Professor

&

Dr. D.V.S.S. Siva Sarma Professor(HAG)

Department of Electrical Engineering
National Institute of Technology Warangal
(An Institute of National Importance)
Warangal – 506 004, Telangana, India

AUGUST – 2022

APPROVAL SHEET

This Thesis entitled "**Investigations on PD Source Localization in Power Transformer using Non-Invasive Monitoring Techniques**" by **M. Kalyan Chakravarthi** is approved for the degree of Doctor of Philosophy

Examiners

_____

_____

_____

Supervisor(s)

Dr. A.V. Giridhar
Associate Professor
&

Dr. D.V.S.S.Siva Sarma
Professor (HAG)
EED, NIT Warangal

Chairman

Dr. M. Sailaja Kumari
Professor & Head,
EED, NIT Warangal

Date: _____

DEPARTMENT OF ELECTRICAL ENGINEERING
NATIONAL INSTITUTE OF TECHNOLOGY WARANGAL
WARANGAL – 506 004

DEPARTMENT OF ELECTRICAL ENGINEERING
NATIONAL INSTITUTE OF TECHNOLOGY WARANGAL

CERTIFICATE

This is to certify that the thesis entitled **"Investigations on PD Source Localization in Power Transformer using Non-Invasive Monitoring Techniques"**, which is being submitted by **Mr. M. Kalyan Chakravarthi** (Roll No. 701410), is a bonafide work submitted to National Institute of Technology Warangal in partial fulfilment of the requirements for the award of the degree of **Doctor of Philosophy** in Electrical Engineering. To the best of my knowledge, the work incorporated in this thesis has not been submitted elsewhere for the award of any degree.

Date:
Place: Warangal

Dr. A.V.GIRIDHAR
(Thesis Supervisor)
Associate Professor
Department of Electrical Engineering
National Institute of Technology Warangal
Warangal – 506004

Dr. D.V.S.S. SIVA SARMA
(Thesis Co-Supervisor)
Professor (HAG)
Department of Electrical Engineering
National Institute of Technology Warangal
Warangal – 506004

DECLARATION

This is to certify that the work presented in the thesis entitled "**Investigations on PD Source Localization in Power Transformer using Non-Invasive Monitoring Techniques"** is a bonafide work done by me under the supervision of **Dr. A.V. Giridhar & Dr D.V.S.S. Siva Sarma**, Department of Electrical Engineering, National Institute of Technology Warangal, India and was not submitted elsewhere for the award of any degree.

I declare that this written submission represents my ideas in my own words and where other's ideas or words have not been included; I have adequately cited and referenced the original sources. I also declare that I have adhered to all principles of academic honesty and integrity and have not misrepresented or fabricated or falsified any idea/date/fact/source in my submission. I understand that any violation of the above will be a cause for disciplinary action by the institute and can also evoke penal action from the sources which have thus not been properly cited or from whom proper permission has not been taken when needed.

Date:
Place: NIT Warangal

M. Kalyan Chakravarthi
(Roll No: 701410)

ACKNOWLEDGEMENTS

It gives me immense pleasure to express my deep sense of gratitude and thanks to my supervisor(s) **Dr. A.V.Giridhar,** Associate Professor**,** and **Dr. D.V.S.S. Siva Sarma,** Professor (HAG), Department of Electrical Engineering, National Institute of Technology Warangal, for their valuable guidance, support, and suggestions. Their knowledge, suggestions, and discussions helped me to become a capable researcher.

I am very much thankful to **Prof. M. Sailaja Kumari**, Chairman & Head, Department of Electrical Engineering for her constant encouragement, support and cooperation.

I take this privilege to thank all my Doctoral Scrutiny Committee members, **Dr. S. Srinivasa Rao**, Professor, Department of Electrical Engineering, **Dr. P. Suresh Babu**, Associate Professor, Department of Electrical Engineering and **Dr. P. Bangarubabu**, Professor (HAG), Department of Mechanical Engineering for their detailed review, constructive suggestions and excellent advice during the progress of this research work. I would also like to thank **Dr. D. Vakula**, Professor, Department of Electronics and Communication Engineering and **Dr. G. Arun Kumar**, Assistant Professor G-I, Department of Electronics and Communication Engineering for their valuable suggestions, support and cooperation.

I also appreciate the encouragement from teaching, non-teaching members, and fraternity of Department of Electrical Engineering of NIT Warangal. They have always been encouraging and supportive.

I wish to express my sincere thanks to **Prof. N.V. Ramana Rao**, Director, NIT Warangal for his official support and encouragement.

I convey my special thanks to contemporary Research Scholars Dr. D.Sudha Rani, Dr. Sachidananda Prasad, Dr. B. Kiran Babu, Mr Y.Darmesh, Mr. K.K.Rai, Mr. T.Praveen Kumar, Dr. S. Madhu Babu, Mr. K. Hema Sundara Rao, Mr. M.F Baba, Dr. G. Sunil Kumar and Mr T. Murali Krishna for their technical and personal support.

I acknowledge my gratitude to all my teachers and colleagues at various places for supporting and co-operating me to complete the work.

I express my deep sense of gratitude and reverence to all my **family members** for their sincere prayers, blessings, constant encouragement, shouldering the responsibilities and moral support rendered to me throughout my life, without my family's sacrifice and support which my research work would not have been possible. It is a great pleasure for me to acknowledge and express my appreciation to all **my well-wishers** for their understanding, relentless supports, and encouragement during my research work. Last but not the least, I wish to express my sincere thanks to all those who helped me directly or indirectly at various stages of this work.

Above all, I express my deepest regards and gratitude to "**ALMIGHTY**" whose divine light and warmth showered upon me the perseverance, inspiration, faith and enough strength to keep the momentum of work high even at tough moments of research work.

M. Kalyan Chakravarthi

ABSTRACT

Power transformers are substantial and key elements of electrical energy networks. The power transformers should be insulated to provide reliable and safe service in the power systems. Due to the continuous operation of power transformers sudden failure and outages may occur as the insulation degrades with time. Hence continuous insulation quality monitoring of power transformers is essential and widely accepted assessment is the identification of partial discharges. PD monitoring techniques can be performed either online or offline. These online monitoring techniques do not interrupt its normal operation whereas offline monitoring techniques require disconnection from the power supply. The recommendations for transformers condition assessment and monitoring facilities had been reviewed in technical brochure of Cigre working group A2.27, 2008.

PD is a quite cumbersome incident and random in nature. There are still distinct challenging aspects like accurate evaluating PD measurements, analysing the captured PD signals relevantly and thereafter preparing a report on insulating system of the condition assessment. The present work is focused on design of a non-invasive monitoring type of sensor technique for PD detection and source localization in power transformer using distinct metaheuristic methods.

In this thesis, metaheuristic techniques such as particle swarm optimization, bat algorithm and fuzzy adaptive particle swarm optimization have been investigated for localization of PD source in power transformer using non-invasive monitoring techniques. These approaches are applied to laboratory as well as field PD measurements of acoustic emission case studies. These case studies demonstrate merits of the proposed metaheuristic techniques when compared to conventional techniques in the localization of PD source.

A broadband printed log periodic dipole array ultra high frequency sensor has also been designed for detection of distinct incipient discharges falling on UHF frequency range i.e. 0.5 - 3GHz. To validate the designed UHF sensor, four distinct test cells have been designed and manufactured to capture respective incipient discharges falling in that UHF range i.e. corona, particle movement, free metal particles and surface discharges. After detection of PD sources, time difference of arrival measurements can be acquired from PD source to the respective non-invasive sensors i.e. acoustic and UHF sensors. In this thesis, an investigation on these TDOA measurements acquired from the narrow and broad band LPDA UHF sensors for localization of PD source has been performed. The PD source localization results were found to be within acceptable limits.

Keywords: Partial Discharge (PD), Acoustic Emission (AE), Bat Algorithm (BA), Particle Swarm Optimization (PSO), Fuzzy Adaptive Particle Swarm Optimization (FAPSO), Time Difference of Arrival (TDOA), Log Periodic Dipole Array (LPDA) , Ultra High Frequency (UHF).

CONTENTS

APPROVAL SHEET ..... **ii**

CERTIFICATE ..... **iii**

DECLARATION ..... **iv**

ACKNOWLEDGEMENTS ..... **vi**
ABSTRACT ..... **viii**
LIST OF FIGURES ..... **x**
LIST OF TABLES ..... **xii**
LIST OF ABBREVIATIONS ..... **xiv**
LIST OF SYMBOLS ..... **xv**

CHAPTER-1 INTRODUCTION **1**

1.1 Overview 1

1.2 Motivation 4

1.3 Research Contributions 5

1.4 Organization of the Thesis 6

CHAPTER-2 LITERATURE REVIEW **8**

2.1 Introduction 8

2.2 PD and Its Mechanisms 8

2.3 PD Monitoring Techniques 9

2.3.1 Direct or Invasive Technique (Electrical Method) 12

2.3.2 Indirect or Non-Invasive Technique (Acoustic Emission Method) 13

2.3.3 Indirect or Non-Invasive Technique (UHF / RF Method) 14

2.4 Importance of UHF PD Technique 15

2.5 Challenges of UHF PD Technique 16

2.6 Literature Survey on PD Source Localization in Power Transformer 16

2.6.1 PD Source Localization in Power Transformer Using Acoustic Sensors 16

2.6.2 PD Source Localization in Power Transformer Using UHF Sensors 18

2.6.3 Different types of UHF Sensors used for PD Measurements in Power Transformer 20

2.7 Summary 22

CHAPTER-3 ACOUSTIC SENSOR BASED PD SOURCE LOCALIZATION IN POWER TRANSFORMER USING BAT ALGORITHM ……... 24

3.1 Introduction....24
3.2 Acoustic Emission Localization Concept and Its Mathematical Model....25
3.3 Implementation of Bat Algorithm for AE PD source Localization....27
3.3.1 Bat algorithm....28
3.3.2 Bat motion....28
3.3.3 Loudness and Pulse emission rate....29
3.3.4 Pseudo code of Bat algorithm....30
3.4 Results and Discussion....32
3.4.1 Laboratory data case study....32
3.4.2 Field data case study....36
3.5 Summary....39

CHAPTER-4 LOCATION OF PD SOURCE UTILIZING ACOUSTIC SIGNALS IN POWER TRANSFORMER BY FUZZY ADAPTIVE PARTICLE SWARM OPTIMIZATION…….....40

4.1 Introduction....40
4.2 Formulation of PD Source Localization Problem....40
4.2.1 Objective function....41
4.3 Proposed method....41
4.4 Formulation of Fuzzy System....47
4.5 Fuzzy Adaptive PSO Formulation....48
4.6 Results and Discussion....48
4.6.1 Case study of Field data....49
4.6.2 Case study of Laboratory data....53
4.7 Summary....55

CHAPTER-5 DETECTION AND LOCALIZATION OF PD SOURCE USING LOG PERIODIC DIPOLE ARRAY PRINTED UHF SENSORS…… 56

5.1 Introduction....56
5.2 Basic Principles for LPDA Antenna Design....56
5.3 LPDA Antenna Structure and Design....59
5.4 Parametric Study and Analysis....62
5.4.1 Variation of Feed Line width....62

5.4.2 Variation of distance between dipole elements 63
5.4.3 Variation of Length Ly_1 and Ly_2 63
5.4.4 Variation of Length Ly_5 64
5.5 Measured Results and Discussion.....65
5.6 Partial Discharge Experiment and Results.....69
5.7 Localization of PD source using Narrow band LPDA UHF Sensors 75
5.7.1 Particle Swarm Optimization Algorithm……..78
5.8 Localization of PD source using Broad band LPDA UHF Sensors.....81
5.9 Summary.....82

CHAPTER-6 Conclusions and Future Scope.....84
6.1 Conclusions.....84
6.2 Future Scope of work.....86

REFERENCES.....87

List of Publications 94

Appendix…….....95

LIST OF FIGURES

Figure Title **Page. No**

Figure 1.1 Root causes of insulation degradation in any HV power apparatus due to PD sources 2
Figure 1.2 Different types of maintenance strategies followed by the industries....2
Figure 1.3 Detailed plan of research work....5
Figure 1.4 Organization of the thesis....7
Figure 2.1 Distinct forms of PD (a) corona discharge (b) surface discharge (c) internal discharge (d) treeing phenomena....9
Figure 2.2 Physical effects of PD and its monitoring methods.... 10
Figure 2.3 Direct electrical PD measurement circuit for transformer 13
Figure 2.4 PD monitoring system for acoustic and UHF signal transmission path....15
Figure 3.1 Schematic visualizing the sensors placed on the transformer tank 26
Figure 3.2 Flow chart of bat algorithm for PD source localization in power transformer 31
Figure 3.3 Comparison of PD source location results among literature with proposed bat algorithm for trail 1 laboratory measurements 35
Figure 3.4 Comparison of PD source coordinates maximum deviation error among literature with proposed bat algorithm for trail 2 laboratory measurements 35
Figure 3.5 Comparison of PD source coordinates maximum deviation error among literature with proposed bat algorithm for trail 3 laboratory measurements 36
Figure 3.6 Comparison of PD source coordinates maximum deviation error among literature with proposed bat algorithm for field measurements 37
Figure 4.1 PD source and the sensors placement on the transformer tank 41
Figure 4.2 Representation of triangular membership functions for normalized fitness input....46
Figure 4.3 Representation of triangular membership functions for input inertia weight input 46
Figure 4.4 Representation of triangular membership functions for output change in inertia input 46
Figure 4.5 Fuzzy logic system with two inputs and one output of FAPSO-I method....47
Figure 4.6 Flow chart of FAPSO-I and FAPSO 50
Figure 4.7 Comparison of convergence characteristics of FAPSO-I and FAPSO methods for field measurements 51

Figure 4.8 Inertia weight adjustment of FAPSO-I method 52
Figure 5.1 Schematic diagram of a generalized LPDA antenna 57
Figure 5.2 (a) Top layer and (b) Bottom layer of the proposed LPDA UHF sensor 60
Figure 5.3 Simulated S11 of the initial LPDA UHF sensor 61
Figure 5.4 Simulated S11 for variation in feed width of the antenna 62
Figure 5.5 Simulated S11 for variation in d_4 of the antenna 63
Figure 5.6 Simulated S11 for variation in L_{y1} of the antenna 64
Figure 5.7 Simulated S11 for variation in L_{y2} of the antenna 64
Figure 5.8 Simulated S11 for variation in L_{y5} of the antenna 65
Figure 5.9 Top and bottom side of the fabricated LPDA antenna prototype (inset picture shows feed position) 65
Figure 5.10 Simulated and measured S11 of the antenna 66
Figure 5.11 Simulated and measured radiation patterns for the fabricated antenna (a) 0.7GHz (b) 1GHz (c) 1.5GHz (d) 2 GHz (e) 2.2GHz 67
Figure 5.12 Simulated and measured realized gain of the proposed LPDA antenna 68
Figure 5.13 Effective Height of the proposed LPDA antenna 69
Figure 5.14 (a) Block diagram of the PD test system using oscilloscope (b) PD test cells (Particle movement, corona, free metal particles and surface discharge) (c) PD experimental set up for antenna in lab using spectrum analyzer 72
Figure 5.15 Particle movement defect at an inception voltage of 7.6 kV in transformer oil (a) Time domain (b) Normalized FFT of the UHF signal 72
Figure 5.16 Corona defect at an inception voltage of 8.7 kV in transformer oil (a) Time domain (b) Normalized FFT of the UHF signal 73
Figure 5.17 Free metal particles defect at an inception voltage of 10.6 kV in transformer oil (a) Time domain (b) Normalized FFT of the UHF signal 74
Figure 5.18 Surface defect at an inception voltage of 11.8 kV in transformer oil (a) Time domain (b) Normalized FFT of the UHF signal 75
Figure 5.19 Localization of PD source of equal positions using narrow band UHF sensors 77
Figure 5.20 TDOA measurements of the four narrow band UHF sensors from the PD source at 14.5 kV 77
Figure 5.21 Localization of PD source of unequal positions using narrow band UHF Sensors 78
Figure 5.22 Flow chart of proposed PSO algorithm for PD source localization 80
Figure 5.23 Localization of PD source for experimental set up using broad band UHF

Sensors 81

LIST OF TABLES

Table Title **Page. No**

Table 3.1 Parameters of particle swarm optimization algorithm 29

Table 3.2 Parameters of bat algorithm 30

Table 3.3 PD Source Location Error results and comparison among different algorithms for laboratory data case study 33

Table 3.4 Maximum deviation error and relative error results comparison among different algorithms for laboratory data case study……..34

Table 3.5 Comparison of PD Source Location results among available literature with proposed method.....36

Table 3.6 Comparison of Location and Maximum Deviation error results among available literature with proposed method 37

Table 3.7 Comparison of PD Location results (4 sensors) among available literature with proposed method 38

Table 3.8 Comparison of error analysis (4 sensors) results among available literature with proposed method 38

Table 4.1 Simple IF –THEN rules of FAPSO-I 43

Table 4.2 Rules of FAPSO.....45

Table 4.3 Comparison of field PD Location results with proposed methods and different methods in available literature 50

Table 4.4 Comparison of field data Error analysis of different methods in literature with proposed methods 51

Table 4.5 Comparison of Laboratory PD source location results among available literature with proposed methods 52

Table 4.6 Error Analysis Comparison of Laboratory PD source among available literature with proposed methods. 54

Table 5.1 Dimensions of the designed antenna structure in millimeters 62

Table 5.2 Performance comparison of designed antenna with other reported antennas in the literature 70

Table 5.3 PSO Algorithm Parameters …….79

Table 5.4 Narrow band LPDA UHF sensor co-ordinates 80

Table 5.5 PD source location results using Narrow band LPDA UHF sensors.....81

Table 5.6 Broad band LPDA UHF sensor co-ordinates 82

Table 5.7 PD source location results using broad band LPDA UHF sensors 82

LIST OF ABBREVIATIONS

AE	Acoustic Emission
AF	Antenna Factor
ASA	Archimedes Spiral Antenna
ATM	Absolute Time Method
BA	Bat Algorithm
CBM	Condition Based Maintenance
CST	Computer Simulation Technology
DOM	Degree of Membership
DSO	Digital Storage Oscilloscope
EM	Electro Magnetic
FAPSO	Fuzzy Adaptive Particle Swarm Optimization
FBW	Fractional Bandwidth
FFT	Fast Fourier Transform
GA	Genetic Algorithm
GIS	Gas Insulated Substation
GPS	Global Position System
HFSS	High Frequency Structure Simulator
HV	High Voltage
ICA	Independent Component Analysis
IEC	International Electro-technical Commission
LPDA	Log Periodic Dipole Array
LPSO	Linear Particle Swarm Optimization
LS	Least square
LSE	Linear System of Equations
LV	Low Voltage

MDO	Mixed Domain Oscilloscope
MMA	Metal Mountable Antenna
NFV	Normalized Fitness Value
NL	Negative Large
NM	Negative Medium
NS	Negative Small
OEFS	Optical Electric Field Sensor
PD	Partial Discharge
PL	Positive Large
PM	Positive Medium
PS	Positive small
PSO	Particle Swarm Optimization
PTM	Pseudo Time Method
QGA	Quadratic Genetic Algorithm
RF	Radio Frequency
RL	Return Loss
RPLPDA	Reconfigurable Printed Log Periodic Dipole Array
SA	Simulated Annealing
SQP-GA	Sequential Quadratic Programming-Genetic Algorithm
TDOA	Time Difference of Arrival
UHF	Ultra High Frequency
VHF	Very High Frequency
VSWR	Voltage Standing Wave Ratio
Z	Zero

LIST OF SYMBOLS

X	X-axis coordinate of PD source and sensors
Y	Y-axis coordinate of PD source and sensors
Z	Z-axis coordinate of PD source and sensors
S1	Position of AE sensor numbered one
Tp	Unknown propagation time
Tn1	Time difference of n^{th} sensor to the first sensor
Va	Acoustic wave velocity in transformer oil
A	Loudness of bats
Q	Wavelength of bats
U	Velocity of bats
X	Position of bats
ζ	Cooling constant
β	Random vector in uniform distribution (0,1)
γ	Cooling constant
r	Pulse emission rate of bats
C1, C2	Social learning parameters of swarm particles
w	Inertia weight of swarm particles
V	Velocity of swarm particles
P_{best}	Local best solution of swarm particles
g_{best}	Global best solution of swarm particles
$rand_1$& $rand_2$	Random numbers
ΔW	Change in inertia weight
f_{gbest}	Global best fitness value
$f_{gbestold}$	Old Global best fitness value
λ_o	Wavelength at centre frequency

L	Light velocity
T	Scaling factor of the Log Periodic Dipole Array Antenna
Σ	Spacing factor of the Log Periodic Dipole Array Antenna
A	Angle of the Log Periodic Dipole Array Antenna
L	Length of the Log Periodic Dipole Array Antenna
N	Number of dipole elements in Log Periodic Dipole Array Antenna
B_s	Structure bandwidth of the Log Periodic Dipole Array Antenna
B_{ar}	Active region bandwidth of the Log Periodic Dipole Array Antenna
D	Directivity of the Log Periodic Dipole Array Antenna
B_{WE}	Half power beam width in E-Plane
B_{WH}	Half power beam width in H-Plane
D	Distance between the dipole elements of the LPDA antenna
W	Feed width of the LPDA antenna
H	Height of the LPDA antenna
S11	Return loss of the LPDA antenna
GHz	Giga hertz
dB	Decibels
dBm	Power ratio in decibels of measured power referenced to 1mW
cm	Centimetre
mm	Millimetre
MHz	Megahertz
kHz	Kilohertz
kV	Kilovolts
mV	Millivolts
µs	Microseconds
Pstd	Standard antenna
P_{AUT}	Prototype test antenna
G_{AUT}	Gain of the prototype test antenna
G_{Pstd}	Gain of the standard antenna

CHAPTER 1
INTRODUCTION

1.1 Overview

A significant difficulty in the operation of any high voltage power apparatus is the accurate and effective process, which in low cost are utmost capital savings and prevailing over technical requirements. In addition, the principal expenditure demanded for an apparatus often recommends safeguarding with reasonable restoration. As a result, the depreciation of operational expenses bears unplanned downtimes, redundant maintenance and limitations of process capabilities have emerged as significant objective of any industry. Thus, the diagnosis and detection of partial discharges (PD) in power transformer is of great feasible relevance. With the precise monitoring and detection of partial discharges in the power transformer, prior warning symptoms can be obtained for better safety, preventive maintenance and enhanced reliability. PD's can give rise to economic and production losses, even human casualties and equipment shut down. Hence early, fast and proper monitoring and detection of PD's is requisite in hindering substantial damage to the system and acknowledge enough timely measures to safeguard the high voltage power apparatus.

The transformers may experience distinct insulation breakdown problems throughout their entire lifetime [1]. Owing to above, an inaccurate transformer functioning consistently accompanies failures and in the end gives rise to production curtailments. In connection to this, PD sources may be either internal or external. These PD sources are generated due to chemical, electrical, mechanical and thermal stresses. The insulation material deterioration in any high voltage power apparatus is affected by synergetic connections of the above stresses originated by PD sources. Figure1.1 shows the root causes of insulation degradation in any high voltage power apparatus caused by PD sources.

Basically industrialists follow three forms of maintenance strategies i.e. corrective maintenance, time-based maintenance and condition-based maintenance. Figure 1.2 elucidates the merits and demerits of the maintenance strategies. Now a day, industrialists have arrived common interest towards the benefit of prognosis approaches in condition-based maintenance (CBM). These approaches depend on the knowledge assigned by condition monitoring and PD detection systems i.e. check out system changes persistently. This type of identification

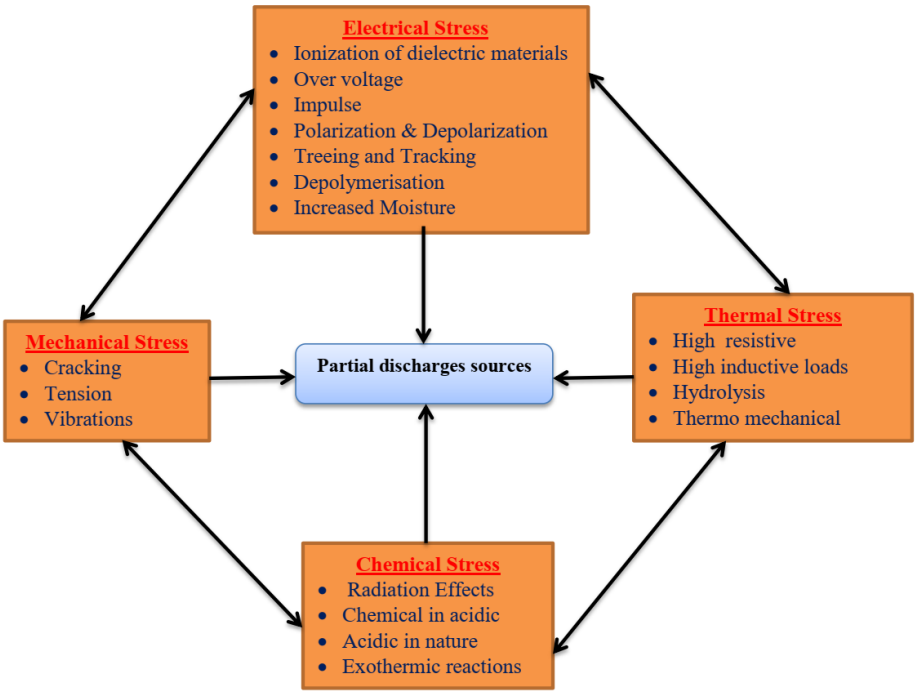

Figure 1.1 Root causes of insulation degradation in any HV power apparatus due to PD sources

techniques must be reliable and potent for PD sources which necessitates non–invasive and able to monitor any type of PD sources in the prior steps. A substantial amount of research has been steered in relation to condition monitoring of power transformers adopting non-invasive monitoring techniques.

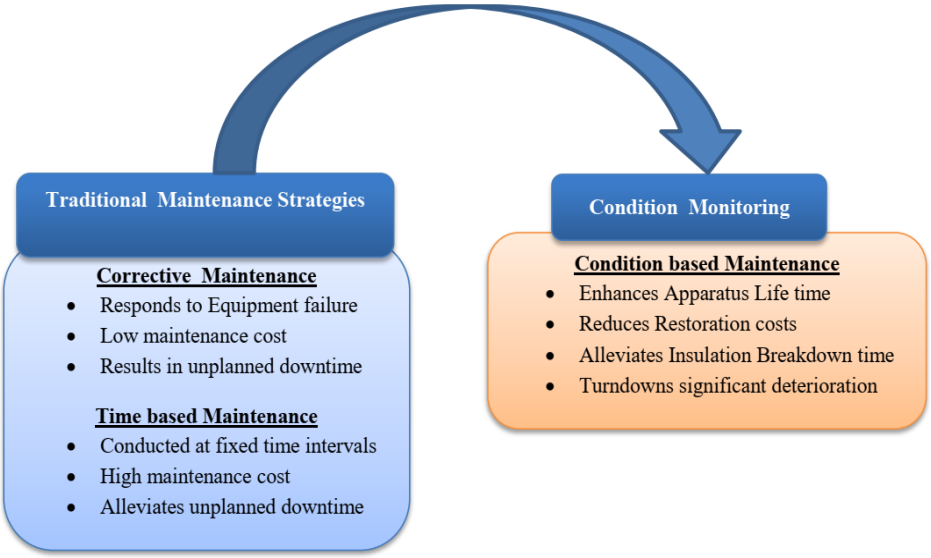

Figure 1.2 Different types of maintenance strategies followed by the industries

The primary goal of PD source identification and monitoring techniques is to attain a raw signal from the incipient discharges. Predominantly, the development of identification and monitoring techniques for PD sources requires a time taking process to detect the sign warnings to be monitored, impart the proper signals for identification of particular PD symptoms and then specify the accurate computational method to process the signals. In fact, in the reported literature, there is not yet any overall algorithm for PD source identification and monitoring system that may surpass the parametric and model uncertainty. As a consequence, researchers have recommended variety of identification and monitoring systems with parameter settings that are elaborated precisely to the system under consideration. As per the survey reports, PD source identification methods are classified into two types i.e. model based and model free approaches.

Model Based Approach takes the help of apparatus model because the concept is to determine such parameters from the models that demonstrate mismatch between healthy and PD condition. In the case of model based approach, exact models of the system are basically demanded to bring out a robust PD monitoring. Normally, the more exact the model, the more stable based PD monitoring process will be i.e. the inputs and outputs of the system make use of the mathematical models. Several methods depend on the idea of logical redundancy rather than actual redundancy. The basic concept in the model based PD source diagnosis technique is to utilize the virtue of the given model process and reproduce remaining PD sources information. In the PD source identification technique, obviously model quality plays the key role.

The model based approach can be classified into three types based on their reasoning i.e. knowledge based models, data based models and analytical based models. Knowledge based models depend on natural knowledge of PD sources like human mind of system [2- 5]. Data based models are employed when the system model is not identified in the analytical instruction and inexperienced system working knowledge on PD sources. Moreover, complex and resolved systems and the development of physical standard models on good precision mathematical models may transform to very troublesome, time taking and even unsolvable sometimes. In general, attaining exact parameter values for the given model turns to be endless task. Analytical models are fixed on the well-known physical interface with the monitoring apparatus and it can be implemented using parameter estimation, observers and parity equations.

The model free approaches can be evaluated using signal processing and monitoring. These approaches utilize desired sensor signals at the beginning juncture. In the second step, it deduces the proper data with the help of signal processing techniques like Fourier transforms, wavelets etc. The PD source is identified and detected based on the derived information in the second step. The condition monitoring is acknowledged as the heart in the final step of this approach. The merit of the model free methods easily excludes parameter mismatches in between the actual and theoretical models.

1.2 Motivation

The partial discharge source localization using non-invasive monitoring techniques are widely utilized by many transformer manufacturers and power utility engineers in routine and critical situation for optimal operation of the electrical power system as well as further risk assessment and restoration scheduling. The PD detection is not just enough to take solution, but also identification of PD source is essential to restore the apparatus condition. In general, the PD source is located geometrically by means of time measurements from respective sensors to the PD source. Many researchers have proposed several heuristic algorithms for solving the PD source localization problem in the literature. Moreover, an effective metaheuristic algorithm is required to attain a global optimal value. The subsequent research gaps have been pinpointed as motivation of the dissertation.

- Majority of literature proposes conventional methods and single parameter tuned optimization algorithms and very few proposed metaheuristic algorithms for PD source localization using noninvasive monitoring techniques.
- Need an effective metaheuristic algorithm that can work for both field and laboratory data for PD source localization using noninvasive monitoring techniques.
- Most of the researchers designed limited bandwidth i.e. narrowband & multiband UHF sensors and very few designed broad band UHF sensors for PD measurements.
- Most of researchers in the literature not yet calibrate the designed UHF sensor sensitivity and very few researchers have mentioned the sensitivity of designed UHF sensor.
- Many researchers designed UHF sensor with higher dimensions and not followed the basic standards in the design and measurements.
- Still today there is no standard method for the calculation of TDOA in the literature.

- Still research is going on various aspects for the localization of PD source using Non-Invasive Monitoring Techniques.

1.3 Research Contributions

From the gaps observed in the literature stated above the following objectives are considered in this thesis.

- Development of a Heuristic Algorithm for PD source localization using the field data available in literature utilizing acoustic sensors.
- Development of Fuzzy Adaptive particle swarm optimization method on existing available field & laboratory data in the literature for PD source localization in power transformer utilizing acoustic sensors.
- Demonstration of PD source localization using narrow band tailor made UHF sensors.
- Development of broad band Log Periodic Planar Dipole UHF Array Sensor using ANSYS HFSS Software for detection of various types of partial discharges.
- Demonstration of PD source localization using broad band Log Periodic Planar Dipole UHF Array Sensors.

To execute the above objectives, in this thesis metaheuristic algorithms and integration of metaheuristic algorithm with fuzzy logic system are developed for non-invasive PD monitoring methods which can enhance effectiveness and system's reliability in the direction of detection and localization of PD source in Power transformer. Figure 1.3 delineates the detailed plan of research work introduced in this thesis.

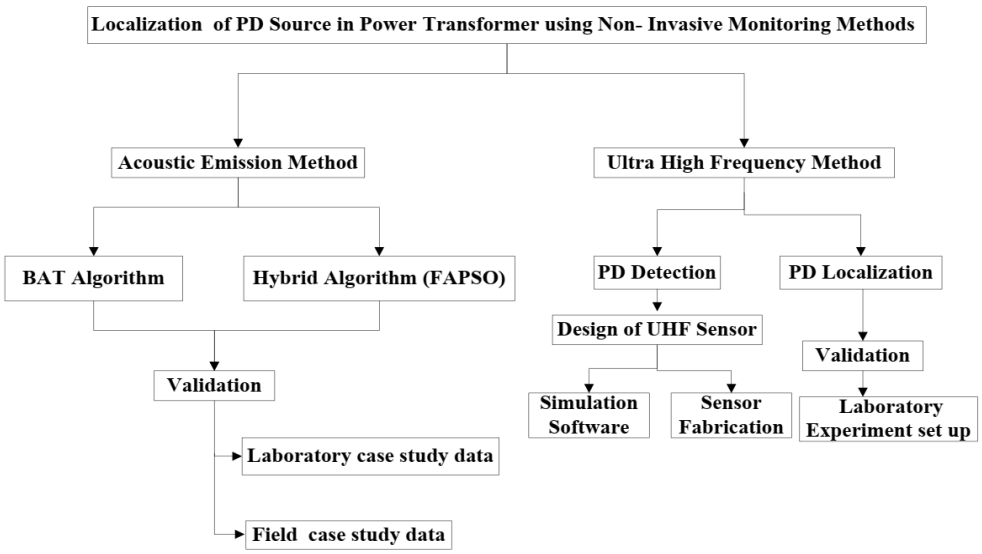

Figure 1.3 Detailed plan of research work

1.4 Organization of the Thesis

The above research work is organized in six chapters in the dissertation and is provided as follows

The first chapter provides the overview, key issues motivated to carry out the research objectives and brief summary of the present research work and organization of the thesis.

The second chapter provides a relevant literature review which is performed on PD source localization in power transformer using Noninvasive monitoring techniques. Concepts of PD and manifestation of physical effects leading to PD. Further different non –invasive PD measurement approaches are explained in depth.

The third chapter presents Acoustic sensor-based PD source localization in power transformer using Bat Algorithm. In this chapter Bat algorithm is proposed for the localization of PD source in power transformer. To validate the efficacy of the algorithm statistical measures have been utilized. From the PD source location results, it is revealed that Bat algorithm converges in less time when compared to other existing algorithms in the literature.

The fourth chapter reports fuzzy adaptive particle swarm optimization (FAPSO) algorithm for localization of PD source utilizing acoustic time measurements. In this method, the inertia weight is effectively regulated by simple IF THEN fuzzy rules to improve the global optimal solution and improves the accuracy in estimating the PD source location.

The fifth chapter addresses the designing of broadband log periodic dipole array (LPDA) UHF sensor and its key issues feasibility in the detection of different PD sources occurrences in the power transformer. The details of various high end devices along with the different designed artificial PD sources for this research work are elaborated. Both narrow band and broad band type LPDA UHF sensors have been validated by conducting an experimental set up for localization of PD source individually. These two types of LPDA UHF sensors detected the partial discharges effectively in their range of applicability. The particle swarm optimization algorithm is utilized for the localization of PD source with these narrow and broad band LPDA UHF sensors.

At last, sixth chapter emphasizes the key resolutions of the dissertation and also the possibility of additional research scope in this field is explored further.

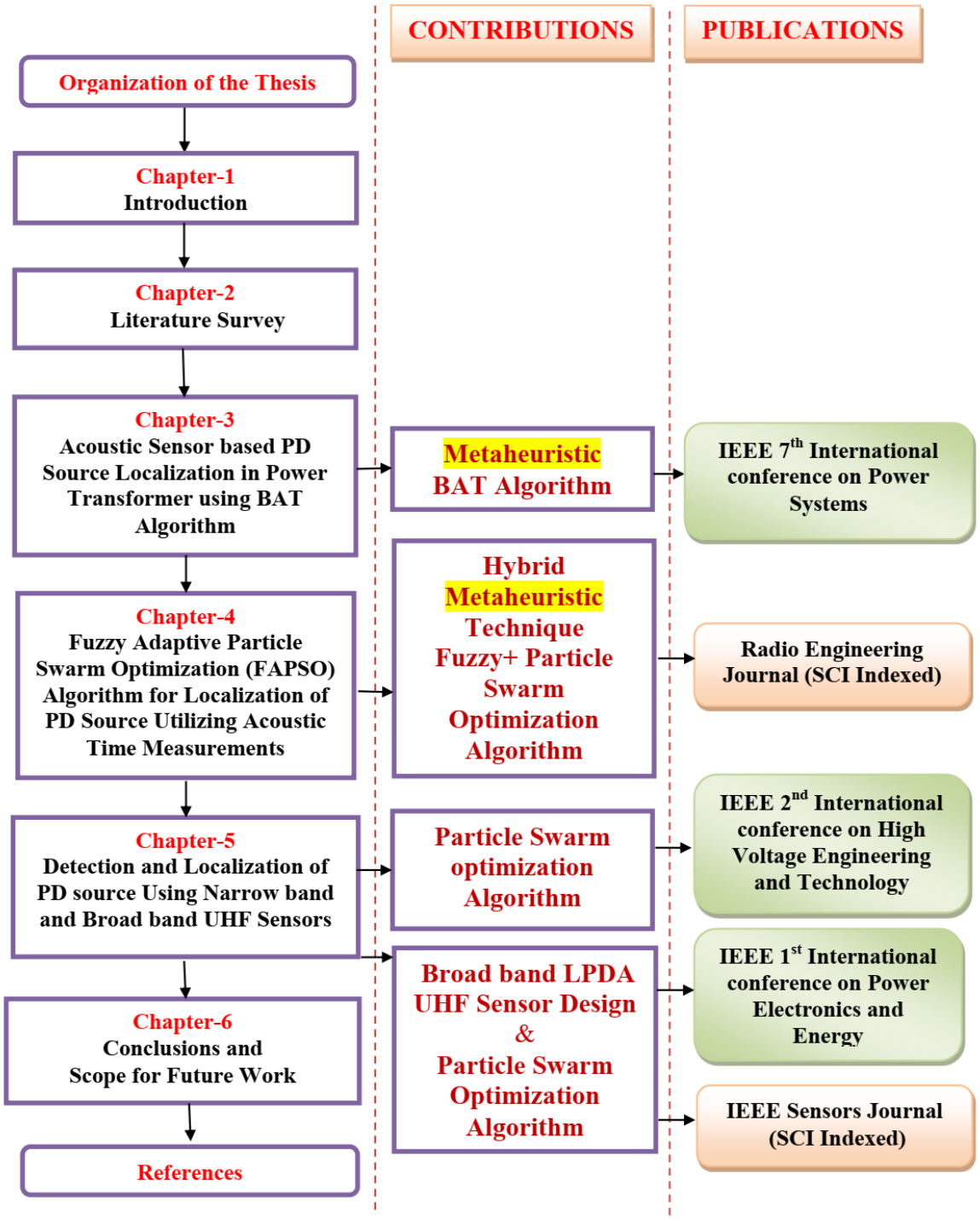

Figure 1.4 Organization of the thesis

CHAPTER 2

LITERATURE REVIEW

2.1 Introduction

Partial discharges are the local electrical stress concentrations in the imperfections of the insulation material and causes very short duration currents pulses which can be electrically monitored and measured. Owing to happening of incipient discharges, the PD sources evolve in various forms that distributes to surrounding medium and also impart differently on insulation media. These electrical discharges can be assessed for condition monitoring of high voltage power apparatus by employing desired monitoring techniques.

2.2 PD and Its Mechanism

The mechanism of PD originates in gas or liquid dielectrics, when an atom hit by free electron which is stimulated to the surrounding field. But the term partial discharge can be used to distinguish the real breakdown occurrence that causes both the streamer and Townsend type PD pulses. Townsend discharge gives rise to the effect of positive ions at the cathode, electron emission exists and the released electrons generate ionization for build-up gap current. The processes of Townsend ionization is mostly direct ionization process and the discharge exists within a fixed short gap on the cathode emission of continuing discharges. The rise time of these partial discharges is in very short duration of nanoseconds [6, 7]. The streamer discharge exists for the longer gaps and causes ionization which spreads to high field regions only. It is important that streamer is chaotic in make out that it may be false with the exact mechanism of streamer breakdown where the breakdown mechanism is regulated by photoionization in gas volume of longer gaps. In general, partial discharges are classified into four types based on the various mechanisms as shown in the Figure 2.1.

A. Corona Discharges

This type of discharge occurs in the gaseous medium either in uniform or non-uniform electric fields electrode configurations.

B. Surface Discharges

This type of discharge occurs if there exists a stress component parallel to dielectric medium. In general, these discharges occur in the transformer's bushings, cable ends and overhanging of generator windings.

C. Internal Discharges

When cavities or voids are occurred in liquid / solid dielectric mediums, these discharges occurs due to overstress in the insulation medium i.e. when the electric stress exceeds the insulation breakdown strength then incipient discharges occurs.

D. Treeing Phenomenon

The continuous impact of partial discharges in solid dielectrics forms as treeing channel.

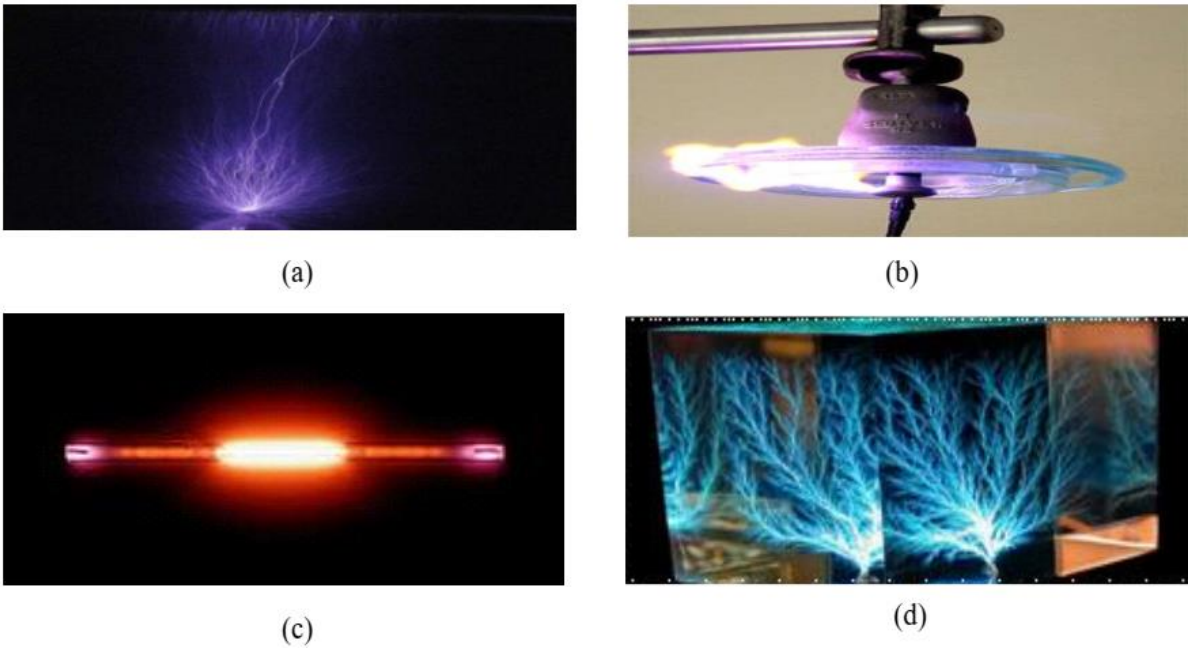

Figure 2.1 Distinct forms of PD (a) Corona discharge (b) Surface Discharge (c) Internal discharge (d) Treeing Phenomena

2.3 PD Monitoring Techniques

Partial discharges are the extreme dangerous process in any high voltage power equipment which deteriorates the equipment life with the damage of insulation. Thus, it is necessary to detect the partial discharges for extending the apparatus lifetime which avails to make undamaged to the whole apparatus. Thus, the continual monitoring necessitates for regular

condition based maintenance (CBM) of any HV power apparatus in order to minimize the revenue losses, power supply interruptions and unexpected failures. In general, PD monitoring techniques are of two kinds i.e. Invasive and Non- Invasive. The Invasive is the direct way of monitoring usually electric method i.e. conventional method. The Non-Invasive is an indirect way of monitoring PD's. The PD's gives rise to manifestation of distinct measurable signals in terms of acoustic, UHF and sometimes optical [8] comes under non-invasive monitoring techniques as shown in the Figure 2.2.

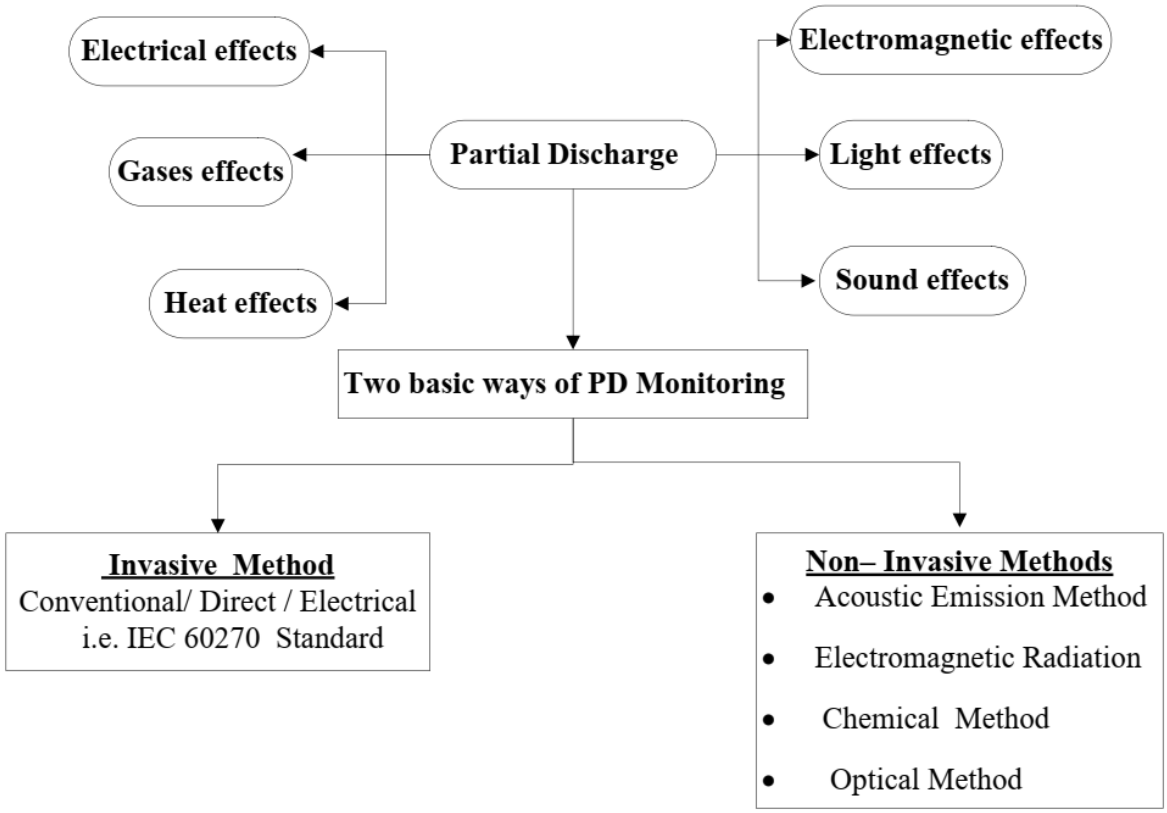

Figure 2.2 Physical effects of PD and its monitoring methods

The reliability of the electrical grid relies on the availability and quality of high voltage power apparatus like power transformer. The internal insulation damages [9, 10] may cause to catastrophic breakdowns and give rise to high outage and penalty costs. To minimize such dangers, it is routine for power transformers to have passed a set of factory tests together with partial discharge (PD) activity before acceptance and commissioning. The acoustic and ultra high frequency (UHF) PD measurement methods are employing either individually or in the combination with the electric method according to IEC 60270 [11,15].

The PD measurements gained popular and accepted test for any high voltage power apparatus insulation system according to IEC 60270 standard. Now- a- days there is a growing challenge to assess the PD measurements for installed apparatus in service being powerful monitoring tool. The conventional or invasive methods have some limitations and demerits if executed online and onsite conditions [12, 13]. Normally two things are required as for PD its intensity level and position. Possessing knowledge on PD origin is crucial to evaluate e.g. the hazard capacity of the defect [14]. It is of vast significance to understand about the PD origin for scheduling and commissioning repair/ maintenance measures results in time and cost systematically.

According to IEC 60270, the direct electrical PD measurement setup typically has sensitivity constraints for online /onsite measurements as a consequence of field noise levels. The three phases being coupled in a transformer, only one partial discharge pulse in one particular phase can also be measured as cross coupling signals in all phases. The analysis of multi terminal PD measurements acknowledges a procedure to visibly discriminate multiple PD sources and get rid of external disturbances.

The ultra-high frequency PD measuring method is based on the reality that the incipient discharges under oil are relatively short duration electrical pulses and emits electro- magnetic waves in the UHF range of 300-3000MHz. The electromagnetic waves are sensitively detected inside the transformer tank since the propagation of these waves attenuates moderately. The UHF probes can be placed through the oil valve into the transformer during full energization.

When acoustic or UHF PD measurements confirm PD activity, a three-dimensional PD source localization is the following step for hazard assessment of PD activity. The time measurements corresponding to particular PD event and three space co-ordinates, the number of unknowns requires four sensors for time difference of arrival (TDOA) measurements and location. The UHF method has this possibility however it limits the sensor number to three or less. Since there is a greater number of piezo-electric acoustic sensors that can be fixed on transformer tank. However, acoustic sensors are generally more attenuated to external disturbances rather than internal PD generated sound waves.

The merits of the noninvasive PD measurement procedures[16-18] are their broad immunity over external noise signal disturbances onsite and these sensors do not require electrical connection to high voltage circuit and the fundamental feasibility of determining three

dimensional PD defect location utilizing these signal arrival time measurements. The UHF method renders very low noise levels

PD measurements may help in understanding the insulation damage that has occurred or not in any high voltage power apparatus, but they cannot estimate the PD source location itself. The specific amplitudes of PD may be allowed in particular locations, but their existence can be adverse at some locations in power transformer. The PD source location diagnosis in power transformer guides to effective evaluation of PD measurements results and beneficial for restoring a damaged transformer. Moreover, it is informative for developing the better design of the transformer. The main aim of locating PD inside the transformer or entire substation is more difficult because it is three dimensional. The PD source is located in 3D space by minimum of four sensors time difference of arrival measurements. Additional difficulty may include when the line of sight path from the PD source to the respective sensors can obstruct by materials inside the monitoring region and determining paths to enhance this issue rests a focused area of research.

2.3.1. Direct or Invasive Technique (According to IEC 60270 Standard i.e. Electrical Method)

According to IEC 60270 standards, [19] the PD is defined as a localized electrical discharge that only partially bridges the insulation between conductors and which can or cannot occur adjacent to a conductor. The observed beginning voltage at which PD initiated when the voltage is gradually increased from a lower level at which no PD is developed from the test object is known as inception voltage. The voltage at which PD come to end when the voltage is gradually decreased from a higher level at which PD is observed is termed as extinction voltage. In general inception voltage is greater than the extinction voltage.

The electrical location methods are established on the measured time resolved PD signals analysis at the transformer terminals [20]. The PD current pulse shape is highly dependent on the respective dielectrics medium like oil, paper, gas etc. In [21] illustrated the sensitivity limitations of UHF method for PD source location in power transformers.

The main limitation of electrical method is it’s prone to noise.

- It is an Invasive method, requires measuring device for every PD source is to connect with the test system.

- Difficult in installation, as it requires extending power supply.
- Requisite of more electrical equipment arrangements are required like voltage source of PD free & blocking capacitor.
- Faraday cage shielding is needed for prevention of external noise disturbances.
- It is tough to detect localization of PD sources.

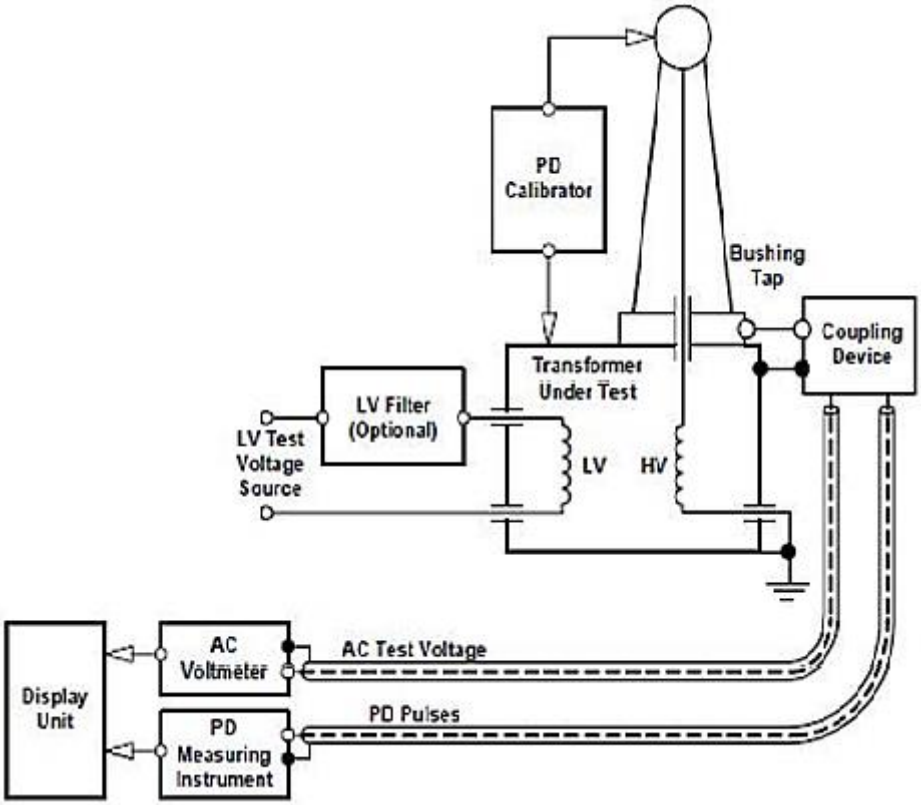

Figure 2.3 Direct electrical PD measurement circuit for transformer

2.2.2. Indirect or Non-Invasive Technique (Acoustic Emission Detection)

This technique is arousing substitute for online detection of partial discharge in power transformers. With the happening of partial discharge, the current streamer is established in the void, the medium around the hot streamer is vaporized and the acoustic waves are produced. The streamer induces a discharge of mechanical energy, which then spreads through the high voltage power apparatus surface in the shape of pressure field [22]. The PD defect acts as primary source of acoustic wave's propagation around the medium in spherical form [23]. During the propagation, the wave endures from absorption and dispersion caused by effects of insulation material. The waves at the boundary surface of the liquid and gas insulation medium endures from destructive and constructive interference due to the acoustic impedance of the two dissimilar media.

In acoustic sensor based PD detection, the acoustic waves are sensed by sensors from the PD source in the frequency range of 30 – 300 kHz. These acoustic sensors are fixed on the surface of the transformer tank which captures the mechanical pressure waves and converts into electrical PD signals which could be acquired by appropriate data acquisition and processing system. These sensors can be placed in two different ways. The acoustic sensors which are fixed on the outside of the transformer wall come under external acoustic detection system and the acoustic sensors which are fixed inside the transformer tank comes under internal acoustic detection system. The limitations of acoustic sensor based detection system are

- The mechanical waves emitted from the acoustic sensors to the PD source do not form in spherical wave fronts owing to its complex nature and the non-homogeneity of power transformers structure.
- The perturbation by absorption and dispersion in the oil insulation and multiple reflections in the material of the transformer tank causes noise and reduced level of signal strength.
- The acoustic sensors require more sensitivity for PD detection owing to various attenuation processes.

2.2.3. Indirect or Non-Invasive Technique (Electromagnetic / Radio Frequency / UHF Detection)

The impulsive current of very small magnitude is produced in the ultra high frequency range if the PD is emitted in the weakness region of the insulation medium. The frequency spectra of the electromagnetic (EM) waves vary based upon the partial discharge source variation and the defects which are in and around the insulation medium. The different partial discharges have their own spectra fall in the frequency range of 300-3000MHz. This frequency range is termed as ultra high frequency range.

In this method, a suitable UHF sensor or antenna has to be placed around the high voltage power apparatus to capture the PD signals in the UHF range. The UHF detection system depends on properties of sensor type, source and insulation medium of EM wave propagation. The UHF sensor is connected to the measuring system to capture the PD signals. An amplifier can be connected to the UHF sensor and measuring system if the PD signals strength is too low. The noise is primarily arising from mobile phone or television in the

UHF range. The PD signals can be evaluated by using various advanced signal processing techniques and methods.

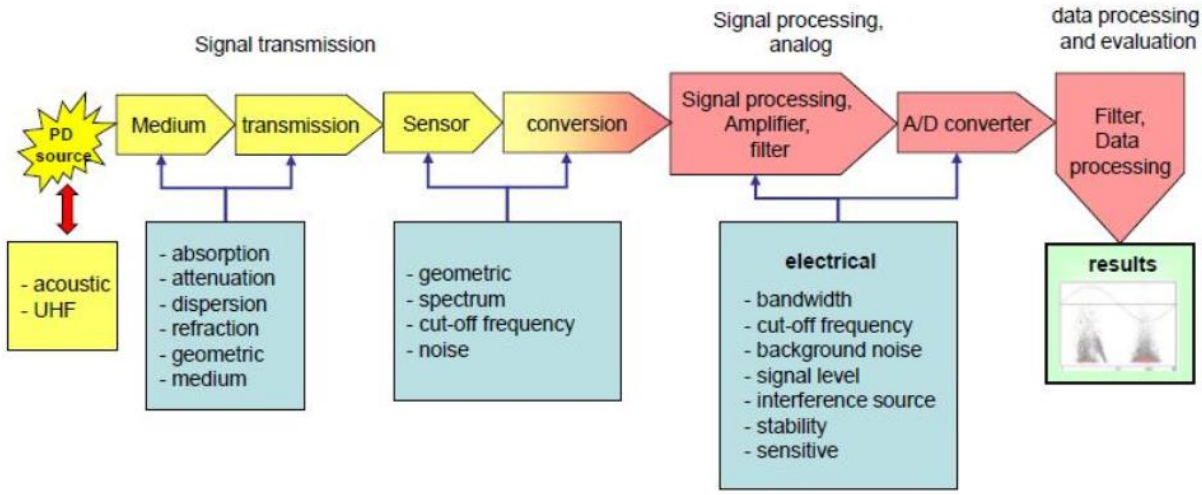

Figure 2.4 PD monitoring system for acoustic and UHF signal transmission path

2.4 Importance of UHF PD Detection Method

Among various online PD detection methods demonstrated, UHF PD detection method is popularly gained currently by many researchers all over the world. This UHF method is promoted owing to certain merits compared to other detection methods. Most of the reported works in the literature performed by researchers to build the PD detection system more precise, transparent and well-built till the date. The advantages of the UHF method are

- The UHF signals have more Signal to noise ratio and immunity over external noise disturbances.
- The UHF signals travels as the velocity of the light i.e.; $3*10^8$ m/sec.
- This method is powerful and performed both in online and offline modes of operation.
- The multi-source location with minimum number of sensors is possible.
- The dangerous harms connected with detection system are ignored because it is a non-invasive method unlike direct electrical method.
- This method can employ in hard physical conditions.

2.5 Challenges of UHF PD detection

1. *Drawbacks with digitization:* The raw analog signals detected by UHF sensors is further pre-processed by data acquisition system in which the data is stored and the captured signals are visualized in digitized form through high speed digital storage oscilloscope (DSO). This digitization needs high sampling rate for further signal processing analysis.

2. *Sensor/Antenna Parameters*: The UHF detection method typically depends on design, structure and antenna parameters. The parameters of an antenna that influence the measurement are return loss, bandwidth, radiation pattern, gain, directivity and input impedance. Based on these parameters different types of antennas have been developed in the literature like Archimedean spiral, log spiral, planar spiral, conical, monopole, micro strip patch and log periodic antennas. Several researchers still making their effort in the antenna structure and ease of its handling the detection for cheaper.

3. *Detection and Location of PD source*: The occurrence of PD is an arbitrary mechanism, its signal level and form vary every time. Several researchers have presented their ideas for detection of PD sources with precise results, efficacy utilizing few apparatus and small effort. After the identification of PD, locating the PD source is also important and many were used TDOA (Time Difference of Arrival) method for three dimensional localization of PD source.

2.6 Literature Survey on PD Source Localization in Power Transformer

2.6.1 PD Source Localization in Power Transformer Using Acoustic Sensors

This acoustic method has several merits over direct electrical method because they are non-contact, non-interference prone and ease of installation. The Time Difference of Arrival (TDOA) method is popularly gained for accurate localization of PD source [24]. In the present work, the above method makes use of arrival time differences of AE signals with respect to reference sensor to other sensors there by PD source is determined. However, several conventional PD localization methods have been found in literature.

In [25], M. Kozako et al carried out the basic study on PD induced acoustic wave propagation in simulated transformer composite insulation system. Xie.Q et al made a comparison of three distinct types of acoustic arrays i.e. cross, circular and square shaped for PD detection and finally concluded that circular array shaped is the best for detection of AE signals [26]. Al-Marsi et al proposed an algorithm for bias fault (ageing of oil) AE PD detection [27].

E.Mohammadi et al implemented the PD localization and classification using AE sensors in power transformer [28]. A.Hekmati et al demonstrated the optimum placement of AE sensors for distinct PD origins in the tank of the transformer [29]. Majority of the reported works in the literature have considered line of sight path from PD source to AE sensor in the transformer and velocity of sound in oil as acoustic wave velocity [30, 31].

Lu et al. proposed pattern recognition method to acoustic PD source localization in an oil filled transformer and in the simulation, the transformer tank is partitioned into a number of sub -modules, the PD site is located by finding the small spatial distance between the two pattern vectors of each sub-module's i.e. standard pattern vector and its undetermined pattern vector, and the location error is also more. Hence, this methodology is inappropriate for the on-line checking and field approaches owing to approximation scope [32]. M.M. Sacha et al. applied Global Position System (GPS) algorithm which utilizes pseudo time analysis for acoustic PD source localization and the demerit is sometimes it may produce complex solution [33, 34].

Veloso.et al. used the genetic algorithm for PD source localization and the source is accurately located after large number of iterations with more population size [35].The iterative least square method is always dependent upon the initial guess value, it takes more number of iterations and there is no guarantee of attaining a feasible PD location result. Hence, it also suffers from local premature problem. Kundu et al. reported a non-iterative algorithm for acoustic PD source localization and the drawback is, it also gives two sets of solutions like GPS algorithm but only one solution is within boundary, the location error is also more even though it has no convergence problem [36].

L. Tang et al. applied particle swarm optimization algorithm for PD source localization using AE sensors in the laboratory model [37]. T. Bozcar et al [38] used artificial neural network for recognition of PD defects in paper oil insulation damaged by aging action. G. S Punekar et al applied Newton iterative method and genetic algorithm for the localization of PD source adopting AE sensors [39, 40]. I. Buanuenz et al demonstrated how the instrument system helps the PD source localization in power transformer adopting AE sensors [41]. Liu. H. L et al. applied sequential quadratic programming-genetic algorithm for PD source location with more population size [42]. C. Boya et al applied blind signal separation approach for the identification of multiple PD sources using AE sensors [43]. Liu. H. L et al. employed quantum genetic algorithm for PD source location with more population and iterations [44].

S. Biswas et al utilized cross wavelet transform for the identification of distinct types of PD sources and ensemble binary support vector machine for the classification of PD sources. At least five acoustic sensors are required in order to get rid of plane of symmetry for multiple PD sources [45]. R. Ghosh et al developed source filter model for the extraction of PD pulse estimation from PD source to the respective sensors and cross correlation method is used for TDOA measurements and determined the PD source location without using any denoising method [46]. Y. B. Wang et al proposed particle swarm optimization route search algorithm for the localization of PD source on 35 kV and 110kV power transformer using AE sensors [47]. Y. B. Wang et al made a quantitative comparison on the PD source location results with other algorithms [48]. M. Schrammer et al described the blind estimation of microphone position on orthogonal geometrical projection using 2Dand 3D AE sensor arrays [49]. L. Zhou et al proposed differential evolution particle swarm optimization algorithm for PD source localization in the testing transformer using four AE sensors, two temperature sensors outside & twenty two sensors inside the transformer and compared the PD location results with GA, ICA algorithms [50].

2.6.2 PD source localization in Power Transformer using UHF Sensors

P.J. Moore et al. introduced the location of PD source by UHF method using TDOA signals [51]. Several researchers are employing shortest signal propagation path principle for locating PD source by UHF sensors TDOA signals till date. In the years 2005-2013, most of the researchers worked on different aspects like UHF Propagation, optimal placement of UHF sensors, arrival time recognition are carried out [52, 53, 54 & 62]. Judd et al. addressed the problems like installation, practicability, capabilities of UHF sensors to power transformer and explained the PD source location procedure to the prototype transformer model with 0.3m accuracy [53, 54]. In [53], the space grid search method was proposed to solve nonlinear TDOA equations to localize PD source but, it locates the PD source with more computational load and time. Z. Tang et al applied hyperboloid genetic algorithm for non-linear TDOA equations using diamond shape sensor array and cross correlation method was utilized for TDOA measurements to locate PD source but the approximate location range is more [55].

Localization of PD source by UHF method involves two key steps, i.e. acquiring TDOA measurements and solving the non-linear TDOA equations. Three methods to quantify the TDOA measurements are first peak method, cross correlation and cumulative energy method

adopted by UHF sensors in which utilized by many researchers in this field. Sinaga et al. compared all the above three methods to calculate TDOA measurements captured by four UHF monopole sensors array and concluded that first peak method yielded best accuracy when compared to other methods [56].

Shibuya et al. developed the analysis of electromagnetic waves generated by PD measurement using rectangular patch antenna considering with and without active part elements [57]. B. Sarkar et al developed a low cost RF sensor for the detection of PD source in high voltage apparatus [58].

Tang et.al proposed energy accumulative based TDOA measurements in which a window is added to TDOA signal waveform in order to reduce error from PD reflected waveform there by located the PD source [59]. Xu et al. applied Finite difference time domain (FDTD) approach to study the UHF PD signal propagation characteristics in simulated transformer model and the simulation results showed that PD signal has different electric field intensity [60].

Robles et al. investigated experimental study on zigzag, log periodic and two monopole antenna of 5cm &10cm for different frequency response to detect PD and concluded that 5cm monopole antenna is simple & low cost and gains 60% UHF radiated energy signal which proves best choice for effective PD measurements [61, 62].

C. Boya et al explained blind source separation algorithm for the separation of mixed time domain signals received by the UHF sensors in the PD source identification [63]. E. M. Amin et al used RF sensors as multi resonator passive circuit for the detection of PD sources [64]. S. Zheng et al used planar equiangular spiral antenna as UHF sensor for the location of PDs in the windings of the power transformer [65]. P.J Moore et al addressed the issues on detecting the PD's using radio frequency methods, as it provides improved sensitivity and vigorous anti interferences [66]. S. Tenbohlen et al used monopole antenna for detection of PD under noisy conditions [67]. S. Coenen et al illustrated the location of PD sources in power transformer using acoustic and UHF sensors [68]. H. R. Mirzaei et al explained the issues in the placement of UHF sensor on the power transformer tank and the propagation paths in the localization of the PD source [69]. H. R. Mirzaei et al applied the particle swarm optimization algorithm for the localization of PD source considering non line of sight effect [70]. F. Zeng et al applied semi definite relaxation approach for non-linear TDOA equations

using diamond shape sensor array to locate PD source but the approximate location range is more [71].

2.6.3 Different types of UHF Sensors used for Partial Discharge Measurements in Power Transformer

Partial Discharge (PD) is the dominant diagnostic quantity that manifests incipient discharges in the transformer. For any kind of PD antenna design, the effectiveness and ability of the antenna for monitoring the condition of the equipment is given by the effective antenna height which is the figure of merit for the sensor [73]. Though, the PD discharge frequency range is from 0.3 GHz to 3 GHz, however, the criticality in compactness of antenna design is due to lower frequency range requirement for PD i.e. from 0.3 GHz to 1 GHz.

The important sensors used in radio frequency (RF) method are broad band antennas. E. Al. Almazan et al. demonstrated an RF antenna working in the frequency range of 0.5 GHz to 2 GHz for detecting PDs and also for examination of transformer oil [74]. A. H. EI-Hag et al. [75], the performance of three different RF antennas i.e.; dipole, axial helix and circular loop are compared with the commercial acoustic sensor for detection of PD signals. Y. Hai-Feng et al developed multi band loop antenna which works at resonant frequencies in the UHF frequency range to detect the PD sources [76]. A. Akbari et al addressed the challenges associated with the UHF PD monitoring method [77].

A. M. Ishak et al. have designed Ultra high frequency (UHF) sensor using FDTD simulation tool is demonstrated and its performance is tested [80]. J. Lopez Roldan et al. made a comparison of various broadband antennas such as different shaped monopole, spiral, and loop antennas are used as UHF sensors for PD detection in power transformer [81]. C. Zachariades et al. designed a dual slot barrier sensor [82] for PD detection in gas insulated substation apparatus and working from 1 GHz to 2.6 GHz frequency range.

Several antennas are used for wideband performances such as bow tie antennas, Vivaldi antennas and Archimedean spiral antennas. W. U. Qiuuen et al. analyzed the performance of Archimedean antenna for different types of PD defects [83]. Bow tie antennas are non-planar structures whereas spiral and Vivaldi antennas are planar structure but all these antennas are not compact. The feeding is also very complex for these antennas as balun is required which further increases cost and complexity during the integration of other components of the system.

W. Li et al. have designed Fractals such as Hilbert, stacked Hilbert, Sierpinski, and Koch structures are used for miniaturization of these antennas [84-86]. However, the radiation patterns of these antennas have to be oriented for proper measurement of the PDs. Printed log periodic dipole antenna exhibits broad bandwidth characteristics with compact dimensions. As the antenna is in planar form, its integration with other circuit components is easy. Since these antennas are specifically used for PD measurements they have to be small, compact and provide end-fire radiation for proper measurement of PD faults in the transformers [87-88].

H. Naomi et al. designed a thirty element log periodic dipole array (LPDA) type optical electric field sensor (OEFS) for computing the electromagnetic field interferences which operates in the frequency range of 1.8 to 6 GHz [89]. The antenna provides a fractional bandwidth (FBW) of 107.69% with the dimensions of $1.391\lambda_0$ x $0.91\lambda_0$ x $0.195\lambda_0$ (L x W x H) and λ_0 is the wavelength at center frequency. Though the sensitivity of the OEFS sensor is highly desirable and minimum detectable electric field strength at 2 GHz is 70 µV/m at 1 MHz resolution bandwidth, however the complexity of the antenna increases with the use of $LiNbO_3$ optical waveguide and the antenna also uses high dielectric constant substrate which results in feeding line losses.

X. H. Zhen et al demonstrated a low profile log periodic monopole array consists of 15 monopole hats of elliptical shape is designed which operates from 1.5 - 6.8 GHz frequency range [90]. The antenna which provides a fractional bandwidth of 127.7% and occupying a size of ($5.81\lambda_0$ x $5.81\lambda_0$ x $0.0032\lambda_0$), however, the structure is complex as it contains top hat monopole in a multi-layer printed circuit board configuration.

L.Xiuyuan et al. designed a miniaturized log periodic dipole array antenna with complementary split ring resonators consisting of eighteen dipoles working from 0.4 - 1.8 GHz frequency range ($1.35\lambda_0$ x $1.1\lambda_0$ x $0.008\lambda_0$) with 127.3 % FBW and the size is large [91].

A.Mirkamali et al. designed a reconfigurable printed log periodic dipole array (RPLPDA) antenna consisting of eight dipoles on FR4 substrate and the diverse frequency bands over a wide frequency range can be yielded by switching the eight printed dipoles. The RPLPDA covers frequency range of 0.75 - 2.7 GHz within size of ($1.093\lambda_0$ x $0.863\lambda_0$ x $0.0092\lambda_0$) with 113% FBW [92].

C.Zachariades et al. developed a wideband spiral shaped coupler consists of tuning nodules for detection of PD's [93]. The UHF coupler size is ($1.033\lambda_0$ x $1.033\lambda_0$ x $0.0155\lambda_0$) with 135.5% FBW and working from 0.5 - 2.6 GHz frequency range with peak gain of 4.8 dBi. Though, the FBW is good, the antenna is not compact, moreover the gain for the antenna

falls at higher frequencies resulting in variation of measured PDs. The Archimedes Spiral Antenna (ASA) is particularly designed for detection of PD in rotating machines [94]. The ASA size is ($0.842\lambda_0$ x $0.842\lambda_0$ x $0.008\lambda_0$) with 120% FBW and from 0.5-2 GHz bandwidth with simulated gain of -11 to 3 dBi.

X. Han et al. demonstrated an integrated sensor is fabricated by placing a fluorescent fiber optic on the disc UHF sensor top surface for GIS application [95]. The sensor size is ($0.5\lambda_0$ x $0.5\lambda_0$ x $0.006\lambda_0$) with 100% FBW and operates from 0.5 - 1.5 GHz with sensitivity of 8 mm. Y.Qi et al. designed an ultra-wideband Metal Mountable Antenna (MMA) for PD detection in contaminated insulator [96]. The MMA size is ($1.598\lambda_0$ x $1.37\lambda_0$ x $0.05\lambda_0$) with 152.94% FBW and works from 0.4 - 3 GHz bandwidth exhibiting a gain from -5.2 to -10.5 dBi. G.V.R.Xavier et al. illustrated a circular printed monopole antenna is designed for PD detection in oil cell [97]. The antenna size is ($0.9\lambda_0$ x $0.9\lambda_0$ x $0.013\lambda_0$) with 130% FBW and operates over 0.3 - 1.5 GHz with S11 less than -10 dB. The simulated gain of the antenna is -1 to 5 dBi.

Compact LPDA have been designed by J.X.Chen et al., C. Lei et al., K.Anim et al., W.Jia et al., K.K.Mistry et al., loading single & double T-shaped structures, dielectric loading with sinusoidal curves, dual band dipole and radial stubs [98-102]. However, FBW and frequency range of these antennas are not sufficient for PD measurements. The effect of transformer tank on the PD measurements is experimentally validated and their accurate simulation models are presented in [103, 104]. The PD acquisition depends on antenna frequency response, tank enclosure resonance modes, and frequency content distribution of PDs [103]. The amplitude and cumulative energy of EM waves are accurately modeled using CST simulations and experimentally validated. It is concluded from the results that attenuation is greater and energy ratio is less at higher frequencies [104].

2.7 Summary

In this chapter, an exhaustive literature survey has been provided. It revealed that degradation of insulation in the transformer imparting to its failure. The distinct types of incipient defects, particularly leading to PD in the transformers have been presented in this thesis and different PD monitoring techniques have been explained. The standard IEC 62478 High Voltage test techniques- measurement of partial discharges by electromagnetic and acoustic methods may be framed in the coming years. The emphasis of this thesis is to

elaborate metaheuristic algorithms for localization of PD source in power transformer adopting non- invasive techniques. Distinct metaheuristic algorithms have been emerged within this layout and they have been explained from chapter 3 to chapter 5.

CHAPTER 3

ACOUSTIC SENSOR BASED PD SOURCE LOCALIZATION IN POWER TRANSFORMER USING BAT ALGORITHM

3.1 Introduction

PD initiates acoustic waves which propagate within transformer tank surface. Acoustic sensors are placed on the outside of the transformer tank wall to capture these acoustic waves that propagates from the PD source. This acoustic method has several merits over direct electrical method because they are non-contact, non-interference prone and ease of installation. The Time Difference of Arrival (TDOA) method is popularly gained for accurate localization of PD source. In the present work, the above method makes use of arrival time differences of AE signals with respect to reference sensor to other sensors there by PD source is determined.

The classic or conventional optimization algorithms are deterministic. A few deterministic optimization algorithms utilize step by step procedure in their search process known as gradient based algorithms. Moreover, if there is little discontinuous in the objective function, these gradient based algorithms cannot work well. Owing to that, non-gradient based algorithms are desired. Non- gradient or gradient free based algorithms generally called stochastic algorithms which employ objective functions for solving the real time engineering problems.

These stochastic algorithms are categorized into two types i.e. heuristic and metaheuristic, however their dissimilarity is negligible. For a tough optimization problem obtaining good quality solutions in a realistic time, yet there is no assurance that they have attained optimal solutions. It can be demanded that these heuristic algorithms work often still not always. To a greater extent development of heuristic algorithms are termed as metaheuristic algorithms [72]. These stochastic algorithms use the combination of both randomization and local search features as metaheuristic. Randomization imparts a good way to pull from local search to global search. Thus, relatively all metaheuristic algorithms swing to be apt for global optimization. In view of above, the bat algorithm has been adopted in this chapter for improving the accuracy of PD source localization.

3.2 Acoustic Emission Localization Concept and Its Mathematical Model

A Partial discharge develops in a localized, closely instantaneous release of energy. A tiny part of released energy heats the material besides to the PD and can vaporize some of it, developing a small or micro discharge. The discharge behaves as a source point of AE Pressure waves. When PD happens, the resultant acoustic signal can extend the piezo electric sensors placed on the outside wall of the transformer tank along different ways. These ways can be classified to direct and indirect ways. In the direct way, the AE signal travels easy way to extend the sensor on the outside wall. In the indirect propagation path, the AE signal arrives at the internal wall and then extends the sensor through the tank wall. The direct way of AE wave is a compression wave and the indirect way of AE wave is a shear wave. However, liquids like transformer oil will carry compression waves only. The direct wave amplitude is more compared to indirect wave.

In the acoustic PD source localization approaches, AE sensors capture acoustic signals at specific time of arrivals. Usually the sensors time of arrivals are of difference between two sensors. Based on the difference of timing method, the ultrasonic localization methods can be classified into the absolute time method (ATM), time difference of arrival method (TDOA) and pseudo time method (PTM). By virtue of the TDOA, without considering concrete arrival time of AE signals reaching specific sensors, is approved extensively and the potency of positioning is comparatively effective. Hence, the TDOA method is studied in detail here.

The Figure. 3.1shows a schematic visualizing the PD source and positions of sensors placed on the transformer tank. The chosen space position system is fixed by taking one of the bottom areas of the transformer tank as the origin O (0, 0, 0) for the determination of forming the tank is positioned in the positive and first quadrant. As shown in Figure.3.1, the PD source is detected at P(x,y,z) and the sensors positions are $S_1(x_1,y_1,z_1)$, $S_2(x_2,y_2,z_2)$, $S_3(x_3,y_3,z_3)$ and $S_n(x_n,y_n,z_n)$.

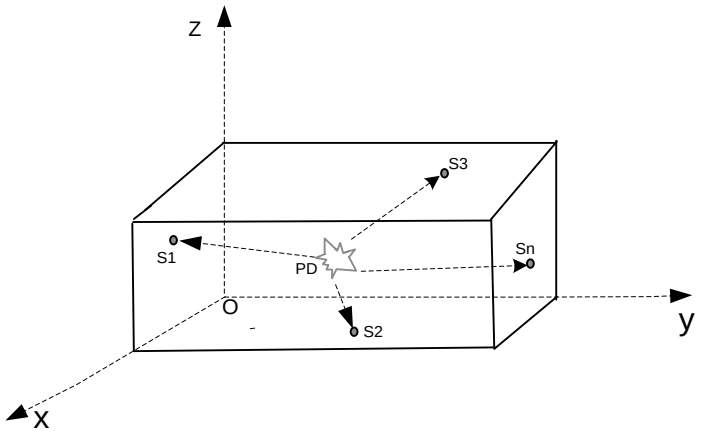

Figure 3.1 Schematic visualizing the sensors placed on the transformer tank

The sensor S_1 is selected as the reference sensor to activate the further sensors and $\tau_{n1} = \tau_n - \tau_1$shows the time difference of acquiring AE signal between sensor n and sensor 1.

The set of 'n' equations describing the position of sensors and acoustic PD source are given by Eqn (3.1)

$$\left.\begin{aligned}
&(x-x_1)^2+(y-y_1)^2+(z-z_1)^2=(v_aT_p)^2\\
&(x-x_2)^2+(y-y_2)^2+(z-z_2)^2=\{v_a(T_p+\tau_{21})\}^2\\
&(x-x_3)^2+(y-y_3)^2+(z-z_3)^2=\{v_a(T_p+\tau_{31})\}^2\\
&\ldots\ldots\\
&(x-x_n)^2+(y-y_n)^2+(z-z_n)^2=\{v_a(T_p+\tau_{n1})\}^2
\end{aligned}\right\} \quad (3.1)$$

Where v_a is the acoustic wave velocity. The Eqn (3.1) can be illustrated shortly as

$$f(x,y,z,v_a)=\{(x-x_n)^2+(y-y_n)^2+(z-z_n)^2\}^{1/2}-\{(x-x_1)^2+(y-y_1)^2+(z-z_1)^2\}^{1/2}-v_a(t-\tau_n)=0 \quad (3.2)$$

The above equation (3.2) is complex combinatorial equation and yielding solution of it is not very easy, so only the best solution can be obtained. To estimate the PD source correctly, the mathematical representation of the ultrasonic localization methods based on the TDOA can be expressed as a constrained optimization problem as shown in Eqn (3.3)

$$min\{D_f(x,y,z,v_a)\} = \sum_{n=2}^{5}\{[(x-x_n)^2+(y-y_n)^2+(z-z_n)^2]^{\frac{1}{2}} - [(x-x_1)^2+(y-y_1)^2+(z-z_1)^2]^{\frac{1}{2}} - v_a(t-\tau_n)\}^2$$

Subject to

$$\left.\begin{array}{l} 0 \le x_n \le x_{max} \\ 0 \le y_n \le y_{max} \\ 0 \le z_n \le z_{max} \\ 1200 \le v_a \le 1500(m/s)\} \end{array}\right\} \qquad (3.3)$$

where x_{max}, y_{max}, $z_{max}$and v_a are the length, width and height of the transformer tank and acoustic wave velocity, respectively. Due to the difficulty of the travelling paths of the acoustic waves in transformers, some factors such as temperature and pressure relies on acoustic wave velocity; normally, the acoustic wave velocity is taken as a constraint in the experimental approaches; examining like this the locating accuracy can be enhanced to a certain value.

Normally, the best solution of Eqs. (3.3) is attained by the LS method, although it has local minima problem and falls into the local convergence because it is a single searching route, which the actual PD source cannot be positioned precisely and the initial guess value should be known; so the efficacy of localization method is not accurate. Then some intelligent (random search) algorithms are better.

3.3 Implementation of Bat algorithm for AE PD source Localization

For single objective global optimization problems, if the functions are very nonlinear, it is great difficult to obtain global best. In general, real-world optimization problems involve certain level of uncertainty. Metaheuristic algorithms are starting to evolve as a key player for global optimization; they repeatedly mimetic the efficient features in nature, particularly biological systems. Many new algorithms are exploring for broad range of applications.

This chapter presents a metaheuristic bat search (real coded) algorithm for localization of AE PD source. Initial studies reveal that it is extremely optimistic and could perform effectively than existing algorithms. The BA results are tested with LS and PSO& other intelligent algorithms and shown to be effective.

3.3.1 Bat algorithm

The basic three steps involved for single objective optimization bat algorithm are presented here.

1. All bats avail echolocation to recognize distance, and they also 'know' the difference between food/prey and circumstances in some unique way;
2. Bats move randomly with velocity u_1 at position x_i with a frequency Q_{min}, with fluctuating wavelength w and loudness A_0 to search for prey. They can automatically tune the wavelength (or frequency) of their emitted pulses and tune the pulse emission rate rϵ [0, 1], based on the proximity of their target;
3. But the loudness can differ in multiple ways; the loudness fluctuates from a large (positive) A_0 to a small constant value A_{min}. Normally frequency f is chosen in the range of [Q_{min}, Q_{max}] matching to the wavelength range of [w_{min}, w_{max}]. For example, frequency in the range of [20 kHz, 500 kHz] matches to wavelengths of range of 0.7–17 mm. The ranges can be freely selected to outfit different applications.

3.3.2 Bat motion

Bat position x_i and velocity u_i in a D-dimensional search space at a time step 't' are upgraded using (3.4) – (3.6).

$$Q_i = Q_{min} + (Q_{max} - Q_{min})\beta \quad (3.4)$$

$$u_i^t = u_i^{t-1} + (x_i^{t-1} - x^*)Q_i \quad (3.5)$$

$$x_i^t = x_i^{t-1} + u_i^t \quad (3.6)$$

Where $\beta \epsilon [0, 1]$ is a random vector drawn from a uniform distribution. Here 'x' is the current global best location (solution) which is located after comparing all the solutions among all the 'n' bats at each iteration 'i'. As the product (w_iQ_i) velocity increment, we can use Q_i (or w_i) to tune the velocity change while fixing the other factor w_i (or Q_i), based on the interest of problem type. In this work Q_{min}= 0 and Q_{max}= 0.15 are used. At first, each bat is randomly set a frequency which is drawn equally from [Q_{min}, Q_{max}].

For the local search part, once a solution is chosen from among the current best solutions, a new solution for each bat is produced locally using random walk using Eqn (3.7)

$$x_i^{t+1} = x^* + (0.01 \times rand) \quad (3.7)$$

The velocities and positions of bats up gradation have some similarity to the procedure in the standard particle swarm optimization, as Q_i necessarily checks the pace and range of the movement of the swarming particles. To a degree, BA can be considered as a balanced combination of the standard particle swarm optimization and the rigorous local search checked by the loudness and pulse emission rate.

3.3.3 Loudness and Pulse emission

Moreover, the loudness A_i and the pulse emission rate r_i have to be upgraded accordingly as the iterations begin. If bat has found its prey then loudness reduces, whereas the pulse emission rate increases, the loudness can be selected as any value of ease. For simplicity, we can also use $A_o = 1$ and $A_{min} = 0$, assuming $A_{min} = 0$ means that a bat has just found the prey and temporarily stop emitting any sound. Where and ζ and γ are constants.

$$A_i^{t+1} = \zeta A_i^t, r_i^t = r_i^0[1 - \exp(-\gamma t)] \quad (3.8)$$

For any $0 < \zeta < 1$ and $\gamma > 0$, and in the simplest case use $\zeta = \gamma = 1$, and in our simulations

$\zeta = \gamma = 0.9$.

$$A_i^t \to 0, r_i^t \to r_i^0, as\ t \to \infty \quad (3.9)$$

If we replace the variations of frequency 'Q_i' by a random parameter and $A_i = 0$, $r_i = 1$, then Bat algorithm becomes standard PSO. Similarly, if we do not use the velocities, and for fixed loudness and rate values, the Bat algorithm reduces to a simple harmony search algorithm. Bat algorithm is very promising for solving nonlinear global optimization problems. The flowchart of Bat Algorithm is shown in Fig 3.2.

Table 3.1 Parameters of PSO Algorithm

Parameter name	Assigned Value
Population of Swarm Size	50
Maximum number of generations	200
C_1	2
C_2	2

Table 3.2 Parameters of Bat Algorithm

Parameter name	Assigned value
Population of Bat Size	20
Maximum number of generations	100
Loudness	0.2
Pulse emission rate	0.6

3.3.4 Pseudo code of Bat Algorithm

1. Assign the bat population x_i, y_i, z_i (i=1,2,3,4,…..n) and velocity u_i

Assign frequencies Q_i ,Pulse emission rate r_i and loudness A_i

2. Iteration begins

for i =1 to iter_max(maximum number of iterations)

3. Produce new solutions by tuning frequency

and upgrading velocities and solutions using Eqns (3.4-3.6)

Choose a solution among the global solutions

if (rand > r_i)

Produce a local solution near the selected global solution

end //if

Assess new solutions

if(rand < A_i & & $f(x_i) \leq f(x)$)

Acquire the new solutions

Increase r_i and decrease A_i

end // if

Rank the bats and identify the current global x Y z^*

end // for maximum number of iterations

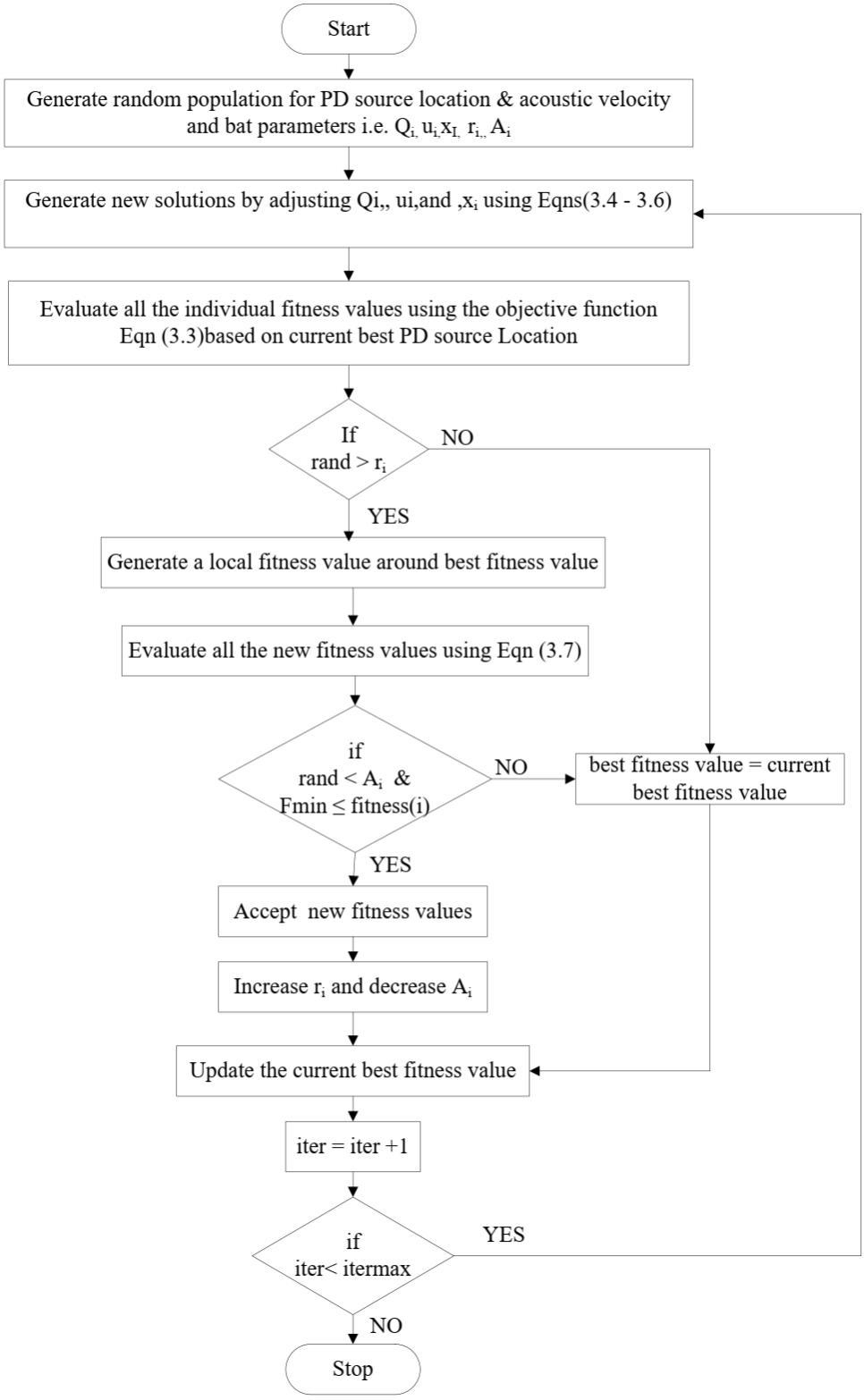

Figure 3.2 Flow chart of bat algorithm for PD source localization in power transformer

3.4 Results and Discussion

3.4.1 Laboratory data Case Study

The laboratory experimental setup and related data is taken from [42] is adopted for BA based AE partial discharge source localization .The simulation experiments were set up on steel oil tank size of 1000 mm x 800 mm x 1200 mm and 4 acoustic sensors were placed on the tank outer wall by magnets. The discharge source position was fixed for every measurement. By moving the pin-plate electrode, they got different discharge position, measured time-differences for four times to each PD point. The sensors are located at S_1(800,820,0), S_2(1000,420,346), S_3(345,782,800) and S_4(0,468,386); the time differences of each trail is given in the Table 3.3.

For validation of proposed method with the existing literature, the laboratory experimental data i.e. actual PD Source location, time delays from [37] are adopted and analyzed. The PD Source location results using proposed method and available literature results are shown in the table 3.3. From the table 3.3,PSO locates the PD Source within 13.67 to 31.45mm,whereas the Proposed BA locates within 12.24 to 24.74 mm for trail 1 and for trail 2, PSO locates the PD Source within 12.17 to 21.66mm,whereas the Proposed BA locates within 3.93 to 10.29 mm and for trail 3, PSO locates the PD Source within 13.19 to 19mm,whereas the Proposed BA locates within 9.22 to 14.76 mm and for Table 3.4 shows that proposed method locates the PD Source within overall location error maximum of 24.74 mm and minimum of 3.93mm for laboratory data case . From the table 3.3, it is noted that the PD location error decreases for accurate time delay measurements from the sensors and increases for inaccurate time delay measurements from the sensors and also noticed that the proposed algorithm gives minimum PD location error compared with PSO and LSE methods. Table 3.4 shows that for trail 1, PSO locates the PD Source within 9-26 mm of maximum deviation whereas BA locates the PD Source within 10-24 mm and for trail 2, PSO locates the PD Source within 12-16 mm of maximum deviation whereas BA locates the PD Source within 3-9 mm and for trail 3 PSO locates the PD Source within 12-17 mm of maximum deviation whereas BA locates the PD Source within 9-13 mm. Table 3.4 shows that proposed method locates the PD Source within overall maximum deviation of highest value 24 mm and lowest value of 3mm for laboratory data case, which can be allowed negligible for distances of practical interest.

Table 3.3 PD Source Location Error results and comparison among different algorithms for laboratory data case study

S. No	Actual PD Coordinates (mm)	Time Differences (μs)	PD Location results of LS (mm) [37]	PD Location results of PSO (mm) [37]	PD Location results of Bat (mm)	Error of LS (mm) [37]	Error of PSO (mm) [37]	Error of Bat (mm)
1-1	(392,700,490)	(25,-228,-127)	(529,590,501)	(384,719,492)	(381,706,488)	176.04	20.01	12.68
1-2		(27, -210,-131)	(661,1012,672)	(379,712,516)	(398,700,466)	450.37	31.45	24.74
1-3		(23, -225,-126)	(682,793,872)	(383,691,495)	(387,698,479)	488.54	13.67	12.24
1-4		(27, -230,-130)	(485,936,647)	(380,701,483)	(387,710,483)	298.31	13.93	13.17
2-1	(510,700,410)	(37, -61,32)	(694,918,491)	(512,716,421)	(502,704,411)	296.55	19.52	9
2-2		(36, -65,30)	(625,625,275)	(520,715,422)	(509,703,411)	192.54	21.66	3.93
2-3		(40, -58,34)	(650,768,515)	(513,703,424)	(512,703,403)	187.75	14.63	7.87
2-4		(38, -64,29)	(646,895,585)	(510,712,412)	(513,696,401)	295.21	12.17	10.29
3-1	(883,700,690)	(-174,-106,179)	(952,1112,763)	(877,706,707)	(890,700,703)	424.07	19.00	14.76
3-2		(-175,-112,182)	(968,1027,592)	(882,708,702)	(882,689,690)	351.79	14.45	11.04
3-3		(-182,-95,191)	(799,582,833)	(881,701,703)	(879,709,684)	203.54	13.19	11.54
3-4		(-162,-106,187)	(785,592,796)	(895,706,693)	(883,702,681)	180.29	13.75	9.22

Table 3.4 Maximum deviation error and relative error results comparison among different algorithms for laboratory data case study

S. No	Maximum Deviation of LS (mm) [37]	Maximum Deviation of PSO (mm) [37]	Maximum Deviation of Bat (mm)	Relative Error of LS (%)	Relative Error of PSO (%)	Relative Error of Bat (%)
1-1	200	19	11	10.03	1.14	0.722
1-2	312	26	24	25.66	1.79	1.41
1-3	382	9	11	27.84	0.78	0.697
1-4	236	12	10	16.99	0.79	0.75
2-1	218	16	8	16.89	1.11	0.51
2-2	135	15	3	10.97	1.23	0.22
2-3	140	14	7	10.69	0.83	0.45
2-4	195	12	9	16.82	0.69	0.586
3-1	412	17	13	24.16	1.08	0.841
3-2	327	12	11	20.05	0.82	0.629
3-3	143	13	9	11.59	0.75	0.657
3-4	108	12	9	10.27	0.78	0.525

From the table 3.4, it is noted that the maximum deviation of PD source decreases for accurate time delay measurements from the sensors and increases for inaccurate time delay measurements from the sensors. From the figures 3.3-3.5, the maximum deviation error comparison for all the three trails with different algorithms. It can also be noticed that proposed method locates the PD source much better when compared with the available literature results.

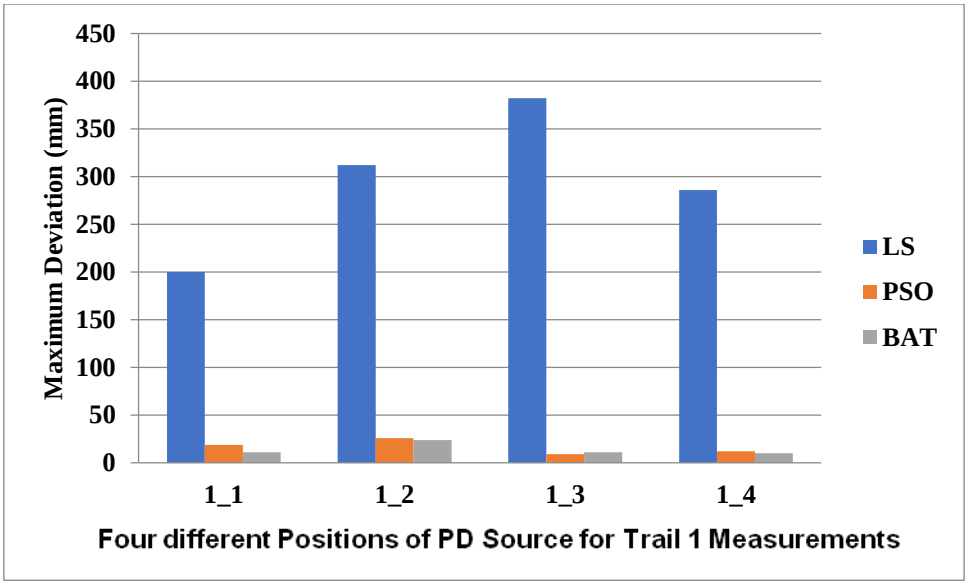

Figure 3.3. Comparison of PD source location results among literature with proposed bat algorithm for trail 1 laboratory measurements

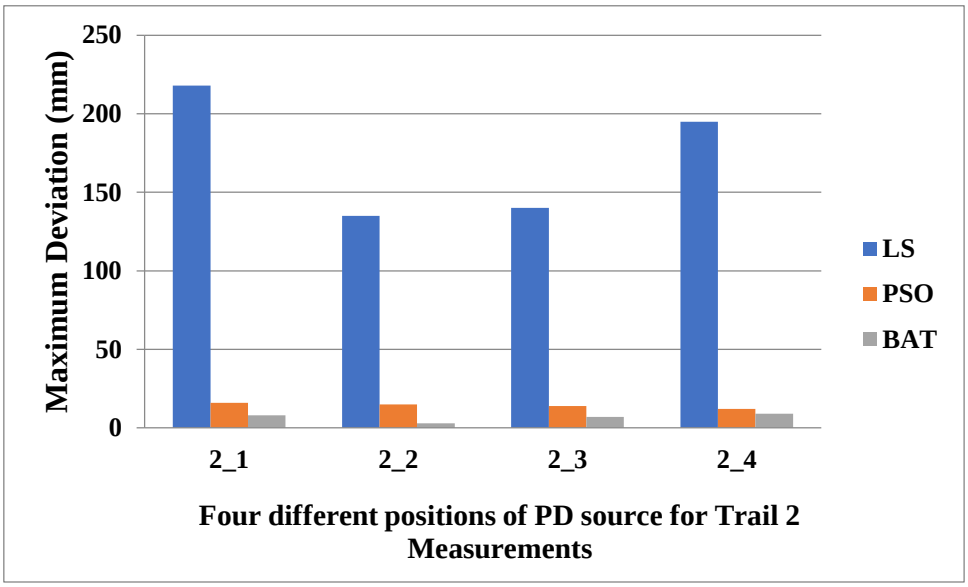

Figure 3.4. Comparison of PD source coordinates maximum deviation error among literature with proposed bat algorithm for trail 2 laboratory measurements

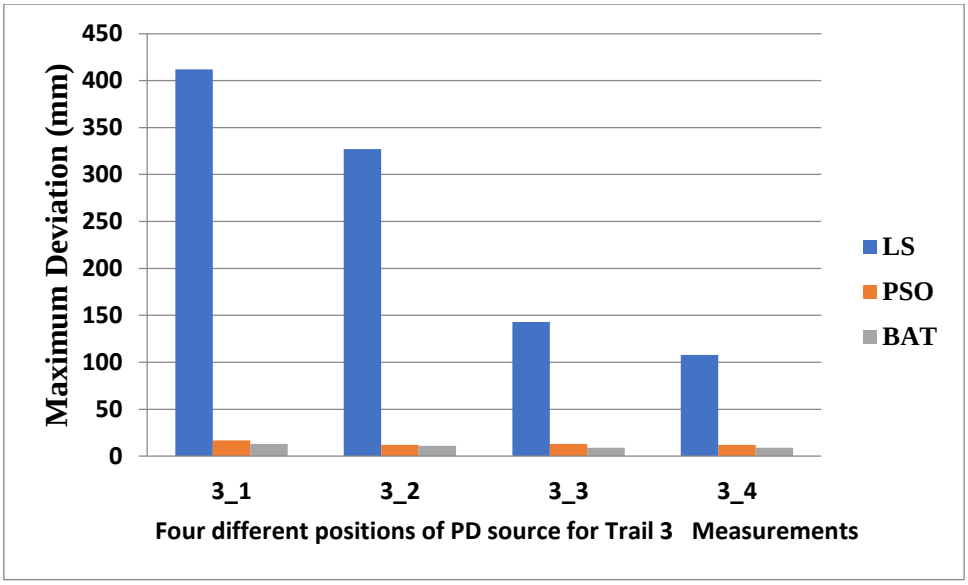

Figure 3.5 Comparison of PD source coordinates maximum deviation error among literature with proposed bat algorithm for trail 3 laboratory measurements

3.4.2 Field data Case Study

The field experimental data of the power supply company from [44] is taken for this case study and five acoustic sensors are placed on the transformer tank wall. The transformer tank size is 5000mm x3000mm x 4000mm, and the actual PD source is at P (4500,2600,3700); the sensors positions are S_1(2500,0,2000), S_2(2500,1500,4000), S_3(5000,1500,2000), S_4(2500,3000,2000) and S_5(0,1500,2000);the t= 2600µs is selected as the reference time, (µs) and the respective sensors time delays are1600, 1500, 1900, 3524.69 µs.

Table 3.5 Comparison of PD Source Location results among available literature with proposed method

Coordi-nates (mm)	Actual PD source (mm)	PD Location results of PSO [42]	PD Location results of SA [42]	PD Location results of Linear PSO [42]	PD Location results of GA [44]	PD Location results of QGA [44]	PD Location results of Bat
X	4500	4383.32	4387.78	4382.14	4223.76	4394.77	4402
Y	2600	2470.53	2470.01	2469.99	2391.71	2475.98	2577
Z	3700	3649.16	3666.64	3648.11	3503.04	3656.17	3689

Table 3.6 Comparison of Location and Maximum Deviation error results among available literature with proposed method

Error	Linear PSO [42]	PSO [42]	SA [42]	GA [44]	QGA [44]	BAT
Location error (mm)	182.99	181.55	174.94	398.10	168.45	101.26
Maximum Deviation (mm)	130.01	129.47	129.99	276.24	124.02	88
Relative Error (%)	2.59	2.57	2.47	5.63	2.38	1.43

Maximum deviation $Deviation_{max}$ of coordinates can be estimated by

$$Deviation_{max} = \begin{Bmatrix} x_{actual} - x_{calculated} \\ y_{actual} - y_{calculated} \\ z_{actual} - z_{calculated} \end{Bmatrix}_{max}$$

Where x_{actual} y_{actual} z_{actual} are actual coordinates;$x_{calulated}$, $y_{calculated}$, $z_{calculated}$ are calculated coordinates.

Relative Error can be calculated as$\left(\frac{LocationError}{TankDiagonal}\right) * 100$

Tank Diagonal is $\sqrt{x^2 + y^2 + z^2}$where *x* is length, *y* is width, *z* is height of the transformer tank in mm.

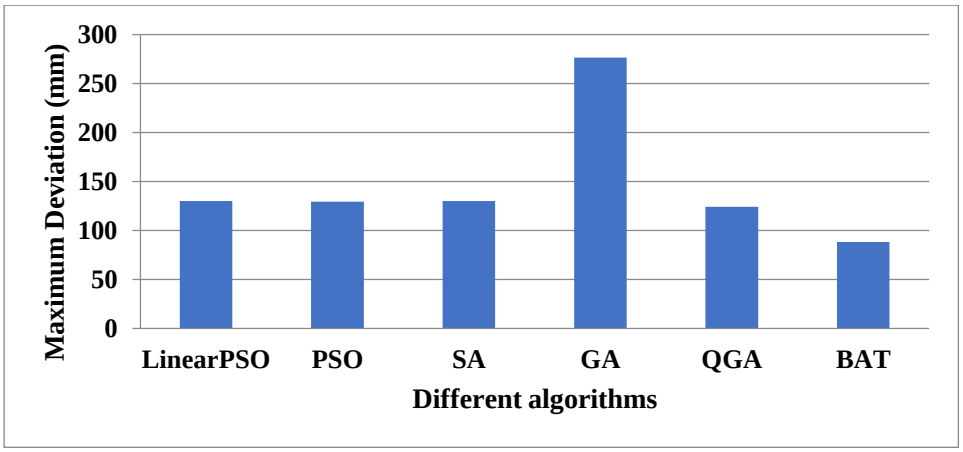

Figure 3.6. Comparison of PD source coordinates maximum deviation error among literature with proposed bat algorithm for field measurements

The performance of proposed method with the existing literature, the field experimental data i.e. actual PD Source location, time delays, PD Source location results from [42] are taken and analyzed. The PD Source location results using proposed method and available literature results are shown in table. Table3.5 shows that proposed method locates the PD Source within location error of 101.26mm and it is noted that the PD location error decreases for proposed algorithm and increases for linear PSO, PSO, SA, GA and QGA algorithms of available literature. Table 3.6 shows that proposed method locates the PD Source within maximum deviation of 88 mm, which can be allowed negligible for distances of practical interest and it is noted that the maximum deviation of PD source decreases for proposed algorithm and increases for linear PSO, PSO, SA, GA and QGA algorithms of available literature. Figure 3.6 shows the maximum deviation error comparison for five sensor time delay measurements with different algorithms. The proposed BA method has less relative error that is obtained with reference to the tank diagonal (D_{tank} =7071.07 mm) when compared with other methods.

Table 3.7 Comparison of PD Location results (4 sensors) among available literature with proposed method

Combinations Number	Coordinates (mm)		
	X	Y	Z
1	4490.5	2544.4	3601
2	4449.1	2558.8	3744.8
3	4356.5	2394.5	3541.2
4	4375.2	2452.3	3510.2
5	4421	2510	3756

Table 3.8 Comparison of Error analysis (4 sensors) among available literature with proposed method

Combinations number	Errors Analysis		
	Location Error (mm)	Maximum Deviation (mm)	Relative Error (%E)
1	113.94	99	1.61
2	79.34	50.9	1.12
3	296.71	205.5	4.19
4	270.95	189.8	3.83
5	132.20	90	1.87

Table 3.7 shows the PD location results of the optimized sensors (i e., 5 combinations of four sensors i.e. 5_{C4} which is similar to above 5 sensors as shown in table 3.5) using bat algorithm.

The second combination outperforms among other combinations as shown in the Table 3.8. The error analysis is analyzed in the Table 3.8. The second combination locates the PD source within 79.84 mm location error, 50.9 mm maximum deviation error and 1.244% relative error.

It is also found that the proposed method locates the PD source much better for both laboratory and field experimental data when compared with the available literature results. Therefore, the proposed method possesses its ability to locate the source with outmost relatively high accuracy in single step of calculation. The Proposed BA gives small location error and maximum deviation error with less execution time when compared to other methods.

3.5 Summary

A metaheuristic-based bat algorithm for AE PD source localization is proposed in this chapter. The proposed bat algorithm is tested for laboratory experimental data as well as field data and it yields superior results compared with existing resolutions from the literature. The accuracy of the results can be better to be of practical interest. When compared to conventional iterative methods and some intelligent optimization methods, this method gives the best global optimal location. It is proved that the proposed method will make easy to the AE PD source location.

CHAPTER 4

Location of PD source utilizing Acoustic Signals in Power transformer by fuzzy adaptive particle swarm optimization

4.1 Introduction

The conventional methods i.e. iterative and non-iterative methods take more computation and time to produce the better results and the iterative method depends on correct starting guess values. The optimization algorithms also take large number of population and iterations for getting better results. Hence, hybridization of optimization method with other methods may enhance the search space to balance the overall exploration and exploitation ability, convergence speed, and ability of searching global optimum, less computation time and better results when compared to conventional and optimization methods. PSO is one of the most widely used evolutionary algorithms in hybrid methods due to its simplicity. Some works reported in the literature which has been controlling either inertia weight or acceleration parameters of PSO methods targeted to reduce the trapping probability of local minimum. In view of above, the FAPSO has been adopted in this chapter for improving the accuracy of PD source localization.

4.2 Formulation of PD Source Localization Problem

The PD source and the sensor positions placement on the transformer tank is shown in the Figure 4.1. The P(x, y, z) is estimated PD source and the sensors positions are S_1 (x_a, y_a, z_a), S_2 (x_b, y_b, z_b), S_3 (x_c, y_c, z_c) and so on S_n (x_n, y_n, z_n). The sensor S_1 is considered as the reference sensor to activate the further sensors. In Eqn 4.1, (x, y, z) is the PD source position, S_1 (x_a, y_a, z_a) is the first sensor fixed position on the transformer tank. In Eqn 4.2, (x, y, z) is the PD source position, S_2 (x_b, y_b, z_b) is the second sensor fixed position on the transformer tank, τ_{21} is the time difference between $sensor_2$ and $sensor_1$. In Eqn 4.3, (x, y, z) is the PD source position, S_3 (x_c, y_c, z_c) is the third sensor fixed position on the transformer tank, τ_{31} is the time difference between $sensor_3$ and $sensor_1$. In Eqn 4.4, (x, y, z) is the PD source position, S_4 (x_d, y_d, z_d) is the fourth sensor fixed position on the transformer tank, τ_{41} is the time difference between sensor4 and $sensor_1$. In Eqn 4.5, (x, y, z) is the PD source position, S_5 (x_e, y_e, z_e) is the fifth sensor fixed position on the transformer tank, τ_{51} is the time

difference between $sensor_5$ and $sensor_1$. In Eqn 4.6, min $\{D_f(x, y, z, v_a)\}$ is minimization objective function with constraints length(min< x< max) mm, width (min< y<max) mm, height (min<z<max) mm and acoustic velocity (1200< v_a <1500) m/s of the transformer tank considered.

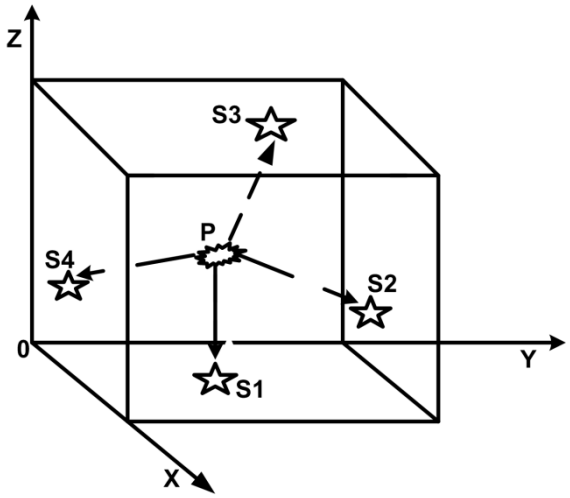

Figure 4.1 PD source and the sensors placement on the transformer tank.

4.2.1 Objective function

The aim of this localization of PD source is to minimize the location error.

$$g = \sqrt{(x - x_a)^2 + (y - y_a)^2 + (z - z_a)^2} \quad (4.1)$$

$$p = \sqrt{(x - x_b)^2 + (y - y_b)^2 + (z - z_b)^2} - \mathrm{g} - v_a\tau_{21} \quad (4.2)$$

$$q = \sqrt{(x - x_c)^2 + (y - y_c)^2 + (z - z_c)^2} - \mathrm{g} - v_a\tau_{31} \quad (4.3)$$

$$r = \sqrt{(x - x_d)^2 + (y - y_d)^2 + (z - z_d)^2} - \mathrm{g} - v_a\tau_{41} \quad (4.4)$$

$$s = \sqrt{(x - x_e)^2 + (y - y_e)^2 + (z - z_e)^2} - \mathrm{g} - v_a\tau_{51} \quad (4.5)$$

$$min\{D_f(x, y, z, v_a)\} = p^2 + q^2 + r^2 + s^2 \quad (4.6)$$

4.3 Proposed Method

PSO is based on the evolution of birds flocking closely to swarming intelligence and it was proposed by Kennedy and Eberhart in 1995.This approach includes in such a way that at each iteration, upgrading the velocity and position of every particle move in the direction of its P_{best} position based on memory and g_{best} position based on information of Eqns. (4.7&4.8) respectively.

$$v_k^{t+1} = wv_k^t + c_1 rand_1(p_{best} - x_k^t) + c_2 rand_2(g_{best} - x_k^t) \quad (4.7)$$

$$x_k^{t+1} = x_k^t + v_k^{t+1} \quad (4.8)$$

In Eqn 4.7, w is the inertia weight, $v_k{}^t$ is the current particle velocity, $v_k{}^{t+1}$ is the new velocity vector, t is the iteration count, c_1& c_2 are learning parameters, $rand_1$& $rand_2$ are random numbers, p_{best} & g_{best} are local best solution & global best solution, $x_k{}^t$ is the current particle solution. In Eqn 4.8, $x_k{}^{t+1}$ is new position vector, $x_k{}^t$ is the current particle position vector, $V_k{}^{t+1}$is the new velocity vector.

Normally, PSO velocity contains three segments i.e. the momentum segment, the cognitive learning segment and the social learning segment. The PSO performance is improved by the equilibrium among these segments i.e., which controls the local and global searching abilities. In PSO, the inertia weight is utilized to balance the global and local searching abilities. A huge inertia weight accelerates a global search while a little inertia weight accelerates a local search. The searching abilities will be dynamically improved by tuning the inertia weight effectively.

The searching procedure of PSO is a non-linear and difficult approach. The sequential or straight-line declining inertia weight process has a linear progression capability from global to local search and not shown the effective searching process for obtaining the optimum solution. Hence, the inertia weight should be changed nonlinearly and dynamically for improvement in the performance and equilibrium between global and local searching abilities. The demanding representation of mathematically adjusting the inertia weight dynamically without having the knowledge on searching process. Conveniently with some ideas of PSO searching procedure is assembled & linguistic relation of the searching procedure for localization of PD source is attainable. This idea & linguistic relation formulates a fuzzy interference system for adjustment of PSO inertia weight dynamically to solve the localization of PD source problem. The remaining part of this paper explains modeling a fuzzy system and adapting inertia weight effectively for localization of PD source problem. The simple IF- THEN fuzzy rules in Table 4.1 and Eqns. (4.9 – 4.12) are utilized for the proposed methods i.e., FAPSO-I consists of 49 fuzzy rules listed in Table 4.1 and FAPSO consist of 9 fuzzy rules listed in Table 4.2.

Table 4.1. Simple IF-THEN Rules for FAPSO-I

Rule Number	**Antecedent**		**Consequent**
	NFV	**W**	**∆W**
1	NL	NL	NL
2	NM	NL	NL
3	NS	NL	NL
4	Z	NL	NL
5	PS	NL	NM
6	PM	NL	NS
7	PL	NL	Z
8	NL	NM	NL
9	NM	NM	NL
10	NS	NM	NL
11	Z	NM	NM
12	PS	NM	NS
13	PM	NM	Z
14	PL	NM	PS
15	NL	NS	NL
16	NM	NS	NL
17	NS	NS	NM
18	Z	NS	NS

19	PS	NS	Z
20	PM	NS	PS
21	PL	NS	PM
22	NL	Z	NL
23	NM	Z	NM
24	NS	Z	NS
25	Z	Z	Z
26	PS	Z	PS
27	PM	Z	PM
28	PL	Z	PL
29	NL	PS	NM
30	NM	PS	NS
31	NS	PS	Z
32	Z	PS	PS
33	PS	PS	PM
34	PM	PS	PL
35	PL	PS	PL
36	NL	PM	NS
37	NM	PM	Z
38	NS	PM	PS
39	Z	PM	PM
40	PS	PM	PL
41	PM	PM	PL
42	PL	PM	PL
43	NL	PL	NL

44	NM	PL	NM
45	NS	PL	NS
46	Z	PL	Z
47	PS	PL	PS
48	PM	PL	PM
49	PL	PL	PL

Table 4.2 Rules of FAPSO

Rule Number	**Antecedent**		**Consequent**
	NFV	**W**	**∆W**
1	S	S	Z
2	S	M	N
3	S	L	N
4	M	S	P
5	M	M	Z
6	M	L	N
7	L	S	P
8	L	M	Z
9	L	L	N

In the Figures 4.2- 4.4, triangular membership functions are considered and they are represented by seven linguistic elements (NL, NM, NS, Z, PS, PM and PH) for negative large, negative medium, negative small, zero, positive small, positive medium and positive high respectively are used for fuzzification of every input and output. The fuzzy logic block diagram with two inputs and one output of FAPSO-I is shown in Figure 4.5. For FAPSO, the triangular membership functions are considered and represented by three linguistic elements (N, Z, P) for negative, zero and positive respectively for fuzzification of every input and output. In this fuzzy logic system, fuzzification block converts crisp value to fuzzy value, fuzzy interference engine has the capability of simulating human decision making based on

fuzzy rules of inference in fuzzy logic and the defuzzifier block converts fuzzy value to crisp value using centroid method.

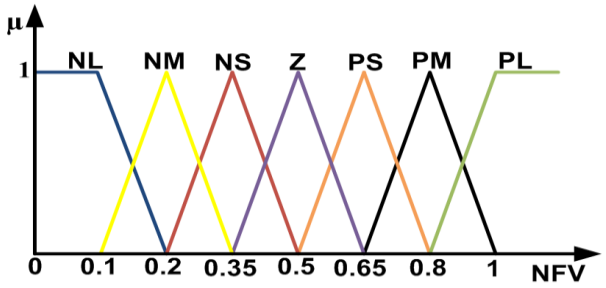

Figure 4.2 Representation of Triangular Membership functions for Normalized Fitness Input

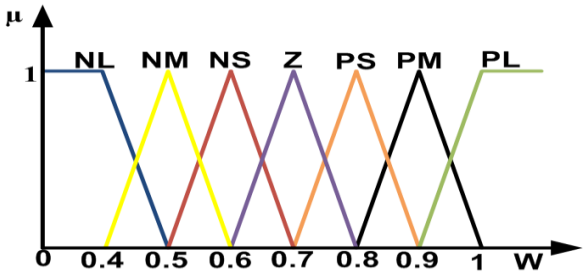

Figure 4.3 Representation of Triangular Membership functions for Inertia weight Input

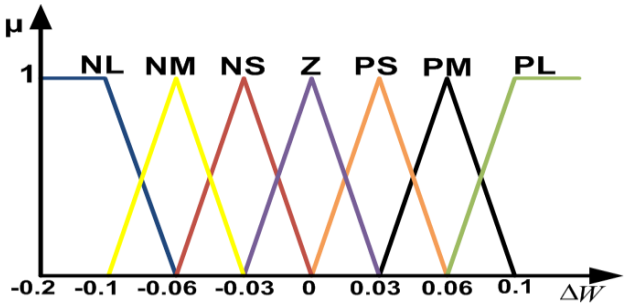

Figure 4.4 Representation of Triangular Membership functions for Change in Inertia weight Output.

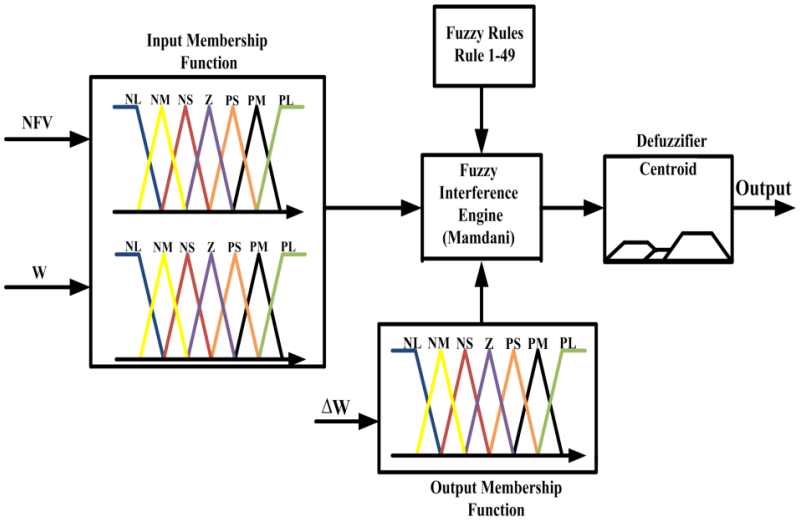

Figure 4.5 Fuzzy Logic System with two inputs and one output of FAPSO-I

4.4 Formulation of Fuzzy system

A fuzzy rule design is developed using inertia weight of the PSO algorithm to get better accuracy in the PD location results. The Fuzzy logic system contains three main segments i.e., fuzzification, inference system and defuzzification. To find a good inertia weight in the fuzzy domain, inputs of the fuzzy system are normalized fitness and the inertia weight while the output is inertia weight. In order to establish a crisp mathematical model for the adaptive PSO, it is very hard to actively modify the inertia weight parameters. Therefore, easily understanding IF-THEN rules are appropriate to compute some portion of inertia weight modification in the fuzzy adaptive PSO procedure to locate the PD source.

Normalized fitness: The current solution fitness is very crucial to guess the inertia weight for the correct choice of the velocity. In general, normalized fitness lies in between 0 and 1 & it is given by

$$Fit_{normalise} = \frac{f_{gbest} - f_{gbestold}}{10 - f_{gbestold}} \quad (4.9)$$

In Eqn 4.9, f_{gbest} is the global best fitness value for considered iterations and $f_{gbestold}$ is the old global best fitness value for first iteration from Eqn 4.8.

Inertia Weight: Its value lies in between 0.4 and 1 for this problem.

Change in Inertia Weight: In this paper, its value is placed in between -0.1 and 0.1.

IF-THEN Rules and Defuzzification: For FAPSO, forty nine rules are constructed using seven linguistic values for every input element. The simple IF-THEN rules are shown in Table 4.1.The arithmetic product operator is used as conjunction for the input and output elements in the formulation of individual rules. For every rule, output element will be scaled based on degree of membership (DOM).

4.5 Fuzzy Adaptive PSO Formulation

The velocity and position computations for the proposed fuzzy adaptive PSO are as follows

$$w_k^{t+1} = w_k^t + \Delta w_k^t \quad (4.10)$$

$$v_k^{t+1} = w_k^{t+1} v_k^t + c_1 rand_1(p_{best} - x_k^t) + c_2 rand_2(g_{best} - x_k^t) \quad (4.11)$$

$$x_k^{t+1} = x_k^t + v_k^{t+1} \quad (4.12)$$

In Eqn 4.10, w_k^{t+1} is the new adaptive weight, t is the iteration count, w^t_k is the k^{th} particle weight, Δw^t_k is the change in weight value. In Eqn 4.11, v_k^{t+1} is the new velocity vector, v_k^t is the k^{th} particle velocity, t is the iteration count, $w_k^{t+1}$is the adaptive inertia weight, c_1 & c_2 are learning parameters, $rand_1$& $rand_2$ are random numbers, p_{best} & g_{best} are local best solution & global best solution, x_k^t is the current particle solution. In Eqn 4.12, x_k^{t+1} is new position vector.

4.6 Results and Discussion:

The simulations are performed on the same experiment measurements data, but the population size is reduced from 50 to 20 and total iterations are reduced from 200 to 100. The simulation parameters of the FAPSO-I and FAPSO for PD source location are swarm population=20, maximum number of iterations=100, learning parameters C_1, C2=2.

Location Error in mm can be determined by

$$\sqrt{(x_{actual} - x_{calculated})^2 + (y_{actual} - y_{calculated})^2 + (z_{actual} - z_{calculated})^2}$$

Maximum deviation $Deviation_{max}$ of coordinates can be estimated by

$$Deviation_{max} = \begin{Bmatrix} x_{actual} - x_{calculated} \\ y_{actual} - y_{calculated} \\ z_{actual} - z_{calculated} \end{Bmatrix}_{max}$$

Where x_{actual}, y_{actual}, z_{actual} is actual PD location and $x_{calculated}$, $y_{calculated}$, $z_{calculated}$ is calculated PD location.

Relative Error can be calculated as$\left(\frac{LocationError}{TankDiagonal}\right) * 100$

Tank Diagonal is $\sqrt{x^2 + y^2 + z^2}$where *x* is length, *y* is width, *z* is height of the transformer tank in mm.

4.6.1 Case study of field data

The onsite measurement data is collected from [42, 44] which is measured data on power transformer. In Eqn. 4.6, five sensors are used in this case study and the Table 4.3 shows the calculated PD location results. The actual PD Coordinates are (X_{PD}, $Y_{PD,}$ Z_{PD}) = (4500, 2600, 3700) mm. The final results for different algorithms are the best values of the PD location solutions. Table 4.3 shows the comparison of final PD source solution obtained with proposed FAPSO-I and FAPSO algorithms with five algorithms in the existing literature. Table 4.4 shows the comparison of error analysis with proposed FAPSO-I and FAPSO algorithms with different methods in reported literature with reference to the tank diagonal (D_{tank} =7071.07 mm).

The location of PD Source results with the proposed methods and available literature are shown in Table 4.3. The proposed methods FAPSO-I and FAPSO locate the PD Source within 58.47&62.83mm of PD source location error and maximum deviation error of 45.1 and 58.3mm in Table 4.4. From the Table 4.4, it is observed that the maximum deviation error and relative error of the proposed algorithm is insignificant when compared to other methods in the available literature. The convergence characteristics comparison of FAPSO-I and FAPSO algorithm for this case study is shown in figure 4.7, the FAPSO-I algorithm takes less number of iterations to locate accurate PD source compared to FAPSO algorithm.

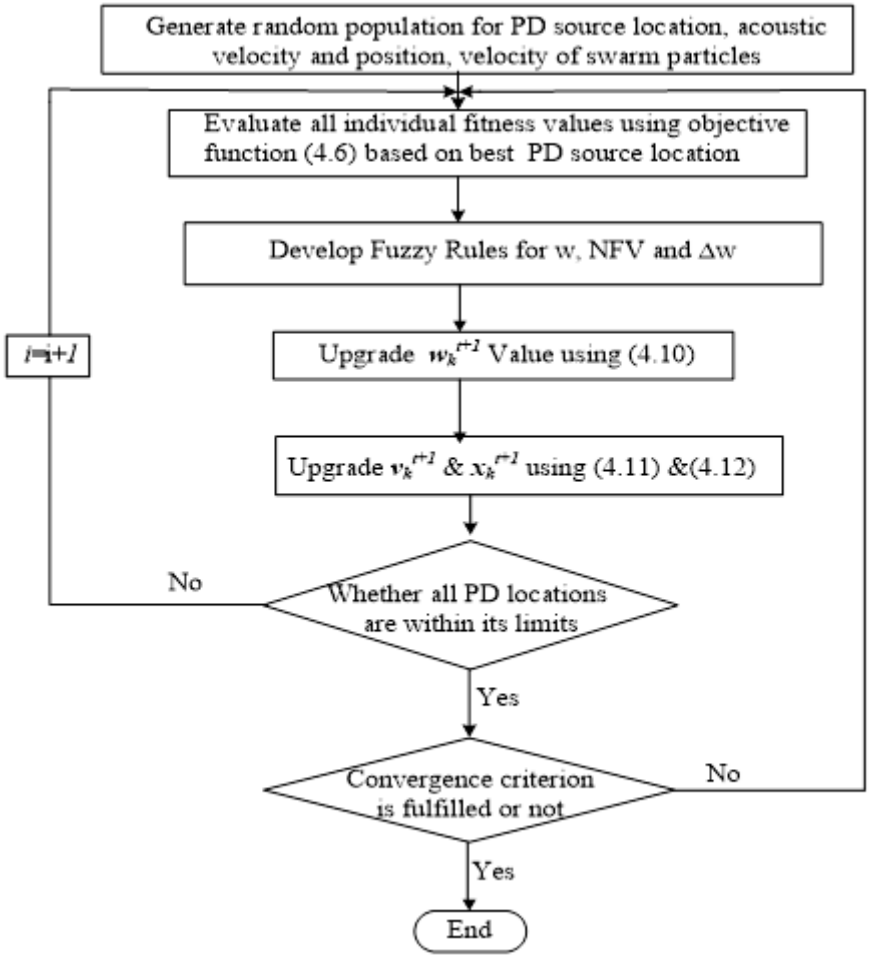

Figure 4.6 Flow chart of FAPSO-I and FAPSO

Table 4.3 Comparison of field PD Location results with proposed methods and different methods in available literature

Methods	Co- ordinates	X(mm)	Y(mm)	Z(mm)
Actual Coordinates		4500	2600	3700.0
FAPSO-I		4465.9	2554.9	3714.9
FAPSO		4485.6	2541.7	3718.5
QGA [44]		4394.77	2475.98	3656.17
GA [44]		4223.76	2391.73	3503.04
SA [42]		4387.78	2470.01	3666.64
PSO [42]		4383.32	2470.53	3649.16
LPSO [42]		4382.14	2469.99	3648.11

It is observed that the Proposed FAPSO-I gives minimum location error, maximum deviation error and relative error with less execution time when compared to other methods. Figure4.8 shows the inertia weight variation for a randomly chosen length and the convergence characteristic of the fuzzy adaptive PSO. The straight segment of the curve specifies that there is no change in the weight tuning of PSO.

Table 4.4 Comparison of field data Error analysis of different methods in literature with proposed methods

Errors / *Methods*	*Location Error (mm)*	*Maximum Deviation Error (mm)*	*Relative Error (%E)*
FAPSO – I	58.47	45.1	0.83
FAPSO	62.83	58.3	0.89
QGA [44]	124.02	168.45	1.75
GA [44]	276.24	398.10	3.91
SA [42]	129.99	174.94	1.84
PSO [42]	129.47	181.55	1.83
LPSO [42]	130.01	182.99	1.84

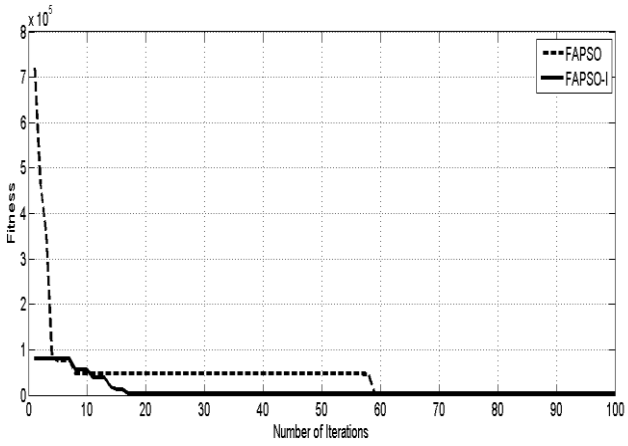

Figure 4.7 Comparison of Convergence Characteristics of FAPSO-I and FAPSO methods for field measurements

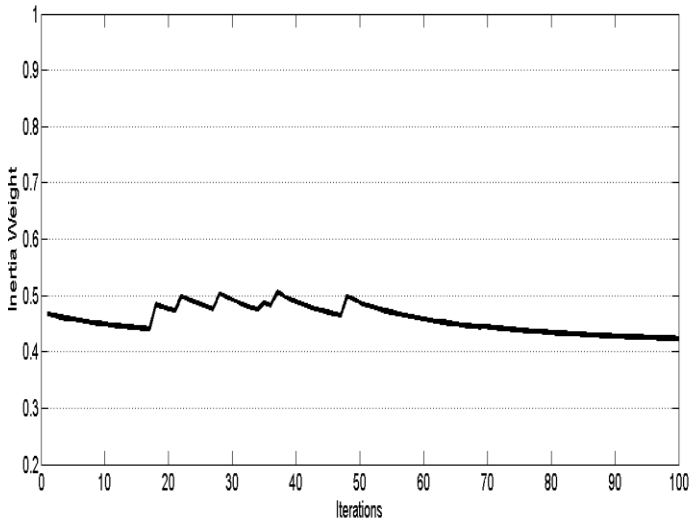

Figure 4.8 Inertia weight adjustment of FAPSO-I method.

Table 4.5 Comparison of Laboratory PD source location results among available literature methods

PD source position No	Actual PD Coordinates(mm)	PD Location results of LS (mm) [10]	PD Location results of PSO (mm) [10]	PD Location results of FAPSO (mm)	PD Location results of FAPSO-I (mm)	Location error of LS (mm) [10]	Location error of PSO (mm)	Location Error of FAPSO (mm)	Location Error of FAPSO-I (mm)
1-1	(392,700,490)	(529,590,501)	(384,719,492)	(383,698,487)	(388,702,489)	176.04	20.01	9.69	4.58
1-2		(661,1012,672)	(379,712,516)	(394,694,486)	(386,704,488)	450.37	31.45	7.46	8.25
1-3		(682,793,872)	(383,691,495)	(388,698,486)	(389,701,488)	488.54	13.67	6	3.74
1-4		(485,936,647)	(380,701,483)	(389,697,485)	(389,702,487)	298.31	13.93	6.56	4.69
2-1	(510,700,410)	(694,918,491)	(512,716,421)	(506,706,408)	(508,702,408)	296.55	19.52	7.48	3.46
2-2		(625,625,275)	(520,715,422)	(507,701,412)	(509,701,409)	192.54	21.66	3.46	1.73
2-3		(650,768,515)	(513,703,424)	(508,702,406)	(508,699,409)	187.75	14.63	4.89	2.45
2-4		(646,895,585)	(510,712,412)	(511,695,405)	(507,701,408)	295.21	12.17	7.14	3.74
3-1	(883,700,690)	(952,1112,763)	(877,706,707)	(887,701,693)	(880,698,688)	424.07	19.00	5.09	4.12
3-2		(968,1027,592)	(882,708,702)	(880,695,688)	(881,697,686)	351.79	14.45	6.16	5.39
3-3		(799,582,833)	(881,701,703)	(880,696,685)	(880,696,687)	203.54	13.19	7.07	5.83
3-4		(785,592,796)	(895,706,693)	(882,700,684)	(881,702,691)	180.29	13.75	6.08	3

4.6.2 Case Study of laboratory data

The laboratory experimental related data is taken from [37] for PD source localization. The actual PD source position was fixed for four different time differences measured by moving the pin-plate electrode for four times. The sensors are located at S_1(800,820,0) ,S_2(1000,420,346),S_3 (345,782,800) and S_4(0,468,386).The Table 4.5 shows the comparison of PD location and its error results with proposed methods and different methods published in literature obtained for each setup (i.e. for each PD source and its TDOA measurements).

It is observed from the table 4.5, that the location error of PD source is lower for accurate time delay measurements from the sensors and higher for inaccurate time delay measurements from the sensors and also observed that the proposed algorithm gives minimum PD location error compared with PSO and LS methods. It is observed from the table 4.6, that the PD source maximum deviation error is significantly lower for accurate time delay measurements from the sensors and higher for inaccurate time delay measurements from the sensors. It can also be found that PD source location by proposed method is much better when compared with the available literature results. It is also reveals that the PD source location by proposed method is much better for both laboratory and field experimental data when compared with the available literature results.

For validation of proposed method with the existing literature, the laboratory experimental data i.e. actual PD Source location, time delays from [10] are adopted and analyzed. The PD Source location results using proposed method and available literature results are shown in the table 4.5. From the table 4.5, the Proposed FAPSO locates the PD Source within 6 to 9.69 mm, whereas the Proposed FAPSO-I locates within 3.74 to 8.25mm for trail 1 and for trail 2, the Proposed FAPSO locates the PD Source within 3.46 to 7.48 mm, whereas the Proposed FAPSO-I locates within 1.73 to 3.74 mm and for trail 3, the Proposed FAPSO locates the PD Source within 5.09 to 7.07 mm, the Proposed FAPSO-I locates within 3 to 5.83 mm .Table 4.5 shows that proposed method FAPSO-I locates the PD Source within overall location error maximum of 8.25 mm and minimum of 1.73 mm for laboratory data case. From the table 4.5, it is noted that the PD location error decreases for accurate time delay measurements from the sensors and increases for inaccurate time delay measurements from the sensors and also noticed that the proposed algorithms FAPSO,FAPSO-I gives minimum PD location error compared with PSO and LSE methods.

Table 4.6. Error Analysis Comparison of Laboratory PD source among available literature with proposed methods.

PD source position No	Actual Coordinates (mm)	Maximum Deviation error of LS (mm)	Maximum Deviation error of PSO (mm)	Maximum Deviation error of FAPSO (mm)	Maximum Deviation error of FAPSO-I (mm)	Relative Error of LS (%)	Relative Error of PSO (%)	Relative Error of FAPSO (%)	Relative Error of FAPSO-I (%)
1-1	(392,700,490)	200	19	9	4	10.03	1.14	0.55	0.26
1-2		312	26	6	6	25.66	1.79	0.43	0.47
1-3		382	9	4	3	27.84	0.78	0.34	0.21
1-4		236	12	5	3	16.99	0.79	0.37	0.27
2-1	(510,700,410)	218	16	6	2	16.89	1.11	0.43	0.2
2-2		135	15	3	1	10.97	1.23	0.19	0.1
2-3		140	14	4	2	10.69	0.84	0.28	0.14
2-4		195	12	5	3	16.82	0.69	0.41	0.21
3-1	(883,700,690)	412	17	4	3	24.16	1.08	0.29	0.23
3-2		327	12	5	4	20.05	0.82	0.35	0.31
3-3		143	13	5	4	11.59	0.75	0.40	0.33
3-4		108	12	6	2	10.27	0.78	0.35	0.17

Table 4.6 shows FAPSO locates the PD Source within 4-9 mm of maximum deviation whereas FAPSO-I locates the PD Source within 3-6 mm and for trail 2 FAPSO locates the PD Source within 3-6 mm of maximum deviation whereas FAPSO-I locates the PD Source within 1-3 mm and for trail 3 FAPSO locates the PD Source within 4-6 mm of maximum deviation whereas FAPSO-I locates the PD Source within 2-4 mm. Table 4.6 shows that proposed method locates the PD Source within overall maximum deviation of highest value 6mm and lowest value of 1 mm for laboratory data case ,which can be allowed negligible for distances of practical interest. From the table 4.6, it is noted that the maximum deviation of PD source decreases for accurate time delay measurements from the sensors and increases for inaccurate time delay measurements from the sensors. The relative error of the LS method varies from 10.03 -27.84% and for PSO method varies from 0.75 - 1.79% whereas for the proposed methods FAPSO varies from 0.19 -0.55% & FAPSO-I varies from 0.1- 0.47%.

4.7 Summary

In this paper, fuzzy adaptive PSO (FAPSO-I & FAPSO) has proposed to obtain search capabilities of the particles. The PSO result greatly influences on inertia weight (w) and learning factors (c_1&c_2) and it may trap into local premature convergence problem. To prevail over this problem, inertia weight is tuned dynamically by using conditional IF -THEN statements in order to obtain the global best solution. From the output results, it is noticed that the proposed FAPSO-I method converge to global optimum solution owing to inertia weight fuzzification. To analyze the fuzzy adaptive PSO correctly, the good choice of inertia weight and learning factors results in such a way that all the particles tend to move in the direction of global optimum location compared to PSO. Thus, the proposed FAPSO-I takes very less time owing to inertia weight has been tuned dynamically using fuzzy rules. This FAPSO-I method is more superior in terms of minimum location error and maximum deviation error for the accurate PD source localization in giving global best solution in comparison to FAPSO, LS, PSO, SA, LPSO, QGA and GA. Finally, this proposed method has shown good implementation and appropriate for localization of PD source and the output results of proposed method when compared to other methods reported in the literature attained desired better results.

CHAPTER 5

DETECTION AND LOCALIZATION OF PD SOURCE USING LOG PERIODIC DIPOLE ARRAY PRINTED UHF SENSORS

5.1 Introduction

Partial discharge detection has been acknowledged as the diagnostic tool for degradation of the insulation in power apparatus. Locating PD sources accurately not only helps to know the insulation of that particular electrical apparatus but also secures the long term reliable operation by eliminating potential faults occurring on them. UHF technique has gained more importance because of its high sensitivity and good signal to noise ratio than acoustic technique as explained in chapter 3 &4.

In this chapter, a seven element log periodic dipole array antenna is designed and validated. The structure is modified by selectively optimizing the elements of the array and the dipoles are shaped to provide additional capacitance which results in overall size reduction and flat gain performance. The coupling capacitance between the dipoles improves low frequency bandwidth and matching due to increase in electrical length of dipoles. The measured fractional bandwidth for the antenna is 126 % in a compact area of 110 mm **x** 140 mm ($0.495\lambda_0$ x $0.63\lambda_0$).

The PD Source Localization using narrow band and broad band LPDA UHF Sensors is performed in the laboratory. The PD signals received by the four LPDA UHF Sensors are then computed to yield the TDOA values. The first peak approach is utilized to determine the TDOA values of each case. These nonlinear equations are solved using PSO algorithm for every case.

5.2 Basic Principles for LPDA Antenna Design

The LPDA antenna is usually composed of a sequence of half wavelength dipole elements lying along the boom length as shown in Figure 5.1. These dipole elements are distributed in a planar array geometry at distances covering a logarithmic function of frequency. The basic terms like return loss, voltage standing wave ratio, bandwidth, input impedance, radiation

pattern, directivity and gain for any type of antenna or sensor are defined in the appendix[78] and the basic design principles of the designed LPDA Antenna is followed from [79] .

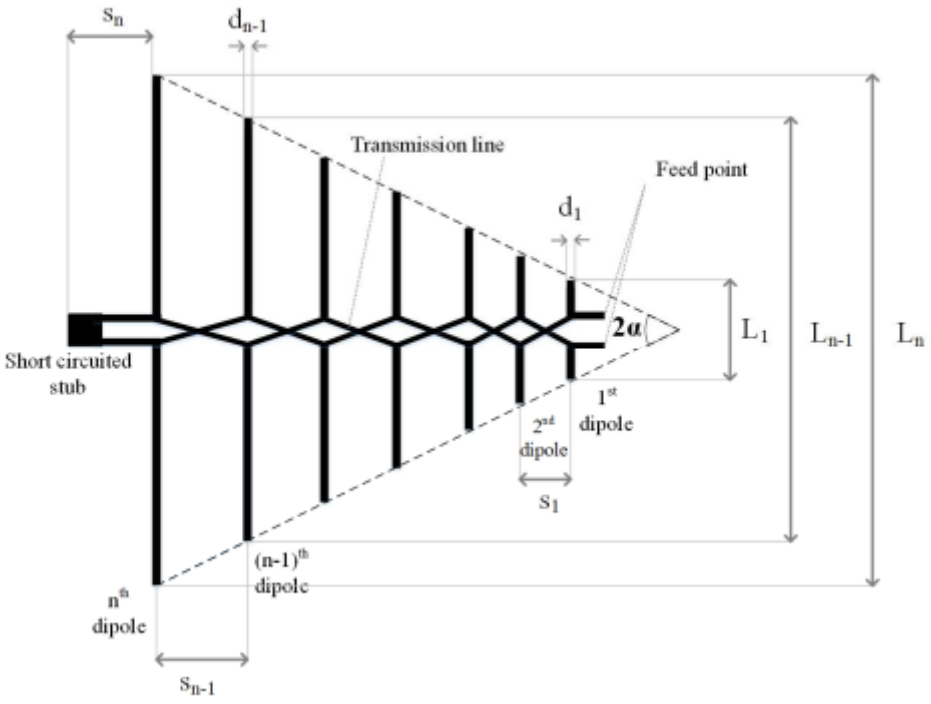

Figure 5.1 Schematic diagram of a generalized LPDA antenna

The lengths of consecutive dipole elements make a geometric progression with the common ratio $\tau < 1$. τ is called the scale factor. The spacing factor σ is defined as the ratio of the distance between close by elements to two times the longest dipole element length and is constant for a given antenna. The ratio of dipole element height (h) to radius (a) is similar for every dipole element in a particular LPDA antenna and will be designated by h/a. When the LPDA antenna is working at a wavelength inside the design limits. i.e. $4hN < \lambda < 4h1$. N is the total number of dipole elements; a linearly polarized unidirectional beam is noticed along the lower elements. The n^{th} dipole element half wavelength is h_N and the longest dipole element half wavelength is h_1.

The fluctuation in operation over a log span is nominal thereby frequency independent functioning results in most of the cases. The infinite structure of the LPDA antenna can be approximated by the truncated active region of the LPDA. The total number of dipole elements connected to the feeder is termed as active region. The information of active region width is essential in the designing of LPDA antenna to consider a specific bandwidth. The

longest dipole element length determines the lower cutoff frequency of the LPDA antenna. If the active region is very narrow, the considerable working bandwidth of the LPDA antenna is given by the ratio of longest to lowest dipole element and this ratio is named as structure bandwidth, B_s. As active region has some width, it is evident that the working bandwidth 'B' is always smaller than B_s by a factor named B_{ar} active region bandwidth.

The LPDA antenna input impedance is calculated at the junction of the lowest dipole element and the feeder. Theoretically, the input impedance at the top of an infinite log periodic design must be similar for all frequencies specified by the scaling factor.

The characteristic pattern of this LPDA antenna does not relies on number of dipole elements [90, 91]. Hence, according to the definition, this LPDA antenna can be named frequency independent with respect to its radiation pattern. This response is distinct of measured and computed patterns [98, 99]. When there is an end effect, the deviations may occur. The exceptions like pattern expand and side lobes may be seen sometimes described by patterns which alter with frequency. This trend is proof for all LPDA antennas, the H-plane pattern results are strong dependent on array factor of the LPDA antenna whereas the E-plane pattern results hides less changes in the array factor. The H-plane beam width graph depicts that the active region covers distinct dipole elements, since the bandwidth of the pattern is considerably lower than the structure bandwidth [100, 101].

The scaling factor (τ) and the spacing factor (σ) mainly focus on the LPDA antenna radiation pattern shapes. The calculated directivity (dB) shown in the figure A.1 of appendix are performed based on the Kraus formula,

$$D = 10 * log\left(\frac{41253}{(BW_E)(BW_H)}\right)$$

where BW_E, BW_H are the half power beam widths in degrees. The comparison of measured and calculated directivity for distinct LPDA models are shown in the Table A.1 of appendix.

If the spacing factor (σ) is larger than the optimum spacing factor (σ_{opt}) then the directivity decreases and the patterns is either inclined toward broad side or side lobes may occurs. Besides, the length of LPDA antenna for a required bandwidth becomes desirable. The scaling factor (τ) less than 0.8, only the single dipole element is at near resonance for a given frequency and it couples with limited energy from the feeder which may give rise to end effect there by damaging log periodic performance.

Table A.2 of the appendix tabulates the parameters and qualitatively defines how these values impact the performance. The LPDA antenna directivity relies on the integration of scaling factor (τ) and the spacing factor (σ) and does not depend on the feeder impedance.

The generalized LPDA design procedure is given below

- The number of dipole elements is decided by the scaling factor (τ), as the scaling factor value increases, the number of dipole elements increases.
- The size of the LPDA antenna is governed by the distance between the lowest and longest dipole element called boom length which usually relies on the angle α. As angle increases the size decreases and vice- versa.
- The selection of one set of scaling and spacing factors values guides to boom length and another gives rise to least number of dipole elements.
- Structure Bandwidth decides the boom length and total number of dipole elements. For some values of B_s lowest boom length may not be achieved for the values of scaling and spacing factors within the working range.
- Probably, the initial guess values of scaling and spacing factors will not decrease the boom length and total number of dipole elements. Continuing the process for distinct values of scaling and spacing factors may determine the trend and base design will get readily visible.

5.3 LPDA Antenna Structure and Design

The log periodic dipole array antenna with seven dipole elements is shown in Figure 5.2. The planar dipoles are arranged on top and bottom copper layers of the FR4 substrate with a dielectric constant of 4.4 and substrate thickness of 3.2mm. The initial elements are designed based on Carrel table for the log periodic antenna [105]. The length of the dipole (L), distance between the elements (d) and the width of the dipoles (W) are varied logarithmically to achieve wide bandwidths and flat gain performance for the antenna array. Traditionally, this method is used for UHF and VHF antennas to achieve broadband characteristics. Since, the dipole structure is on either side of the substrate, it results in a single back lobe radiation, as back lobe radiation is dependent on the angle between the dipole arrays. The basic principle and mathematical analysis are presented here for completeness. The geometry constant (τ), angle (α) and space constant (σ) are defined as in equation (5.1) and (5.2)

$$\tau = \frac{W_k}{W_{k-1}} = \frac{L_k}{L_{k-1}} = \frac{d_k}{d_{k-1}} \quad (5.1)$$

$$\alpha = tan^{-1}\left(\frac{1-\tau}{4\sigma}\right) \quad (5.2)$$

where W_k, L_k and d_k (the subscript k=2,3,….N and N is the number of the dipoles) are the width, length and distance between the elements for the k^{th} element and W_{k-1}, L_{k-1} and d_{k-1} are the width, length and distance between the elements for the $k\text{-}1^{th}$ element. k^{th} element is the largest dipole element.

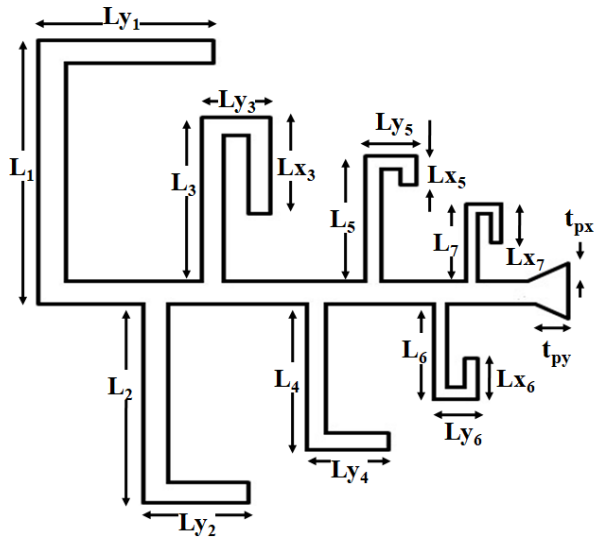

Figure 5.2a Top layer of the proposed LPDA UHF sensor

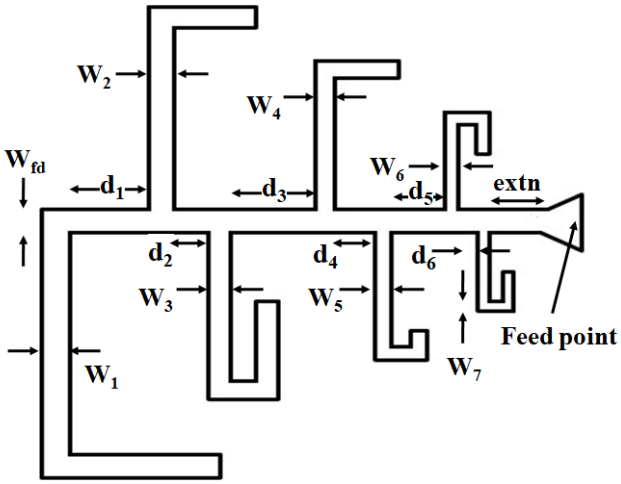

Figure 5.2b Bottom layer of the proposed LPDA UHF sensor

The dipoles are resonant at their corresponding half wavelengths. The bandwidth depends up on the values of τ and σ, the required number of dipole elements are high, if the value of τ is high and the length of antenna increases, if the value of σ is small. Hence, to keep the antenna

to a reasonable length the values of τ and σ are chosen to be 0.78 and 0.14, respectively. The substrate height and width of the feed line is chosen so that the input impedance of the line is 50 Ohms. This is achieved using taper lines at the coaxial to microstrip transition. This improves the return loss of the antenna. Coaxial feed is chosen in this design to simplify the feed mechanism by eliminating the balun structure which performs impedance match between the antenna and the feed. The match between the port impedance of 50 Ohms and input impedance for initial LPDA antenna is substantiated by plotting the S11 as shown in Figure. 5.3. The initial design values are obtained from the Eqns (5.1) and (5.2). The selection of the dipole elements for improving the return loss performance of the antenna array are L_1, L_2 and L_5 as the return loss represented by S11 in dB at the mid-band frequencies (i.e. 1.2 GHz to 1.7 GHz) and at 2 GHz is poor compared to other frequencies. The dimensions of the fabricated LPDA are given in Table 5.1.

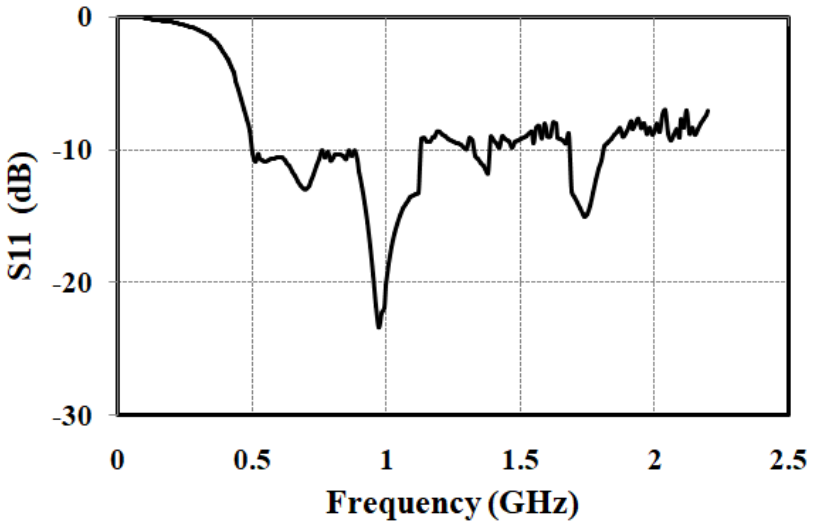

Figure 5.3 Simulated S_{11} of the initial LPDA UHF sensor

TABLE 5.1 DIMENSIONS OF THE DESIGNED ANTENNA STRUCTURE IN MILLIMETERS

L_1	L_2	L_3	L_4	L_5	L_6	L_7	Ly_1	Ly_2
42	35	27	23	18	14	9.5	50	28
Ly_3	Ly_4	Ly_5	Ly_6	Ly_7	Lx_3	Lx_4	Lx_5	Lx_6
7	12	9	6	4	22	6	7	6
Lx_7	W_1	W_2	W_3	W_4	W_5	W_6	W_7	W_{fd}
5.2	6.5	6	5.4	6.5	4.2	2.8	1.8	6
d_1	d_2	d_3	d_4	d_5	d_6	extn	t_{px}	t_{py}
15	10	20	12	13	9.6	15	1.4	15

5.4 Parametric study and Analysis

Parametric analysis is performed to investigate the effects of dipole length, width and distance between the elements on antenna return loss and bandwidth using ANSYS HFSS 3D EM simulation software. In this analysis, one parameter is varied while keeping other parameters constant.

5.4.1 Variation of feed line width

The feed line width affects the input match of the antenna and is matched to an impedance of 50 Ohms. The variation in width is performed in steps of 0.5 mm and return loss is shown in Figure 5.4. The variation of return loss is not considerable and the overall bandwidth is not varying. Hence, feed line width does not affect the bandwidth to a larger extent.

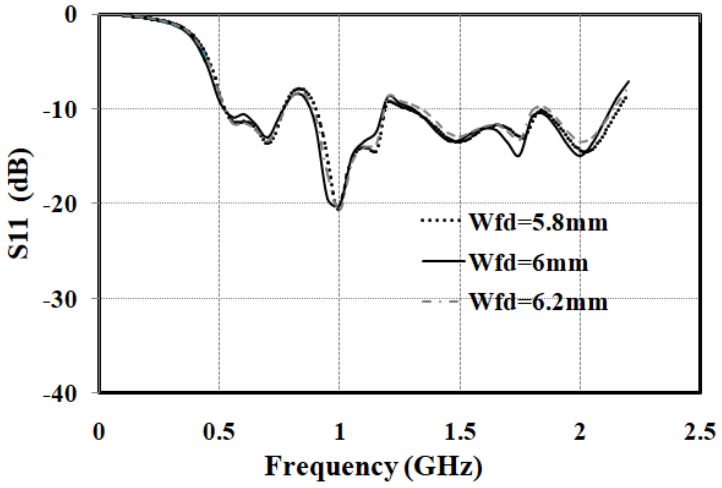

Figure 5.4 Simulated S11 for variation in feed width of the antenna

5.4.2 Variation of distance between dipole elements

The variation of distance between the dipoles is studied by considering the distance between the fourth and fifth dipole elements. This is considered as it is the smallest distance and hence, the interaction between these two dipoles would be high. This also affects the length of the dipoles as mutual coupling between the elements increases with closely spaced dipoles. It is observed that there is an improvement in the return loss at 1.5 GHz and 2 GHz as shown in Figure 5. 5. However, bandwidth is almost same for all the values of d_4.

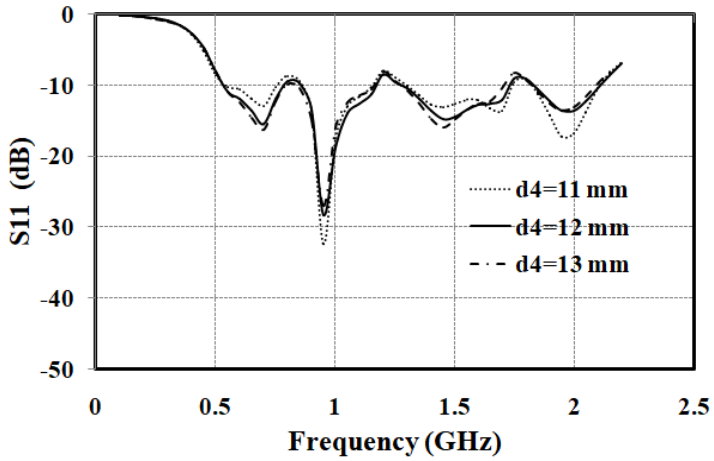

Figure 5.5 Simulated S11 for variation in d_4 of the antenna

5.4.3 Variation of length Ly_1 and Ly_2

The length L_{y1} is length of the lowest frequency dipole elements. The first dipole element is shaped along with other dipole elements to fit the antenna into a compact size. The length L_{y1} and L_{y2} act as coupled lines due to which the effective electrical length of both the dipoles increases without increasing the physical lengths of the elements. The increase in electrical length results in improvement of the return loss of the antenna array at lower frequencies. It is observed from the variation of L_{y1} that the return loss bandwidth is increasing at the lower frequency range and the variation of L_{y2} causes the return loss to improve by providing better matching at lower frequencies as can be observed from Figure 5.6 and Figure 5.7.

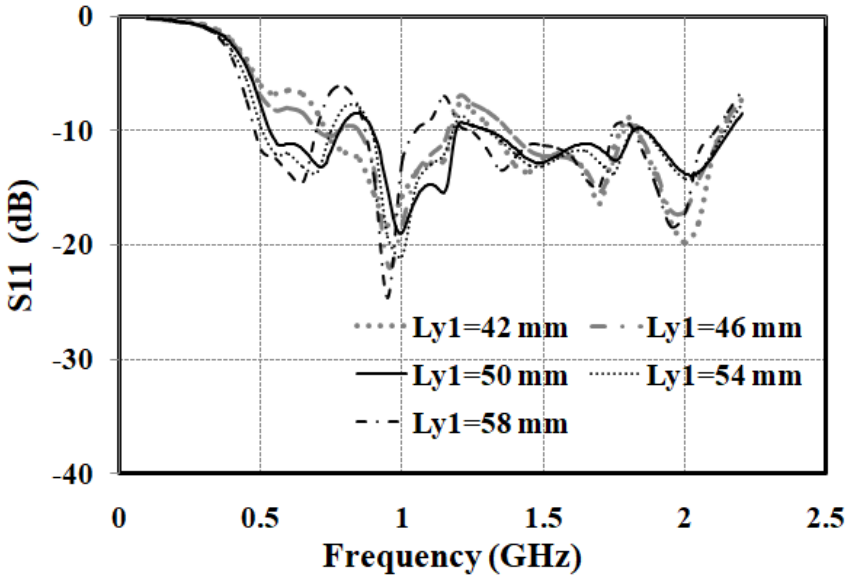

Figure 5.6 Simulated S11 for variation in Ly_1 of the antenna.

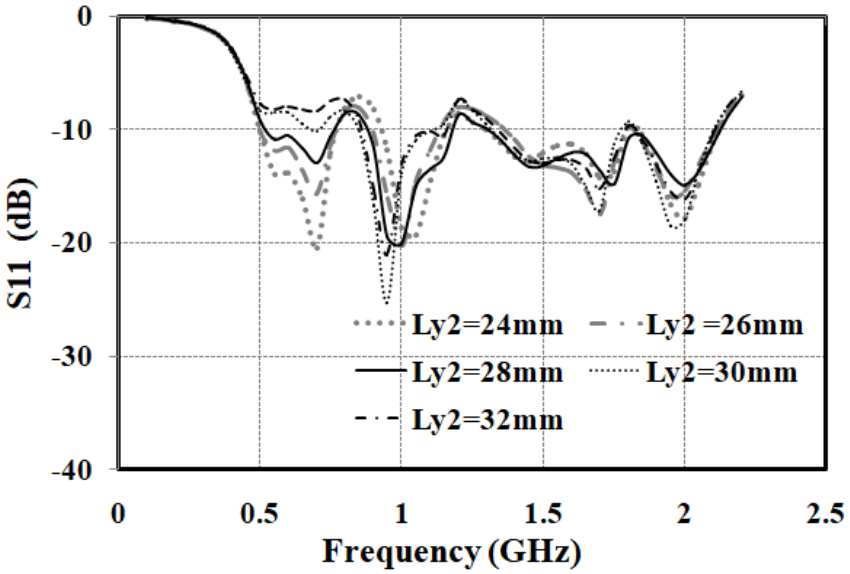

Figure 5.7 Simulated S11 for variation in Ly_2 of the antenna

5.4.4 Variation of length Ly_5

The length of the fifth dipole is considered as the return loss characteristics of the LPDA are poor at mid-band and 2 GHz. As discussed earlier, the largest dipole affects the lowest frequency and smallest dipole affects highest frequency. Hence, the lengths of the middle elements would affect the return loss at mid-band frequencies of the antenna. The fifth element affects the return loss the most which can be observed from the return loss plots shown in Figure 5.8. The return loss in the mid region is drastically affected even though there is no variation in the lower frequencies regions.

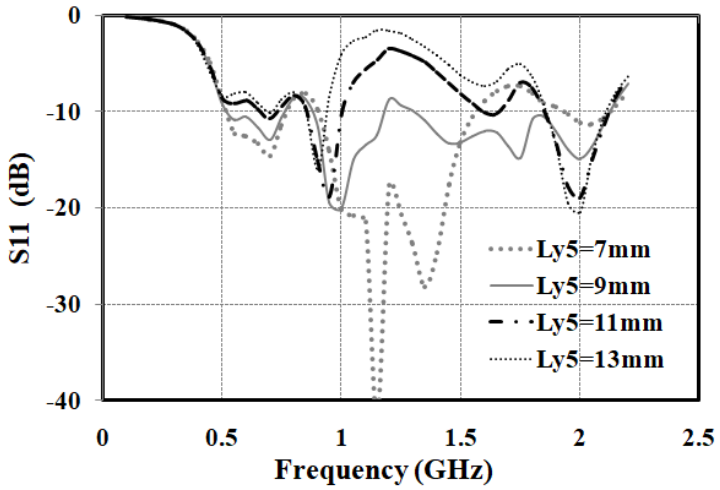

Figure 5.8 Simulated S11 for variation in Ly_5 of the antenna

5.5 Measured Antenna Results and Discussion

The simulations are validated with a fabricated prototype of LPDA antenna and experimentally tested. The fabricated LPDA prototype antenna is shown in Figure 5.9. The coaxial feed is manually soldered across both ends of the feed line with center conductor soldered to top structure and outer conductor is soldered to the bottom structure. The coaxial feed is extended towards the largest dipole from feed point to reduce interference in the radiation pattern of the antenna. The measured and simulated return loss of LPDA UHF sensor is shown in Figure 5.10.

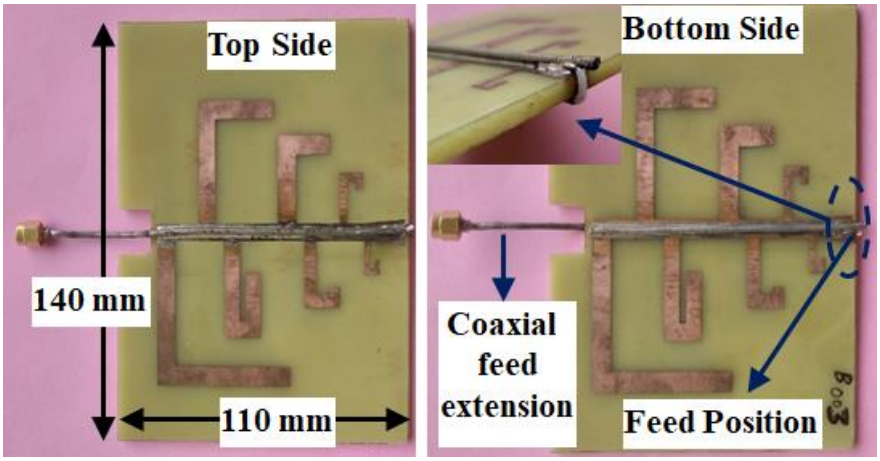

Figure 5.9 Top and bottom side of the fabricated LPDA antenna prototype. (inset picture shows feed position)

The measurements are carried out using HP8719A vector network analyzer. The proposed antenna meets the specification of S11 < -10 dB over 0.5 GHz - 2.2 GHz frequency range. The measured 10 dB return loss bandwidth of the designed antenna is 126%. The simulated results are closely matching the measurement results validating the taper design and lengths of the dipole elements.

The simulated and measured radiation patterns are compared and shown in Figure 5.11 (a-e). The E-plane and H-plane patterns have been measured at 0.7 GHz, 1 GHz, 1.5 GHz, 2 GHz and 2.2 GHz respectively. The patterns could not be measured at the lowest frequency i.e. 0.5 GHz due to non availability of the anechoic chamber at that frequency. The E-plane radiation pattern for the above measured frequencies is a directional pattern and the beam width is also sufficient to capture the partial discharges in transformers. The slight variations in the measured and simulated back lobe patterns of the antenna are due to interference caused by coaxial cable feeding the antenna.

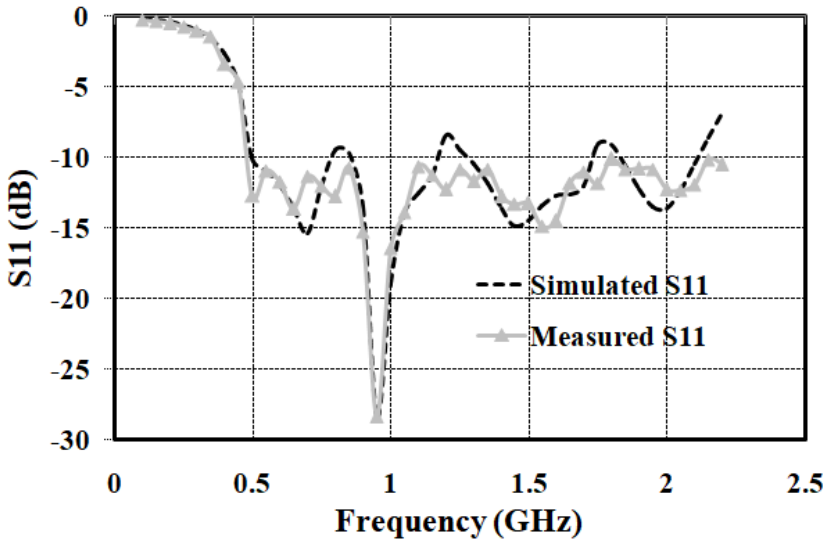

Figure 5.10 Simulated and measured S11 of the antenna

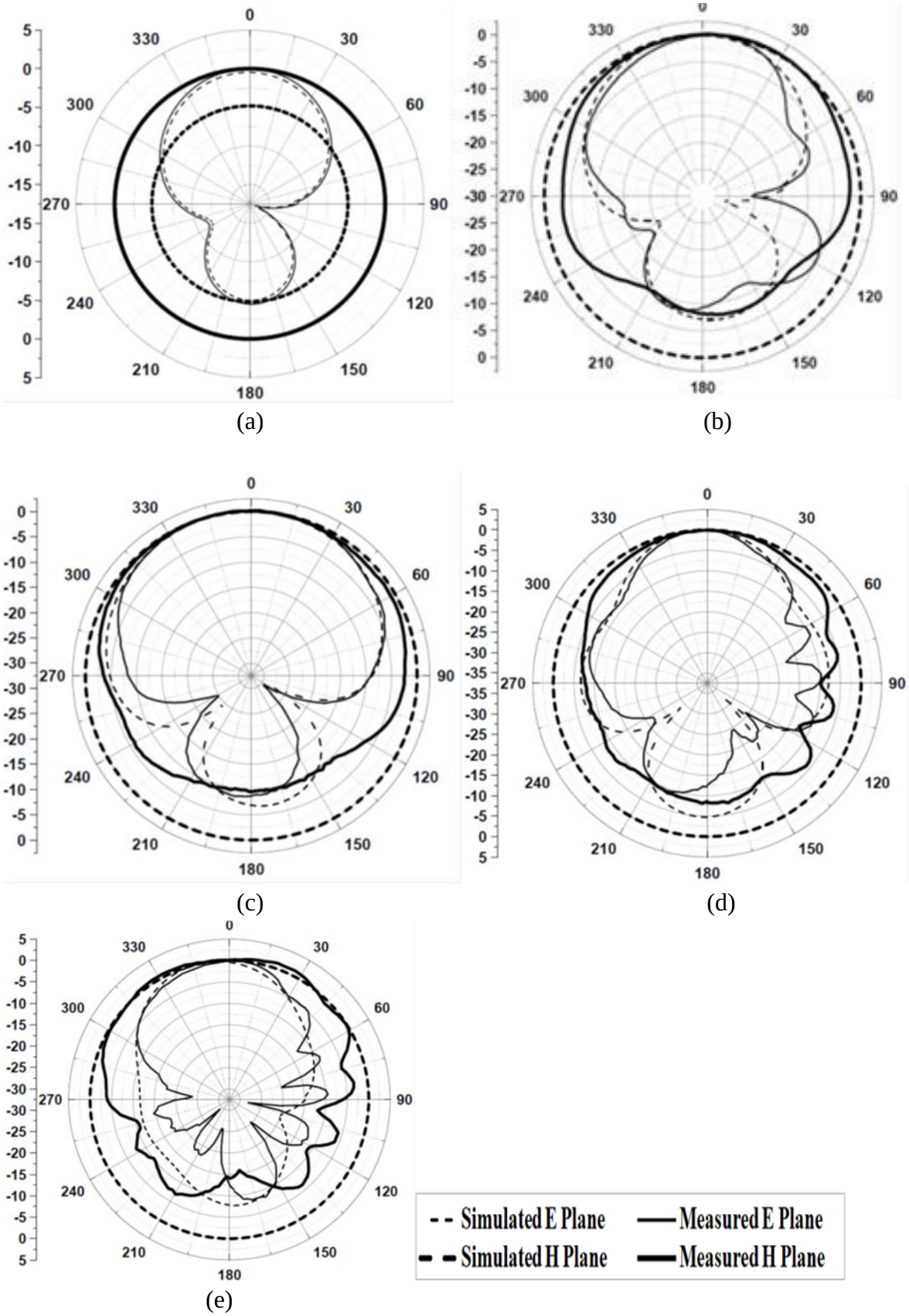

Figure 5.11 Simulated and measured radiation patterns for the fabricated antenna (a) 0.7 GHz (b) 1 GHz (c) 1.5 GHz (d) 2 GHz (e) 2.2 GHz

The gain of the antenna is measured in an anechoic chamber using gain transfer method wherein two sets of received power measurements are performed for standard antenna (P_{Std}) and prototype test antenna (P_{AUT}). The gain of the prototype test antenna (G_{AUT} in dB) is obtained as G_{std} (dB) + P_{AUT} (dBm) - P_{Std} (dBm). The reference antenna used in the radiation pattern and gain measurement is bi-conical antenna EM-6917B-2 (26MHz – 3GHz). The measured gain of the antenna is -1 to 4.3 dBi over 0.7 – 2.2 GHz with almost flat gain of 4 dBi from 0.8 – 2.2 GHz and is shown in Figure. 5.12. Within this bandwidth, the effective antenna height is higher than 15 mm as shown in Figure. 5.13. The designed antenna is compared with other recent reported structures to show its effectiveness in Table 5.2. The comparison is with respect to frequency range, fractional bandwidth, antenna size, return loss, gain and effective antenna height.

The antenna factor (A.F) of the designed LPDA antenna is calculated using Eqn (5.3)

$$A.F = \frac{9.73}{\left({}^{300}\Big/ {}_{(particular\ frequency)*\sqrt{10^{(gain(dB)/100)}}} \right)} \tag{5.3}$$

The effective height of the designed LPDA antenna is calculated as the inverse of antenna factor (A.F).

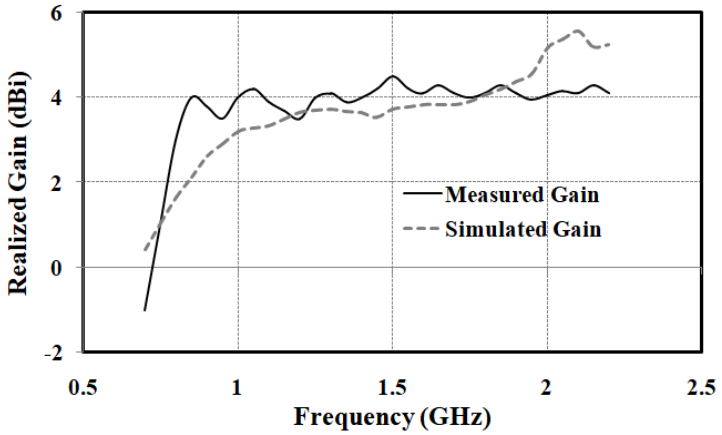

Figure 5.12 Simulated and measured realized gain of the proposed LPDA antenna.

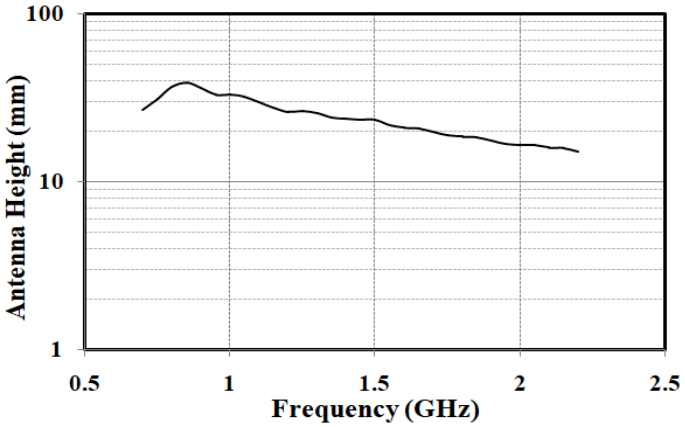

Figure 5.13 Effective height of the proposed LPDA antenna.

Though, the published works in [91, 93, 97, 100] exhibit slightly higher fractional bandwidth compared with proposed antenna but they occupy an area 2.3 times larger than 0.31 λ_0^2. The highest fractional bandwidth among the compared antennas is exhibited by [96] and [100], but it also occupies the largest area among the compared antennas (i.e. 7.1 and 46 times the proposed antenna, respectively). The gain characteristics of the proposed antenna is flat compared to [95] wherein gain varies over a wide range leading to variations in the voltage measurement for different frequencies. Though, [82, 95] proposes a compact antenna (0.41 λ_0^2 and 0.25 λ_0^2), the fractional bandwidth of the antenna are 88% and 100%, respectively when compared to 126% for the proposed antenna. When comparing the antenna dimension the center frequency is used for calculating λ_0.The proposed antenna also achieves an antenna height of 15 mm (0.7 – 2.2 GHz) which is better than antenna height of 13 mm (0.8 - 1.8 GHz) and 8 mm (0.5 - 1.5 GHz) presented in [82, 95] showing the effectiveness and higher sensitivity of the proposed design.

5.6 Partial Discharge Experiment and Results

The designed LPDA UHF antenna is used as a proof of concept for detection of PD's like corona defect, particle movement defect, free particles defect and surface defect. The corresponding frequency range of the above PD defects falls between 0.5 - 2.2 GHz. The block diagram and the experimental set-up of PD detection by the designed LPDA UHF sensor are shown in Figure 5.14(a-c). The test cell used for measurement consists of top and bottom electrodes filled with transformer oil in a cylindrical Perspex tube as shown in Figure 5.14 (b). The particle movement discharge test cell has 25 mm diameter aluminum sphere and a 2 mm diameter aluminum ball is kept on a 55 mm bottom with slightly concave plane

having a 1 cm gap between the two electrodes The test cell of corona discharge has a top copper needle

Table 5.2.Performance comparison of designed antenna with other reported antennas in the literature

Ref	Dimension (LxW) (mm)	Antenna Size (Area)	Freq. range (GHz)	Gain (dBi)	S_{11} (dB)	FBW (%)	Eff. Ant. Ht. (mm)
[82]	190 **x** 60	$1.14\lambda_0$ **x** $0.36\lambda_0$ ($0.41\ \lambda_0^2$)	1.0 – 2.6	-	-6	88.9	> 13
[91]	368 **x** 300	$1.35\lambda_0$ **x** $1.1\lambda_0$ ($1.49\lambda_0^2$)	0.4 – 1.8	-3 to 1.8	-10	127.3	-
[93]	200 **x** 200	$1.03\lambda_0$ **x** $1.03\lambda_0$ ($1.07\ \lambda_0^2$)	0.5 – 2.6	0-4.8	9.55	135.5	-
[94]	202 **x** 202	$0.84\lambda_0$ **x** $0.84\lambda_0$ ($0.71\ \lambda_0^2$)	0.5 – 2.0	-11 to 8*	-10	120	-
[95]	150 **x** 150	$0.5\lambda_0$ **x** $0.5\lambda_0$ ($0.25\ \lambda_0^2$)	0.5 – 1.5	-	-	100	8
[96]	282 **x** 242	$1.59\lambda_0$ **x** $1.37\lambda_0$ ($2.19\ \lambda_0^2$)	0.4 – 3.0	-5 to -11	-10	152.9	-
[97]	300 **x** 300	$0.9\lambda_0$ **x** $0.9\lambda_0$ ($0.81\ \lambda_0^2$)	0.3 – 1.5	-1 to 5*	-10	130	-
[98]	154 **x** 84	$0.77\lambda_0$ **x** $0.42\lambda_0$ ($0.32\ \lambda_0^2$)	0.8 – 2.2	2 to 6	-10	87.3	-
[99]	420 **x** 577	$0.70\lambda_0$ **x** $0.97\lambda_0$ ($0.68\ \lambda_0^2$)	0.2 - 0.8	3.2 to 5.5	-10	120.2	-
[100]	260 **x** 218	$3.45\lambda_0$ **x** $4.17\lambda_0$ ($14.39\ \lambda_0^2$)	0.5 - 10	3 to 6	-10	181	
This work	110 **x** 140	$0.495\lambda_0$ **x** $0.63\lambda_0$ ($0.31\lambda_0^2$)	0.7 – 2.2	-1 to 5	-10	126	> 15

* Simulated results. λ_0 Is the wavelength at centre frequency.
Eff. Ant. Ht. is Effective Antenna Height

attached to aluminum rod having radius of curvature of 40 µm and 50 mm bottom aluminum circular plane has a gap of 1 cm between both electrodes. The test cell for free metal particles discharge has a 25 mm diameter top aluminum sphere and 55 mm slightly concave plane having a 1 cm gap between the two electrodes. Inside the test cell, two different particles i.e. 2 mm aluminum ball and copper bead on the bottom electrode are placed. The test cell for

surface discharge has 25 mm diameter aluminum top sphere and 55 mm bottom slightly concave plane having 1 cm gap. Inside the test cell, a pressboard of 5 cm diameter and 2 mm thickness is placed between the two electrodes.

The four PDs i.e. particle movement, Corona, free metal particles and surface discharges are generated at 7.6 kV, 8.7 kV, 10.6 kV and 11.8 kV, respectively. The antenna is placed at a distance of 1m to capture the PD signals. These signals are then viewed in oscilloscope or spectrum analyzer as shown in Figure 5.14(c).

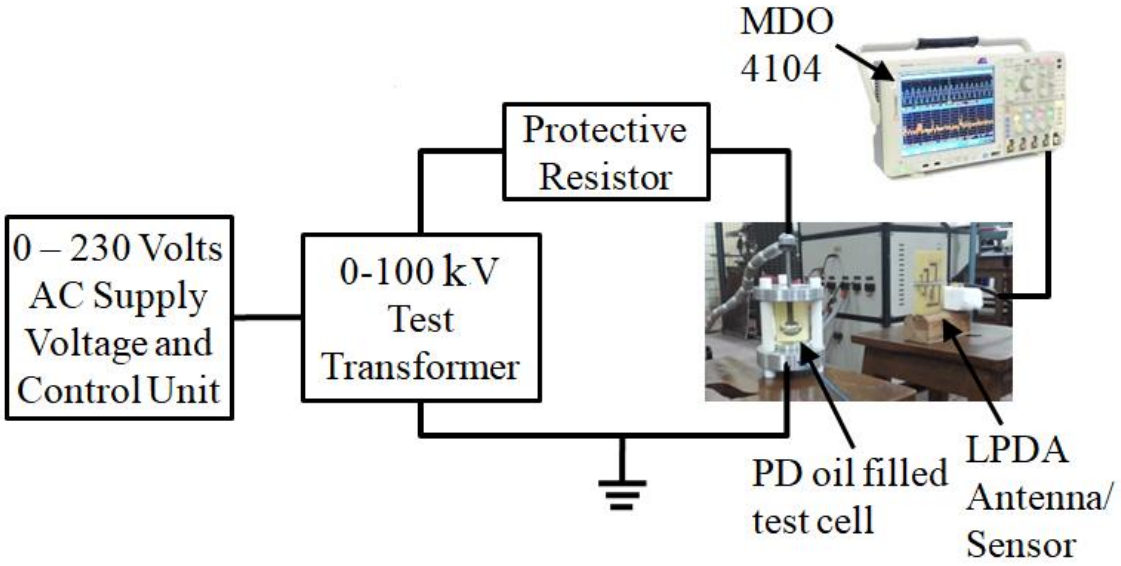

(a)

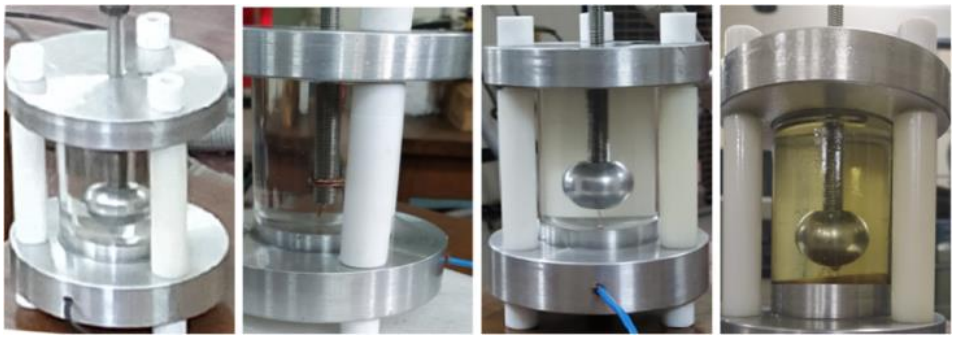

(b)

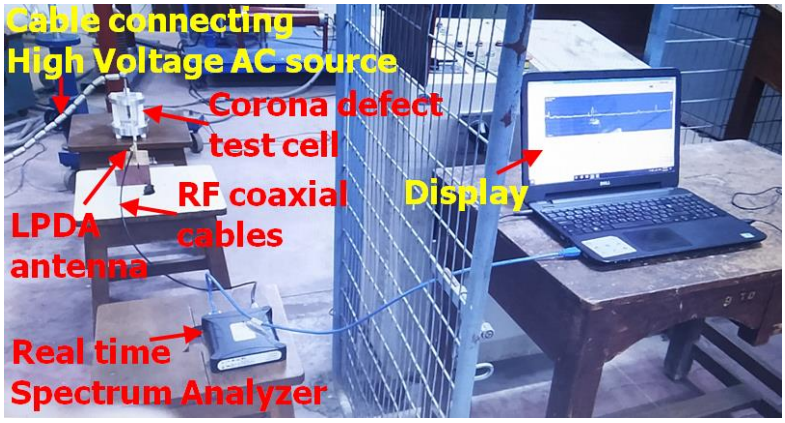

(c)

Figure 5.14 (a) Block diagram of the PD test system using oscilloscope (b) PD test cells (particle movement, corona, free metal particle and surface defect test cells respectively) (c) PD experimental set-up for antenna in lab using spectrum analyser

Figure 5.15 (a) & (b) shows the UHF time domain signal and the respective Fast Fourier Transform (FFT) of the particle movement discharge and its characteristic frequency covers from 0.5 - 1 GHz. The time and frequency domain signals of corona discharge as shown in

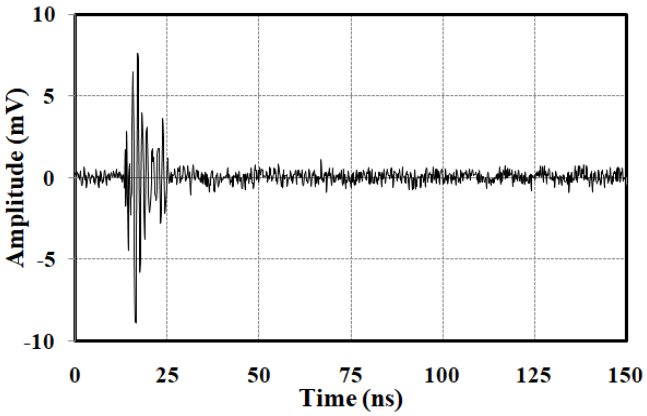

(a)

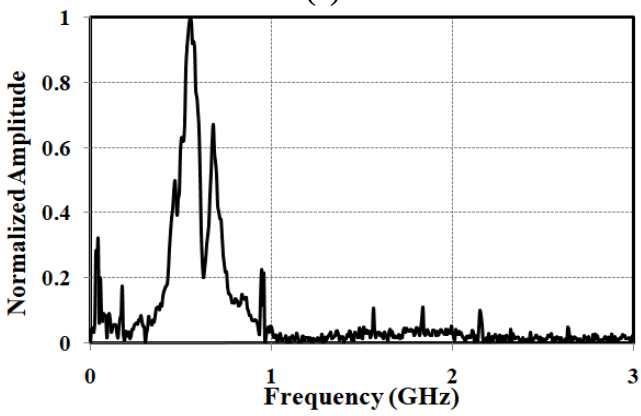

(b)

Figure 5.15 Particle movement defect at an inception voltage of 7.6 kV in transformer oil (a) Time domain (b) Normalized FFT of UHF signal

Figure 5.16 (a) & (b) and its characteristic dominant frequency contents lie in 0.4-0.8 GHz. It is observed from Figure 5.17 (a) & (b) the dominant frequency signals of free particles discharges are from 0.5 - 0.85 GHz and at 1.6 GHz. The characteristic frequency contents of the surface discharges fall in the range of 0.1 - 1 GHz, 1.6 GHz and 2.1 GHz as shown in the Figure 5.18 (a) & (b). The PD experiment result reveals that the designed LPDA UHF sensor is capable of detecting the four different incipient discharge signals with oil filled test object.

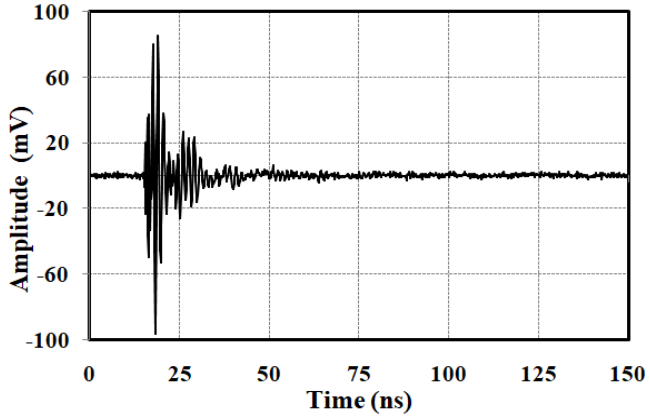

(a)

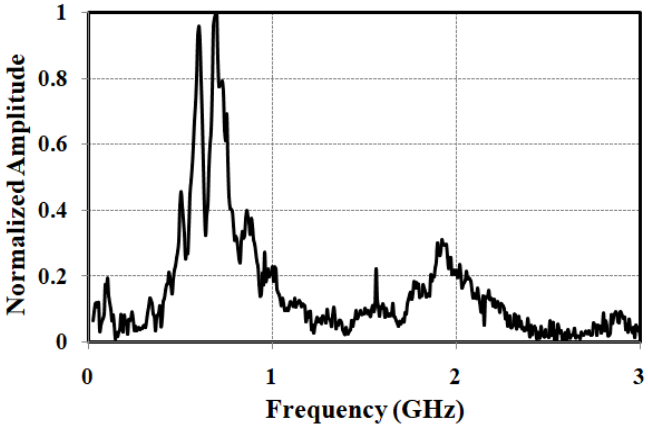

(b)

Figure 5.16 Corona defect at an inception voltage of 8.7 kV in transformer oil (a) Time domain UHF signal (b) Normalized FFT of UHF signal.

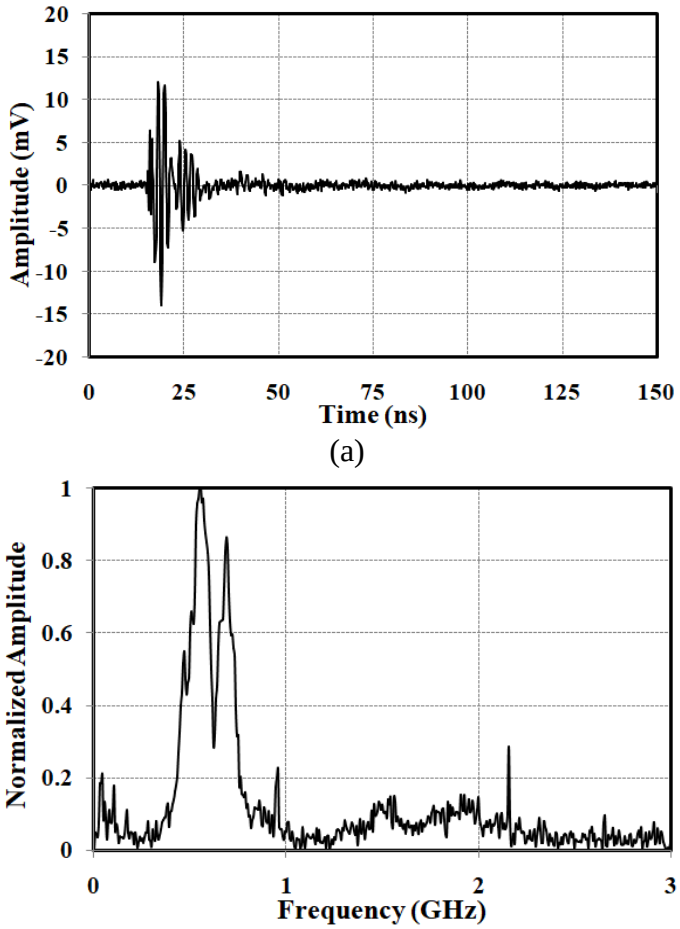

Figure 5.17 Free metal particles defect (aluminium ball and copper bead) at an inception voltage of 10.6 kV in transformer oil (a) Time domain UHF signal (b) Normalized FFT of UHF signal

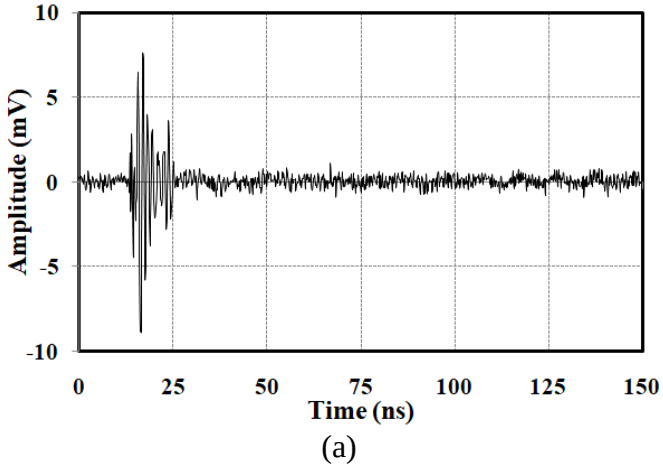

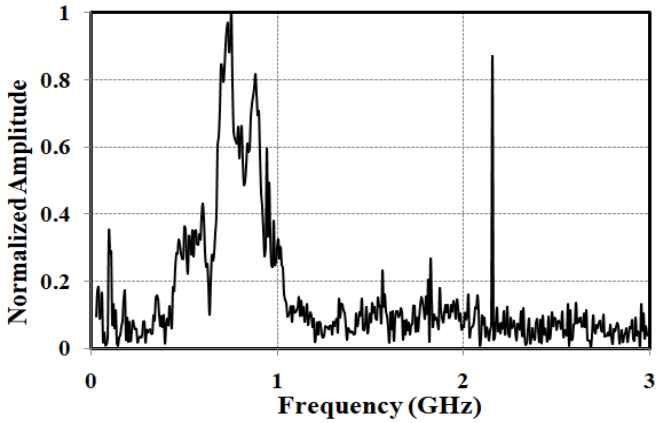

(b)

Figure 5.18 Surface defect at an inception voltage of 11.8 kV in transformer oil (a) Time domain UHF signal (b) Normalized FFT of UHF signal.

5.7 Localization of PD source using Narrow band LPDA UHF Sensors

Let 't' be the uhf signal propagation time travelling from PD source to the reference sensor S_1 , l be the light velocity which is equal to 3*10^8 m/s and τ_{12} ,τ_{13} , τ_{14} are the TDOA measurements of the uhf sensor signals from reference sensor S_1.The nonlinear equations are given in Eqn (5.3)

$$\left.\begin{aligned}(x-x_1)^2+(y-y_1)^2+(z-z_1)^2 &= l^2*t^2\\ (x-x_2)^2+(y-y_2)^2+(z-z_2)^2 &= l^2(t+\tau_{12})^2\\ (x-x_3)^2+(y-y_3)^2+(z-z_3)^2 &= l^2(t+\tau_{13})^2\\ (x-x_4)^2+(y-y_4)^2+(z-z_4)^2 &= l^2(t+\tau_{14})^2\end{aligned}\right\} \quad (5.3)$$

After acquiring the UHF sensors TDOA measurements, the PD source location can be estimated by solving Eqn (1). But, these are nonlinear equations and it is very difficult to calculate directly like traditional approaches. The Eqn (5.1) can be converted as an optimization problem with constraints. Thus, Eqn (1) can be written shortly as

$$d_j = (D_j - D_s) = l * (\tau_{j1}) \quad (5.4)$$

Where D_j is the distance of the PD source to the j^{th} sensor i.e.

$$D_j = \sqrt{(x_j-x)^2+(y_j-y)^2+(z_j-z)^2} \quad (5.5)$$

$$D_s = \sqrt{x^2+y^2+z^2} \quad (5.6)$$

Unfortunately, the'τ' is unknown and it is required to quantify UHF sensors TDOA to estimate the PD source location.

The Eqn (5.4) is then transforms to

$$d_j = \sqrt{(x_j - x)^2 + (y_j - y)^2 + (z_j - z)^2} - \sqrt{x^2 + y^2 + z^2} - l(t_j - t_1) \quad (5.7)$$

In the experiment set up, there is line of sight between PD source &four uhf sensors. The exact calculation of TDOA, ($t_j - t_i$) is important to locate accurate PD source position and even minute changes in this value can results a high uncertainty.

$$min\ d_j = \sum_{j=2}^{4} \{\sqrt{(x_j - x)^2 + (y_j - y)^2 + (z_j - z)^2} - \sqrt{(x_1^2 + y_1^2 + z_1^2)} - l * (\tau_{j1})\} \quad (5.8)$$

The tailor- made UHF sensors are used for incipient discharge localization in a free space. The laboratory experimental set up is developed as shown in the Figure. 5.19. The tailor made log periodic dipole array antenna is used as UHF sensor. This sensor detects the PD signal in the range of (0.7-1) GHZ. The sensor is connected to mixed domain oscilloscope (MDO) through co axial cable. The UHF sensor output signal is displayed in MDO when incipient discharge occurred.

A test cell is designed for the occurrence of PD signal in a laboratory scenario, which consisting of a sphere and concave electrode with a 2 mm aluminum conducting spherical ball. The entire electrode system is filled with transformer oil and housing with Perspex tube. The test cell is energized by a100kV test transformer.

The experiment is conducted for two different positions in the laboratory without any external noise. When the PD is initiated with the applied HV supply, the four UHF sensors will acquire the PD signals simultaneously and displayed in the MDO. This procedure is repeated for different positions of PD source and sensors. The recorded four UHF sensors signals for a particular incipient discharge are shown in Figure 5.20.

Figure 5.19 Experiment Model for localization of PD source position number 1 in table 5.5

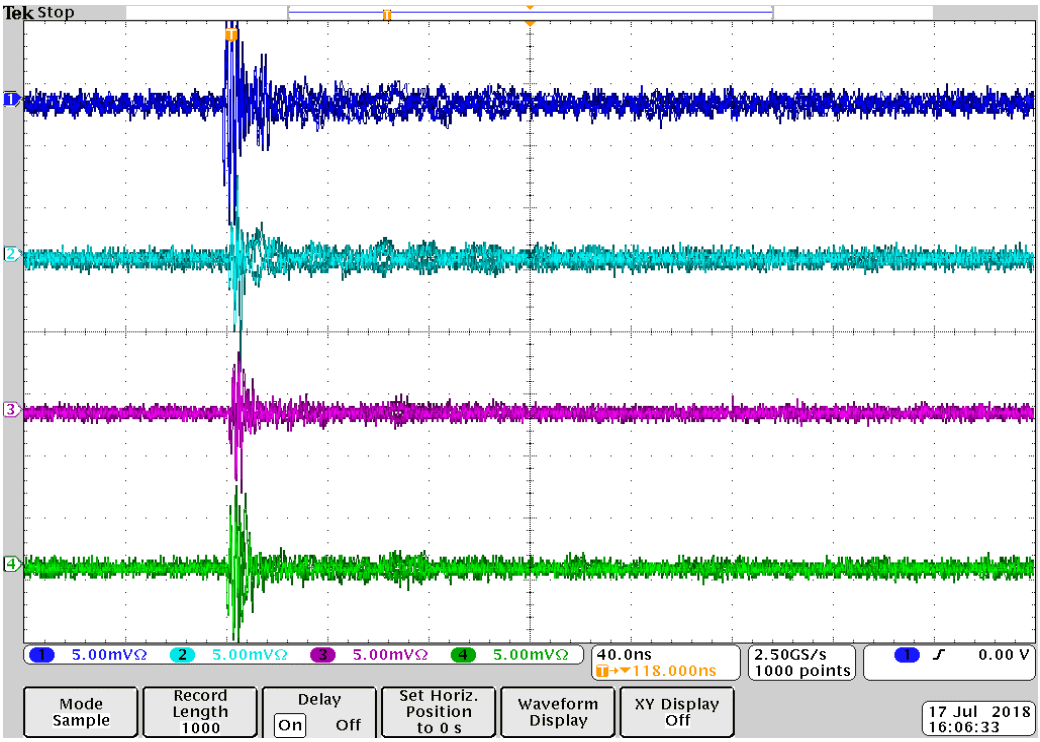

Figure 5.20 TDOA measurements of four UHF sensors for localization of PD source in laboratory scenario at 14.5kV

Figure 5.21 Experiment Model for localization of PD source position number 2 in table 5.5

A threshold value of 25% of signal amplitude is chosen for the calculation of TDOA values of each case using first peak approach.

5.7.1 Particle Swarm Optimization Algorithm

Eberhant and Kennedy developed PSO algorithm which is a population based meta-heuristic method in the year 1995.This algorithm is a nature inspired by flocking of birds. In this algorithm, each bird is treated as a particle and all the birds or particles together form as a group called as swarm. Every particle is constituted by two vectors X_i and U_i which indicates position or location and velocity of the particle. The location of every particle at a particular iteration is assumed as a solution to the problem at that iteration. The particle flies in the search space area and varies their velocities and positions. In a physical k dimensional search space, the velocity and position of every i^{th} particle are shown by the following vectors.

$U_i = [\ U_i^1, U_i^2, , , , , , U_i^k\ ]$

$X_i = [\ X_i^1, X_i^2 , , , , , X_i^k\ ]$

The best location of a particle is the position which gives the minimum objective function fitness value (F) to that particle. Let $Pbest_i$ =[$Pbest_i^1$,$Pbest^2_i$, , , , $Pbest_i^k$] be the local best position obtaining the local best fitness value for the i^{th} particle and similarly $gbest_i$ = [$gbest_i^1$

, $gbest_i^2$, , , , ,$gbest_i^k$] be the best global position in the population of whole swarm. The PSO algorithm upgrades its velocity and position using the following equation.

The learning factors C_1 and C_2 are assumed to be 2 which calculate the relative impact of cognitive and social component to upgrade the position and velocity of the particle. The range of two random numbers rand1 and rand2 are considered in between 0 to 1. $U_i^{K(t)}$ and X are the velocity and position of the i^{th} particle in the k dimension space at t^{th} iteration. The $gbest_i$ is the global best of the i^{th} particle in the k dimension at t^{th} iteration and $Pbest_i$ is the local best of i^{th} particle in k dimension at t^{th} iteration and w is the inertia weight parameter which regulates the exploration and exploitation of the search space.

$$V_k^{t+1} = W * V_k^t + C_1 * rand_1 * (P_{bestk} - x_k^t) + C_2 * rand_2 * (g_{best} - x_k^t) \quad (5.9)$$

$$x_k^{t+1} = x_k^t + V_k^{t+1} \quad (5.10)$$

Location Error can be determined by

$$\sqrt{(x_a - x_c)^2 + (y_a - y_c)^2 + (z_a - z_c)^2} \quad (5.11)$$

Table 5.3 PSO Algorithm Parameters

S. No	Parameters of PSO Algorithm	Assign Value
1	Maximum Number of Generations	100
2	Population Size	20
3	Learning Parameters (c1, c2)	2
4	Inertia Weight (w)	0.4 – 1

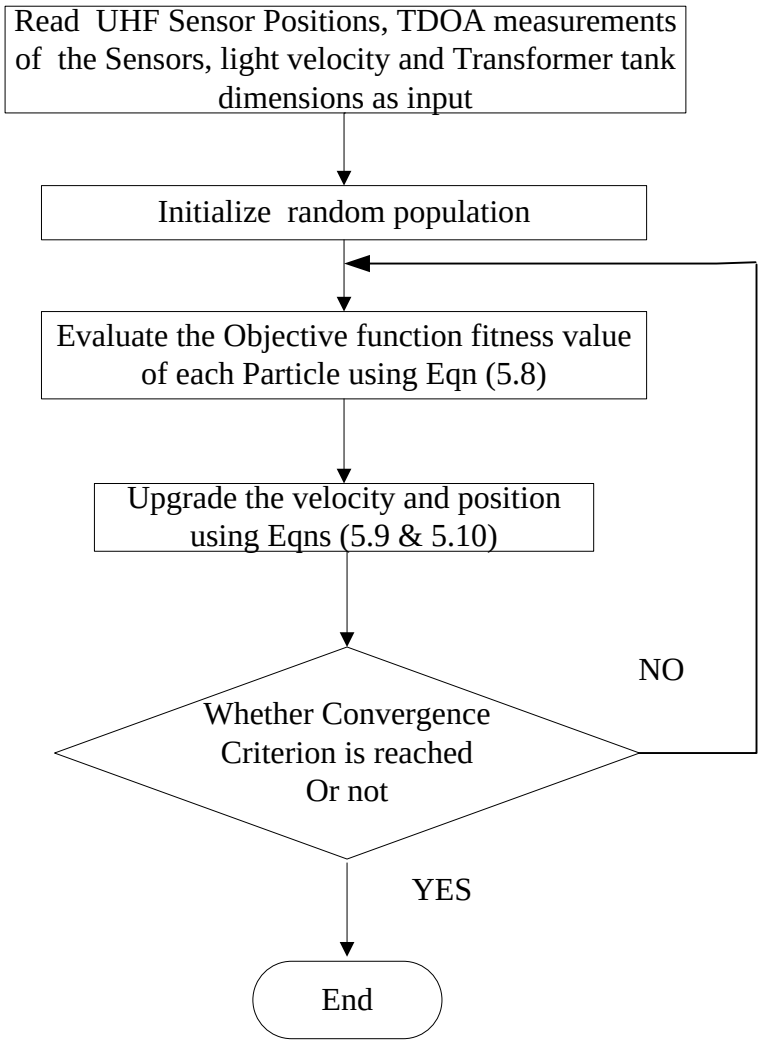

Figure 5.22 Flow chart of Proposed PSO algorithm

where x_a,y_a,z_a are actual coordinates and x_c,y_c,z_c are calculated coordinates.The source and sensors co ordinates are presented in Table 5.4 & 5.5

Table 5.4 Narrow band LPDA UHF Sensors Coordinates

Sensors No	**Coordinates (x,y,z) in cm**
Sensor 1	(47.5,0,0)
Sensor 2	(0,0,47.5)
Sensor 3	(47.5,0,100)
Sensor 4	(94,0,46)

Table 5.5. PD source Location Results using Narrow band UHF Sensors.

S. No	Actual PD source Position (cm)	Calculated PD Position by PSO(cm)	Location error (cm)
1	(47.5, 46.5, 0)	(46.5, 44.8, 2)	2.8
2	(42.2, 41.4, 0)	(40.8, 39.8, 1)	2.35

The PSO algorithm is used for the PD source location with the average value of measured 100 sets of TDOA measurements and an error of 3 cm is observed with the TDOA measurements from the experiment conduction. The actual and calculated PD Position results are shown in the Table 5.5.

5.8 Localization of PD source using Broad band LPDA UHF Sensors

Figure 5.23 Laboratory Experiment Model for PD source Localization using Broad band LPDA UHF sensors

Procedure Steps for PD Source Localization using PSO Method

1. Initialize the random population size for PD source location and light velocity and velocity & position of swarm particles.
2. Evaluate all the individual fitness values using objective function and select the best PD source location.
3. Check whether the PD source location is within its limits, else go to step 2.

4. Check convergence criterion is fulfilled, if it is yes go to step 5 else go to step 2.
5. Stop.

The relative positions of four planar LPDA UHF sensors placed on the four wooden stools are shown in the Figure 5.23 and the sensors positions given in Table 5.6. The two different PD source positions are shown in the Table 5.7. The total length, width and height is (245.5, 184, 52) cm.

Table 5.6 Broad band LPDA UHF Sensors Co-ordinates

Broad band UHF Sensors	Coordinates (x,y,z) in cm
Sensor 1	(131,220,51)
Sensor 2	(16,165.05,51.5)
Sensor 3	(150,48,51.5)
Sensor 4	(58.5,48.5,51.5)

Table 5.7 PD source Location Results using Broad band LPDA UHF Sensors.

	Corona PD Source	Particle Movement PD Source
Actual PD Source Coordinates (cm)	(120, 72, 45)	(133.5, 108.5, 45)
Time Difference of Arrival (ns)	(0.32, 2.08, 3.04)	(0.35, 2.14, 2.89)
Calculated PD Source Coordinates (cm)	(119, 70, 43)	(132, 106.5, 42.5)
Location Error (cm)	3	3.535

The PSO algorithm is used for the PD source location with the average value of measured 100 sets of TDOA measurements and an error of 3.54 cm is observed with the TDOA measurements from the experiment conduction. The actual and calculated PD Position results are shown in the Table 5.7.

5.9 Summary

A broadband log periodic printed dipole array antenna is presented in this paper. The bandwidth is achieved by optimizing lengths of selected dipole elements and shaping them to provide additional capacitance and effectively reducing the length of the dipole elements. The antenna achieves a fractional bandwidth of 126% within a compact size of 110 mm **x** 140 mm. The characteristics of the designed LPDA UHF sensor are simple planar design, light weight and broad bandwidth making it useful for measurement of partial discharges.

This antenna is designed to detect different types of PD defects occurrences generally falling in the 0.5 - 2.2 GHz frequency range which are detected in power transformer. The proposed antenna is effective in measuring the discharges as it exhibits better antenna height and flat gain performance.

The UHF PD signals are acquired by the incipient discharge like with the conducting particle movement in the transformer oil filled test electrode cell. The averaged TDOA measurements are considered for determination of the PD source location using PSO algorithm. The obtained location error is almost 3.5 cm from the conducted experiment. This research may be very much helpful for utilities and manufacturers with low investment.

CHAPTER 6

Conclusions and Future Scope

6.1. Conclusions

In this thesis, non-invasive PD monitoring techniques for the localization of PD source in power transformer have been presented. These approaches have been validated for laboratory and field data case studies in the relevant literature. A broad band UHF sensor is designed, fabricated and various PD defects were detected and localized in the laboratory experimental set up. In this segment, summarization of the major contributions performed in this thesis on merits of non-invasive methods over traditional methods in PD monitoring of power transformer is outlined.

In chapter-1, overview on key aspects of the condition monitoring of power transformer, motivations, research objectives and contributions followed by organization of the thesis have been explained.

In chapter-2, a literature survey on localization of PD source in power transformer using non-invasive PD monitoring techniques has been presented. The detailed description of PD process and PD measurement techniques has been described. Particularly, the merits and demerits of invasive and non-invasive PD monitoring techniques have been elucidated. In this thesis, non-invasive PD monitoring techniques were used for the localization of the PD source in power transformer.

In chapter-3, acoustic sensor based localization of PD source in power transformer using bat algorithm has been proposed. Case study on laboratory and field PD measurements data has been provided to demonstrate the efficacy of the proposed methods. The results of the case study also reveal that the proposed bat algorithm is superior when compared with the reported literature algorithms.

In chapter-4, acoustic sensor based localization of PD source in power transformer using fuzzy adaptive particle swarm optimization algorithm (FAPSO) has been proposed. By the integration of metaheuristic algorithm with fuzzy logic system, the Case study on laboratory and field PD measurements data has been provided to demonstrate the efficacy of the proposed methods. The results of the case study also reveal that the proposed FAPSO-I algorithm is superior when compared with the reported literature algorithms.

In chapter-5, laboratory PD measurement setup has been presented. This measurement set up includes wide band LPDA UHF sensor and its detection circuit. The distinct PD source test objects have been developed and manufactured to simulate distinct incipient discharges from those PD source test objects. The PD source test objects have been elucidated in this chapter. The localization of PD source using narrow band and wideband LPDA UHF sensors is performed in the laboratory. The PD source localization results show that the location error is within the acceptable limit.

The following key outcomes have been attained from the present research work.

- The proposed Bat algorithm for localization of PD source is efficient, robust and with no local optima problems. The bat algorithm converges within 10 iterations compared to other reported works in the literature. The statistical measures like PD source location error, maximum deviation & relative errors illustrate that the bat algorithm has yielded least errors with the other reported literature works.
- The proposed FAPSO-I (49 rules) & FAPSO (9 rules) algorithm has been implemented for PD source localization in power transformer utilizing acoustic time measurements. The Mamdani fuzzy interference system is used for fuzzification and the centroid method is used for degree of membership function. The FAPSO-I algorithm has yielded very low PD location error, maximum deviation & relative errors. In general, more fuzzy rules are better suited for analyzing the location results. At last FAPSO-I is better with other published works in the literature.
- The designed broad band planar LPDA UHF sensor achieves a fractional bandwidth of 126% and the size is ($0.495\lambda_0$ x $0.63\lambda_0$ x $0.0144\lambda_0$) at center frequency of 1.35 GHz. The proposed antenna is experimentally validated on FR4 3.2 mm thickness substrate. The measured gain of antenna is 4 ± 0.5 dBi over 800 MHz to 2.2 GHz which provides lower variation in measured partial discharges. The effective antenna height of the proposed antenna is measured to be over 15 mm. The measured return loss is better than 10 dB over the frequency range. The designed broad band sensor detected the distinct incipient discharges which fall under the UHF frequency range. The time domain and frequency spectrum of those distinct incipient discharges are illustrated in this chapter.

- The partial discharge measurements with oil filled test objects demonstrates that both the UHF sensors i.e., narrow and wide band attained the PD signals effectively in their range of applicability. The localization of PD source results using particle swarm optimization shown by these two sensors is acceptable within the limits.

6.2. Future Scope of Work

- Development of robust algorithms in attaining accurate PD source location results
- Detection and localization of different types of incipient discharges can be attempted on in service power transformer
- Substantial research work has to be required on initiation of less priced sensors with distinct features put together fixing them in destructive conditions that induce in power substations.
- Development of combining the acoustic and UHF sensors with less priced in online monitoring system for high voltage electric power apparatus.
- Multi fusion sensor methodology can be illustrated for power transformer condition monitoring, driving towards penetration of smart grid technology.

REFERENCES

[1] M Minhas, J. Reynders, and P. De Klerk, "Failures in power system transformers and appropriate monitoring techniques," *11th Intl. Sympos. High Voltage Eng.*, London, UK, pp. 94-97, 23-27 Aug. 1999.

[2] H. H. Sinaga, B.T. Phung and T. R. Blackburn, "Recognition of single and multiple partial discharge sources in transformers based on ultra-high frequency signals", IET Gener. Transm. Distrib., Vol. 8, Iss. 1, pp. 160–169, 2014.

[3] S.. Strachan, S. Rudd, S. McArthur, and M. Judd, "Knowledge-based diagnosis of partial discharges in power transformers," *IEEE Trans. Dielectr. Electr. Insul.*, vol. 15, 1, pp.259-268, Feb. 2008.

[4] Homaei, M., Moosavian, S. M., and Illias, H. A. "Partial discharge localization in power transformers using neuro-fuzzy technique." *IEEE Trans. Power Del.*, 29(5), 2066 – 2076, 2014.

[5] Al-Masri, W. M. F., Abdel-Hafez, M. F., and El-Hag, A. H. (2016b). "Toward high accuracy estimation of partial discharge location." *IEEE Trans. Instrum. Meas.*, 65(9), 2145 - 2153.

[6] R. Bartnikas, "Partial discharges their mechanism, detection and measurement," *IEEE Trans. Dielectr. Electr. Insul.*, vol. 9, 5, pp. 763-808, Oct. 2002.

[7] G. Stone, "Partial discharge diagnostics and electrical equipment insulation condition assessment," *IEEE Trans. Dielectr. Electr. Insul.*, vol. 12, 5, pp. 891-903, Oct. 2005.

[8] M. Muhr, T. Strehl, E. Gulski, K. Feser, E. Gockenbach, W. Hauschild, and E. Lemke, "Sensors and sensing used for non-conventional PD detection," *2006 CIGRE Paris Session*, Paris, France, 2006.

[9] Venkatesh, A. S. P., Danikas, M. G., and Sarathi, R. (2011). "Understanding of partial discharge activity in transformer oil under transient voltages adopting acoustic emission technique." *Proc.*, 6*th Int. Conf. on Industrial and Information Syst.*, Kandy, Sri Lanka, 98 – 101.

[10] Fuhr, J., Haessig, M., Boss, P., Tschudi, D., and King, R. A. "Detection and location of internal defects in the insulation of power transformers." *IEEE Trans. Electr. Insul.*, 28(6), 1057 – 1067, 1993.

[11] A.J. Reid, M.D. Judd, R.A. Fouracre B.G. Stewart and D.M. Hepburn, "Identification of simultaneously active partial discharge sources using combined radio frequency and IEC60270 measurement", IET Science, Measurement and Technology, Vol. 5, Iss. 3, pp. 102–108, 2011.

[12] K. Hwang, J. Jung, Y. Kim, and H. Yang, "New locating method of partial dischargesinpower transformers based on electromagnetic wave propagation characteristics"*2014CIGRE Paris Session*, Paris, France, 2014.

[13] S. Hoek, M. Krüger, S. Körber, and A. Kraetge, "Application of the UHF technology to detect and locate partial discharges in liquid immersed transformer " *2014 CIGRE Paris Session*, Paris, France, 2014.

[14] P. Baker, B. Stephen, and M. Judd, "Compositional modeling of partial discharge pulse spectral characteristics," *IEEE Trans. Instrum. Meas.*, vol. 62, 7, pp. 1909-1916, Jul. 2013.

[15] J. Rubio-Serrano, M. Rojas-Moreno, J. Posada, J. Martinez-Tarifa, G. Robles, and J. GarciaSouto, "Electro-acoustic detection, identification and location of partial

discharge sources in oil-paper insulation systems," *IEEE Trans. Dielectr. Electr. Insul.,* vol. 19, 5, pp. 1569- 1578, Oct. 2012.

[16] "Guidelines for Partial discharge detection using conventional (IEC 60270) and unconventional methods", *Cigre Working Group* D 1.37, August 2016.

[17] IEEE Std C57.127 (2007). "IEEE guide for the detection and location of acoustic emissions from partial discharges in oil-immersed power transformers and reactors." 1 - 47.

[18] "Partial discharges in transformers", *Cigre Working Group* D 1.29, February 2017.

[19] IEC 60270 High Voltage test techniques – Partial discharge measurement International Electrotechnical Commission (IEC), Geneva, Switzerland, 3rd Edition, 2000.

[20] K.Rethmeier, M.Kruger, A.Kraetge, R.Plath, W.Koltunowicz,"Experiences in Onsite Partial Discharge Measurements and Prospects for PD Monitoring", No:M-6,pp.1279-1283,Proceedings 2008 International Conference on Condition Monitoring and Diagnosis, Beijing,China,2008.

[21] S.Conen,S.Tenbohlen,S.M.Markalous,S.Strehl,"Sensitivity of UHF PD Measurements in Power Transformers",IEEE Transactions on Dielectrics and Electrical Insulation, Vol.15,No.6,pp.1553-1558.

[22] L. E. Lundgaard, "Partial Discharge – Part XIII: Acoustic Partial Discharge Detection Fundamental Considerations," in *IEEE Electrical Insulation Magazine,* vol. 8, pp. 25-31, 1992.

[23] L. E. Lundgaard, "Partial discharge - XIV: Acoustic partial discharge detection-practical
application," *IEEE Electrical Insulation Magazine*, vol. 8, pp. 34-43, 1992.

[24] S. M. Markalous, S. Tenbohlen and K. Feser, "Detection and Location of Partial Discharges in Power Transformers using Acoustic and Electromagnetic Signals", IEEE Trans. Dielectr. Electr. Insul., Vol. 15, No. 6, pp. 1576-1583, 2008.

[25] M. Kozako, K. Yamada, A. Morita, S. Ohtsuka, M. Hikita, K. Kashine, I. Nakamura and H. Koide, "Fundamental study on partial discharge induced acoustic wave propagation in simulated transformer composite insulation system," ICPADM 2009. IEEE 9th International Conference on the Properties and Applications of Dielectric Materials, 2009, Page(s): 477 – 480, 2009.

[26] Xie, Q., Li, T., Tao, J., Liu, X., Liu, D., and Xu, Y. (2016). "Comparison of the acoustic performance and positioning accuracy of three kinds of planar partial discharge ultrasonic array sensors." *IET Radar, Sonar Navigation,* 10(1), 166 - 173.

[27] Al-Masri, W. M. F., Abdel-Hafez, M. F., and El-Hag, A. H. (2016a). "A novel bias detection technique for partial discharge localization in oil insulation system." *IEEE Trans. Instrum. Meas.,* 65(2), 448 - 457.

[28] Mohammadi, E., Niroomand, M., Rezaeian, M., and Amini, Z. (2009). "Partial discharge localization and classification using acoustic emission analysis in power transformer." *Proc.,* 31*st Int. Telecommunications Energy Conference,* Incheon, South Korea, 1 - 6.

[29] Hekmati, A. and Hekmati, R. (2017). "Optimum acoustic sensor placement for partial discharge allocation in transformers." *IET - Sci. Meas. Technol.,* 11(5), 581 - 589.

[30] Markalous, S. M. and Feser, K. (2004). "All-acoustic PD measurements of oil/paper insulated ransformers for PD-localization." *Proc.,* 2*nd Int. Conf. on Advances in Processing, Testing and Application of Dielectric Materials,* Wroclaw, Poland.

[31] Kraetge, A., Hoek, S., Koch, M., and Koltunowicz, W. (2013). "Robust measurement, monitoring and analysis of partial discharges in transformers and other HV apparatus." *IEEE Trans. Dielectr. Electr. Insul.,* 20(6), 2043 - 2051.

[32] Liu HL, Liu Lu Y, Tan X, Hu X. PD detection and localization by acoustic measurement in an oil-filled transformer. IEE Proc Sci Meas Technology 2000; 147(2):81–85.

[33] Kurz, J., Markalous, S., Grosse, C., and Reinhardt, H. (2005). "New approaches for three dimensional source location-examples from acoustic emission analysis." *In European Geosciences Union-General Assembly,* 7.

[34] M M Sacha, Tenbohlen Stefan, Feser Kurt. New robust non-iterative algorithms for acoustic PD-localization in oil/paper-insulated transformers. In: 14th International symposium on high voltage engineering, Beijing, China, August 25–19; 2005. Paper no. G-40.

[35] Veloso GFC, da Silva LEB, Lambert-Torres G, et al. Localization of partial discharges in transformers by the analysis of the acoustic emission. In: Industrial Electronics, 2006 IEEE International Symposium on, Montreal, Quebec, Canada; 9–12 July 2006. p. 537–541.

[36] Kundu P, kishore NK, Sinha AK. A non-iterative partial discharge source location method for transformers employing acoustic emission techniques. Appl Acoustic 2009; 70(11–12):1378–83.

[37] L. Tang, R. Luo, M. Deng, J. Su., Study of partial discharge localization using ultrasonic in power transformers based on particle swarm optimization". IEEE Trans. Dielectric. Electr. Insul. 2008; 15(2):492–495.

[38] Boczar T, Borucki S, Cichod A, Zmarzby D. Application possibilities of artificial neural networks for recognizing partial discharges measured by the acoustic emission method. IEEE Trans. Dielectric. Electr. Insul. 2009; 16(1):214–23.

[39] Punekar, G. S., Jadhav, P., Bhavani, S. T., and Nagamani, H. N. (2012). "Some aspects of location identification of PD source using ae signals by an iterative method." *Proc., IEEE* 10*th Int. Conf. on the Properties and Appl. of Dielectric Materials,* Bangalore, India, 1 - 4.

[40] Punekar, G. S., Antony, D., Bhavanishanker, T., Nagamani, H. N., and Kishore, N. K. (2013). "Genetic algorithm in location identification of AEPD source: Some aspects." *Proc., IEEE* 1*st Int. Conf. on Condition Assessment Techniques in Electr.Syst. (CATCON),* kolkatta, India, 386 - 390.

[41] Búa-Núñez, I., Posada-Román, J. E., Rubio-Serrano, J., and Garcia-Souto, J. A. (2014). "Instrumentation system for location of partial discharges using acoustic detection with piezoelectric transducers and optical fiber sensors." *IEEE Trans. Instrum. Meas.,* 63(5), 1002 - 1013.

[42] HD. Partial discharge localization in power transformers based on the sequential quadratic programming-genetic algorithm adopting acoustic emission techniques. Eur Phys J Appl Phys 2014; 68(01):10801.

[43] Boya, C., Ruiz-Llata, M., Posada, J., and Garcia-Souto, J. A. (2015). "Identification of multiple partial discharge sources using acoustic emission technique and blind source separation." *IEEE Trans. Dielectr. Electr. Insul.,* 22(3), 1663 - 1673.

[44] Liu HL, Acoustic partial discharge localization methodology in power transformers employing the quantum genetic algorithm .Applied Acoustics 2016; 102:71–78.

[45] Biswas, S., Dey, D., Chatterjee, B., and Chakravorti, S. (2016). "Cross-spectrum analysis based methodology for discrimination and localization of partial discharge

source using acoustic sensors." *IEEE Trans. Dielectr. Electr. Insul.,* 23(6), 3556 - 3565.

[46] Ghosh, R., Chatterjee, B., and Dalai, S. (2017). "A method for the localization of partialdischarge sources using partial discharge pulse information from acoustic emissions." *IEEE Trans. Dielectr. Electr. Insul.,* 24(1), 237 - 245.

[47] Wang, Y. B., Chang, D. G., Fan, Y. H., Zhang, G. J., Zhan, J. Y., Shao, X. J., and He, W. L. (2017). "Acoustic localization of partial discharge sources in power transformers using a particle-swarm-optimization-route-searching algorithm." *IEEE Trans. Dielectr. Electr. Insul.,* 24(6), 3647 - 3656.

[48] Y. B. Wang, Q.R. Shao, L.F. Wang, G.C. Ding, J. L. Li, T.Y.Zhu, G. J. Zhang "Quantitative Comparison of Partial Discharge Localization Algorithms on Power Transformers Based on Acoustic Method" 2018 IEEE Conference on Electrical Insulation and Dielectric Phenomena Cancun, Mexico. pp. 542-545.

[49] M. Schrammen, A. Hamad, P. Jax "Robust Self-Localization of Microphone Arrays Using a Minimum Number of Acoustic Sources" 2019 27th European Signal Processing Conference (EUSIPCO).

[50] L. Zhou, J. Cai, J.Hu, G. Lang, L. Guo and W. Liao "A Correction-Iteration Method for Partial Discharge Localization in Transformer Based on Acoustic Measurement" *IEEE Trans. Power Delivery. 36*(3), 1571 – 1581, 2021.

[51] P.Moore, I. Portugues, and I. Glover, "A nonintrusive partial discharge measurement system based on RF technology", in Proc. IEEE Power Eng. Soc Gen. Meet. ‚Jul. 2003, vol. 2, pp. 1–6

[52] P. J. Moore, I.E. Portugues and I.A. Glover, "Radiometric location of partial discharge sources on energized high-Voltage plant",IEEE Trans. Power Del., Vol. 20, pp. 226-2272, 2005.

[53] M. D. Judd, Y. Li, and I. B. B. Hunter, "Partial discharge monitoring of power transformers using UHF sensors. Part I: sensors and signal interpretation," IEEE Electr. Insul. Mag., Vol. 21, No.2, pp. 5-14, 2005.

[54] M. D. Judd, Y. Li, and I. B. B. Hunter, "Partial discharge monitoring of power transformers using UHF sensors. Part II: Field Experience," IEEE Electr. Insul. Mag., Vol. 21, No.3, pp. 5-13, 2005.

[55] Z. Tang, C. Li, X. Cheng, W. Wang, J. Li, and J. Li, "Partial Discharge Location in Power Transformers Using Wideband RF Detection", IEEE Trans. Dielectr. Electr. Insul., Vol. 13, No. 6, pp. 1193–1199, 2006.

[56] H.H.Sinaga, B.T.Phung and T.R.Blackburn, "Partial discharge localization in transformers using UHF detection method", IEEETrans.Dielectr.Electr.Insul. Vol.19, pp.1891-1900, 2012.

[57] Y. Shibuya, S. Matsumoto, M. Tanaka, H. Muto, and Y. Kaneda, "Electromagnetic waves from partial discharges and their detection using patchantenna,"IEEE Trans. Dielectr. Electr.Insul., vol. 17, no. 3, pp. 862–871,Jun. 2010.

[58] B. Sarkar, C. Koley, and N. K. Roy and P. Kumbhakar, "Low Cost RF Sensor for Partial
Discharge Detection of High Voltage Apparatus," *IEEE 1st International Conference on*
Condition Assessment Techniques in Electrical Systems, 2013, 978-1-4799-0083-1/13/IEEE.

[59] J. Tang and Y. Xie, "Partial discharge location based on time differenceof energy accumulation curve of multiple signals," IET Electric Power Applications, Vol. 5, pp. 175-180, 2011.

[60] Z. Xu, C. Yonghong, M. Yongpeng, W. Kai, and N. Yuhan, "The propagation characteristics of UHF partial discharge in power transformers with complex winding structure," IEEE Conf. Electr. Insul.Dielectr.Phenomena (CEIDP), pp. 60-63, 2012.

[61] G. Robles, J. Martínez-Tarifa, M. Rojas-Moreno, R. Albarracín, andJ. Ardila-Rey, "Antenna selection and frequency response study forUHF detection of partial discharges," inProc. IEEE I2MTC, May 2012,pp. 1496–1499.

[62] G. Robles, M. Sánchez-Fernández, R. Albarracín, M.V. RojasMoreno, E. Rajo-Iglesias and J.M. Martinez-Tarifa, "Antennas parameterization for the detection of partial discharges", IEEE Trans. Instrum. Meas., Vol. 62, pp. 932-941, 2013.

[63] C. Boya, M. V. Rojas-Moreno, M. Ruiz-Llata1 and G. Robles, "Location of Partial Discharges Sources by Means of Blind Source Separation of UHF Signals", IEEE Trans. Dielectr. and Electr. Insul. Vol. 22, No. 4; pp. 2302–2310, August 2015.

[64] Emran M. Amin, and Nemai C. Karmakar, "A Passive RF Sensor for Detecting Simultaneous Partial Discharge Signals Using Time–Frequency Analysis", IEEE Sensor Journal, Vol. 16, No. 8,pp. 2339-2348, April 2016.

[65] Shusheng Zheng, Chengrong Li, Zhiguo Tang, Wenzhi Chang and Meng He, " Location of PDs inside Transformer Windings using UHF Methods", IEEE Transactions on Dielectrics and Electrical Insulation Vol. 21, No. 1; pp 386-393, February 2014.

[66] P. J. Moore, I. E. Portugues, and I. A. Glover, "Partial discharge investigation of a power transformer using wireless wide band wideband radio-frequency measurements," *IEEE Trans. Power Del.*, vol. 21, no. 1, pp. 528-530, 2006.

[67] S. Tenbohlen, D. Denissov, S. M. Hoek and S. M. Markalous, "Partial Discharge Measurement in the Ultra High Frequency (UHF) Range", IEEE Transactions on Dielectrics and ElectricalInsulation Vol. 15, No. 6; pp 1544-1552, December 2008.

[68] Coenen, S. and Tenbohlen, S. (2012). "Location of PD sources in power transformers by UHF and acoustic measurements." *IEEE Trans. Dielectr. Electr. Insul.*, 19(6), 1934 - 1940.

[69] Mirzaei, H. R., Akbari, A., Gockenbach, E., Zanjani, M., and Miralikhani, K. (2013). "A novel method for ultra-high-frequency partial discharge localization in power transformers using the particle swarm optimization algorithm." *IEEE Electr. Insul. Mag.*, 29(2), 26 - 39.

[70] Mirzaei, H. R., Akbari, A., Gockenbach, E., and Miralikhani, K. (2015). "Advancing new techniques for UHF PD detection and localization in the power transformers in the factory tests." *IEEE Trans. Dielectr. Electr. Insul.*, 22(1), 448 - 455.

[71] Zeng, F., Tang, J., Huang, L., and Wang, W. (2015). "A semi-definite relaxation approach for partial discharge source location in transformers." *IEEE Trans. Dielectr. Electr. Insul.*, 22(2), 1097 - 1103.

[72] Yang Xin-She. Nature-inspired metaheuristic algorithms. 2nd ed. United Kingdom: university Press; 2010.

[73] The National Grid Company plc, "Capacitive couplers for UHF partial discharge monitoring," Tech. Guid. Note TGN (T) 121, 1997, no. 1.

[74] E. Al. AlMazam, et al., "Partial discharge and oil quality monitoring using an RF Antenna," *IEEE Industry Applications Magazine*, vol. 16, no. 3, pp. 57-59, 2010.

[75] A. H. EI-Hag, et al., "Multi-Purpose RF Antenna for Partial Discharge and Oil Quality Monitoring," In Proc. of 3rd Intl. Conf. on Electric Power and Energy Conversion Systems, IEEE, Istanbul, Turkey, 2013.

[76] Y. Hai-Feng, Q. Yong, D. Yue, S. Ge-hao and J. Xiu-chen, "Development of multi-band ultrahigh-frequency sensor for partial discharge monitoring based on the meandering technique", IET Sci., Meas. and Tech., Vol. 8, No. 5, pp. 327–335, 2014.

[77] Asghar Akbari, Peter Werle and Mohammad Akbari, Hasan Reza Mirzaei, "Challenges in Calibration of the Measurement of Partial Discharges at Ultrahigh Frequencies in PowerTransformers", IEEE Electrical Insulation Magazine, Vol. 32, No. 2, 2016.

[78] C. A. Balanis, Antenna Theory, Analysis and Design, John Wiley & Sons, INC, New York 1997.

[79] R.L. Carrel, Analysis and Design of the Log Periodic Dipole Antenna, Technical Report No.52.

[80] A. M. Ishak, *et al*, "Design and Optimization of UHF Partial Discharge Sensors using FDTD Modelling," *IEEE Sens. J.,*, vol. 17, no. 1, pp. 127-133, 2017.

[81] J. Lopez-Roldan, T. Tang, and M. Gaskin, "Optimization of a Sensor for Onsite Detection of Partial Discharges in Power Transformers by the UHF method," *IEEE Trans. Dielectr. Electr. Insul.*, vol.15, no.6, pp.1634-1639, 2008.

[82] C. Zachariades, R. Shuttleworth, and R. Giussani, "A Dual-Slot Barrier Sensor for Partial Discharge Detection in Gas-Insulated Equipment," *IEEE Sens. J.*, vol. 20, no. 2, pp. 860–867, 2020.

[83] W. U. Qingyan, L. Guoqiang, X. Zhengwu, and L. Liang, "The Study of Archimedean Spiral Antenna for Partial Discharge Measurement," 4th Intl. Conf. on Intelligent Control and Information Processing (ICICIP), IEEE, Beijing, China. 2013.

[84] J. Li, T. Jiang, and C. Cheng, "Hilbert Fractal Antenna for UHF Detection of Partial Discharges in Transformers," *IEEE Trans. Dielectr. Electr. Insul.*, vol. 20, no. 6, pp. 2017- 2025, 2013.

[85] J. Li, T. Jiang, C. Wang, and C. Cheng, "Optimization of UHF Hilbert Antenna for Partial Discharge Detection of Transformers," *IEEE Trans. Antennas Propag.*, vol. 60, no. 5, pp. 2536- 2540, 2012.

[86] J. Li, P. Wang, T. Jiang, L. Bao, and Z. He, "UHF Stacked Hilbert Antenna Array for Partial Discharge Detection," *IEEE Trans. Antennas Propag.*, vol. 61, no. 11, pp. 5798- 5801, 2013.

[87] A. H. Zahed, *et al*., "Design of Hilbert Fractal Antenna for Partial Discharge Detection and Classification," 4th Intl. Conf. on Electric Power and Energy Conversion Systems (EPEC), Sharjah, UAE, 2015.

[88] M. M. O. Harbaji *et al.,* "Design of Hilbert Fractal Antenna for Partial Discharge Classification in Oil-Paper Insulated System," *IEEE Sens. J.*, vol. 17, no. 4, pp. 1037–1045, 2017.

[89] H. Naomi, *et al*., "A design for significantly improving the measurable sensitivity of log-periodic dipole antenna arrays for optical electric field sensors," *Microw. Opt. Techn. Lett.*, vol. 57 no.6, pp. 1386–1390, 2015.

[90] X. H. Zhen, X. S. Zhong, W. Wen, and L. Jian, "Low-Profile Log-Periodic Monopole Array," *IEEE Trans. Antennas Propag.*, vol. 63 no. 12, pp. 5484 – 5491, 2015.

[91] L. Xinyuan, and Y. Guo-Min, "Miniaturized log periodic dipole array with complementary split-ring resonators," *Microw. Opt. Techn. Lett.*, vol. 58 no. 9, pp. 2217–2221, 2016.

[92] A. Mirkamali and P. S. Hall, "Wideband frequency reconfiguration of a printed log periodic dipole array," *Microw. Opt. Techn. Lett.*, vol. 52, no. 4, pp. 861–864, 2010.

[93] C. Zachariades, R. Shuttleworth, R. Giussani and T. Loh, "A Wideband Spiral UHF Coupler with Tuning Nodules for Partial Discharge Detection," *IEEE Trans. Power del.*, vol. 34, no. 4, pp. 1300–1308, 2019.

[94] W. Zhou, P. Wang, Z. Zhao, Q. Wu and A. Cavallini, "Design of an Archimedes Spiral Antenna for PD Tests under Repetitive Impulse Voltages with Fast Rise Times," *IEEE Trans. Dielectr. Electr. Insul.*, vol. 26, no. 2, pp. 423- 430, 2019.

[95] X. Han, J. Li, L. Zhang, P. Pang and S. Shen, "A Novel PD Detection Technique for use in GIS Based on a combination of UHF and Optical Sensors," *IEEE Trans. Instrum. Meas.*, vol. 68, no. 8, pp. 2890- 2897, 2019.

[96] Y. Qi, *et al*., "Design of Ultra -Wide Band Metal –Mountable Antenna for UHF Partial Discharge Detection," *IEEE Access,* vol. 7, pp. 60163- 60170, 2019.

[97] G. V. R. Xavier, *et al*., "Design and Application of a Circular Printed Monopole Antenna in Partial discharge Detection," *IEEE Sens. J.,* vol. 19, no. 10, pp.3718- 3725, 2019.

[98] Jinxi Chen, Jesse Ludwig, and Sungkyun Lim, "Design of a Compact Log-Periodic Dipole Array Using T-Shaped Top Loadings," *IEEE Trans. Antennas Propag*., vol. 16, pp 1585-1588, 2017.

[99] C. Lei, H. Shuai, Z. Jian Qiang, and L. Dan, "A Compact Dielectric-Loaded Log-Periodic Dipole Array (LPDA) Antenna," *IEEE Antennas Wireless Propag. Lett.*, vol. 16, pp 2759-2762, 2017.

[100] K. Anim and J. Young-Bae, "Shortened Log-Periodic Dipole Antenna Using Printed Dual-Band Dipole Elements," *IEEE Trans. Antennas Propag*., vol. 66, no. 12, pp. 6762-6771, 2018.

[101] W. Jia Min, *et al*., "A Wideband Switched-Beam Antenna Array Fed by Compact Single-Layer Butler Matrix," *IEEE Trans. Antennas Propag*, vol. 69, no.8, pp.5130-5135, 2021.

[102] K. K. Mistry, P. I. Lazaridis, Z. D. Zaharis, T.H. Loh, "Design and Optimization of Compact Printed Log-Periodic Dipole Array Antennas with Extended Low-Frequency Response," *Electronics,*vol.10, pp.1-10, 2021.

[103] R. Albarracin, J. A. Ardila Rey, A. A. Masud, "On the use of Monopole Antennas for Determining the Effect of the Enclosure of a Power Transformer Tank in Partial Discharges Electromagnetic Propagation," *Sensors*, vol. 16 pp. 1-17, 2016.

[104] J. Du, *et al*., "Investigation on the Propagation Characteristics of PD-Induced Electromagnetic Waves in an actual 110 kV Power Transformers and Its Simulation Results," *IEEE Trans. Dielectr. Electr. Insul.*, vol.25, no.5, pp.1634-1639, 2018.

[105] R. Carrel, "The design of log-periodic dipole antennas," in *Proc. IRE Int. Com. Rec.*, New York, NY, USA, Marc. 1966.

LIST OF PUBLICATIONS

SCI / SCIE Journals

1. M. Kalyan Chakravarthi, A.V. Giridhar, G. Arun Kumar and D.V.S.S. Siva Sarma "A Compact Log Periodic Planar Dipole UHF Array Sensor for Partial Discharge Measurements", IEEE Sensors Journal, Vol 21, No 24, Dec 2021, pp 27748-27756, 2021. DOI: 10.1109/JSEN.2021.3124418.

2. M. Kalyan Chakravarthi, A.V. Giridhar, D.V.S.S. Siva Sarma "Location of PD source utilizing Acoustic Signals in Power transformer by fuzzy adaptive particle swarm optimization", Radio Engineering Journal, Vol 27, No 2, Dec 2018, pp 1119-1127, DOI 10.13164/re.2018.1119.

International Conferences

1. M.Kalyan Chakravarthi, A.V.Giridhar, D.V.S.S.SivaSarma "Localization of Partial Discharge Source in Power Transformer using Bat Algorithm", IEEE- ICPS 2017 21st-23rd Dec 2017.

2. M.Kalyan Chakravarthi, A.V.Giridhar, D.V.S.S.SivaSarma "Localization of Incipient Discharge in Power Transformer using UHF Sensors", IEEE- ICHVET 2019 5th-7th Feb 2019.

3. M.Kalyan Chakravarthi, A.V.Giridhar, D.V.S.S.SivaSarma, G.Arun Kumar "Investigation of Log Periodic Dipole Array Printed Antenna for recognizing Incipient Discharges in Power Transformer", IEEE- ICPEE 2021 2-3rd Jan 2021.

APPENDIX

Return loss (RL)

Return loss (or) reflection coefficient is the parameter that describes the portion of signal which will pass through the port and the portion of signal that is rejected (loss) when the antenna port is terminated by a matched load. This parameter is similar to VSWR and it is also known as S11 parameter.

Voltage standing wave ratio (VSWR)

Voltage standing wave ratio indicates the degree of matching achieved between the line and antenna. If an antenna is connected to the input transmission line and the antenna impedance does not match with the transmission line impedance, some of the signal will be lost at the junction point as refracted. The loss due to mismatch impedance is known as VSWR.

Bandwidth (BW)

Bandwidth is the frequency range of the antenna performance with respect to antenna parameters fulfils a specific standard. The frequency bandwidth can be expressed as absolute bandwidth (ABW) or fractional bandwidth (FBW). The ABW is defined as the difference between the maximum and minimum frequency. The FBW is defined as the percentage difference between the maximum and minimum frequency over center frequency.

Input impedance

Input impedance is defined as the impedance presented by the antenna at its terminals or the ratio of the voltage to current at a pair of terminals or the ratio of the appropriate components of the electric to magnetic fields at a point.

Radiation pattern

Radiation pattern is defined either as a mathematical function or a graphical representation of the radiation properties of the antenna as a function of space coordinates. The plots of the radiation patterns may be drawn in three or two dimensions. In this thesis, 2D radiation plots made on a spherical surface of a constant radius r away from the antenna centred at the origin. The electric (E-Plane) and magnetic (H-Plane) field trace plotted shows the normalized amplitude with respect to the maximum values.

There are three radiation patterns that are commonly used to describe the antenna's properties:

Directional is defined as the ability of the antenna to transmit or receive the signal in some direction more effective than others. If that antenna is directional means maximum directivity significantly greater than that of half wave dipole.

Isotropic is a theoretically lossless antenna which also has equal radiation in every direction. Antennas with this pattern type represent ideal cases and are physically realizable. They are usually used as a reference to describe the actual antenna directivity.

Omni directional is a special case of directional antenna, where the antenna has directional capability in any orthogonal plane but has a non- directional pattern in the given plane.

Directivity

The directivity is the ratio of the radiation intensity in a given direction from the antenna to the radiation intensity averaged overall directions. The average radiation intensity is equal to the total power radiated by the antenna divided by 4π. If the direction is not mentioned then it is maximum radiation. It has no units.

Gain

The gain is defined as the ratio of the intensity in a given direction to the radiation intensity that would be obtained if the power accepted by the antenna were radiated isotropically. It has no units.

Antenna Factor

Antenna factor is defined as the ratio of electric field strength at the antenna to the voltage at the antenna terminals.

Effective Height

Effective height is defined as the inverse of antenna factor.

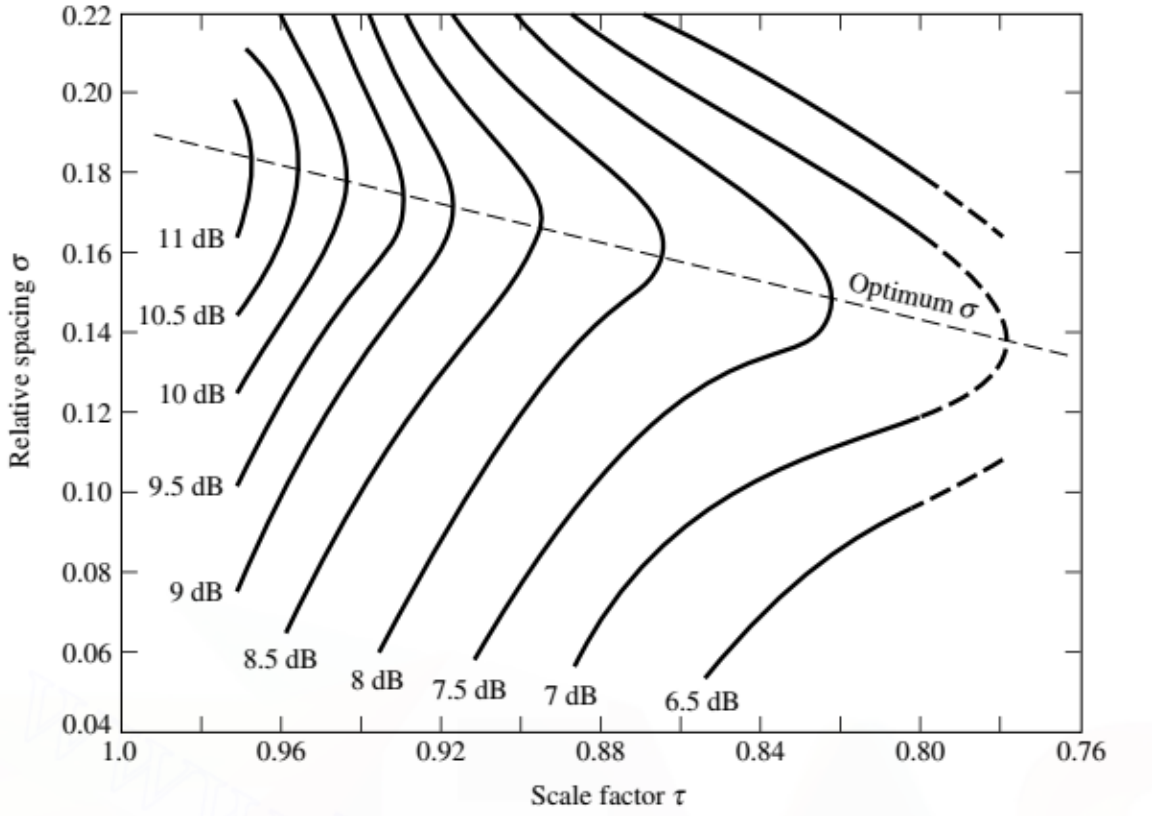

Figure A.1 Computed contours of constant directivity versus spacing &scaling factors of LPDA antenna.

Table A.1 Computed and Measured Directivities of LPDA antennas.

S.No	Scaling factor	Spacing factor	Angle	Characteristic Impedance	height to radius ratio	E-Plane bandwidth	H-Plane bandwidth	Measured Directivity	Computed Directivity
1	0.98	0.057	5	100	125	56.5	85.7	9.31	10.0
2	0.975	0.07/7	5	100	200/151	52.8	76.6	10.08	10.0
3	0.95	0.0268	25	100	100/26	68.7	114.2	7.20	-
4	0.93	0.125	8	65	66	60.0	85	9.08	9.8
5	0.92	0.120	9.5	100	118	57	81.1	9.52	9.4
6	0.91	0.128	10	94	66	59.2	90.8	8.85	9.4
7	0.89	0.103	15	75	80/45	67	106.3	7.63	8.6
8	0.88	0.089	17.5	150	177	65.2	112.0	7.52	8.3
9	0.86	0.08	23.6	200	50	64.3	112.4	7.57	7.9
10	0.85	0.216	10	75	80/49	71.3	109	7.14	7.3
11	0.84	0.068	30.5	215	50	67.8	126.6	6.83	7.5
12	0.81	0.364	7.5	75	80/43	95	180	3.83	-
13	0.80	0.137	20	100	125	58.5	101.9	8.41	8.3

Table A.2 Parameter and their effect on the observed performance.

S. No	LPDA Antenna Parameters	Active Region Bandwidth	Input impedance (always less than Z_o)	Directivity	Boom length for a fixed working bandwidth
1	Scaling factor (Spacing factor constant)	decrease	small decrease	increase	decrease to a point depending on B, then decrease
2	Scaling factor (Angle constant)	decrease	small decrease	small increase	decrease
3	Spacing factor (Scaling factor constant)	increase	increase	increase	increase
4	Spacing factor (Angle constant)	increase	increase	small decrease	increase
5	Characteristic Impedance	independent but active region location moves towards apex	increase	small decrease	small decrease
6	Height to radius ratio	independent but active region location moves away from apex	increase	small decrease	small increase